DYNAMIC VOLATILITY MODELLING OF CRYPTOCURRENCIES USING TIME-VARYING TRANSITION PROBABILITY MARKOV SWITCHING MODELS

TAN CHIA YEN

FACULTY OF SCIENCE
UNIVERSITI MALAYA
KUALA LUMPUR

2021

DYNAMIC VOLATILITY MODELLING OF CRYPTOCURRENCIES USING TIME-VARYING TRANSITION PROBABILITY MARKOV-SWITCHING MODELS

TAN CHIA YEN

DISSERTATION SUBMITTED IN FULFILMENT OF THE REQUIREMENTS FOR THE DEGREE OF MASTER OF SCIENCE

INSTITUTE OF MATHEMATICAL SCIENCES
FACULTY OF SCIENCE
UNIVERSITI MALAYA
KUALA LUMPUR

2021

UNIVERSITI MALAYA

ORIGINAL LITERARY WORK DECLARATION

Name of Candidate: **TAN CHIA YEN**

Matric No: **17029325/2**

Name of Degree: **MASTER OF SCIENCE**

Title of Dissertation ("this Work"):

DYNAMIC VOLATILITY MODELLING OF CRYPTOCURRENCIES USING TIME-VARYING TRANSITION PROBABILITY MARKOV-SWITCHING MODELS

Field of Study:

FINANCIAL MATHEMATICS

I do solemnly and sincerely declare that:

(1) I am the sole author/writer of this Work;
(2) This Work is original;
(3) Any use of any work in which copyright exists was done by way of fair dealing and for permitted purposes and any excerpt or extract from, or reference to or reproduction of any copyright work has been disclosed expressly and sufficiently and the title of the Work and its authorship have been acknowledged in this Work;
(4) I do not have any actual knowledge nor do I ought reasonably to know that the making of this work constitutes an infringement of any copyright work;
(5) I hereby assign all and every rights in the copyright to this Work to the Universiti Malaya ("UM"), who henceforth shall be owner of the copyright in this Work and that any reproduction or use in any form or by any means whatsoever is prohibited without the written consent of UM having been first had and obtained;
(6) I am fully aware that if in the course of making this Work I have infringed any copyright whether intentionally or otherwise, I may be subject to legal action or any other action as may be determined by UM.

Candidate's Signature Date: 21.6.2021

Subscribed and solemnly declared before,

Witness's Signature Date: 21.6.2021

Name:

Designation:

DYNAMIC VOLATILITY MODELLING OF CRYPTOCURRENCIES USING TIME-VARYING TRANSITION PROBABILITY MARKOV-SWITCHING MODELS

ABSTRACT

Motivated by the large price fluctuations and excessive volatility observed in cryptocurrency market, this research aims to model and forecast the volatility dynamics of cryptocurrencies. First, we adopt Bai and Perron (2003) multiple change point model by incorporating exogenous variables to determine the number and location of change points in the price series, return series and squared return series of Cryptocurrency Index, Cryptocurrency Index 30, and the top ten cryptocurrencies that are ranked according to market capitalisation. Results show that change points occur very frequently in the price series, followed by squared return series and return series. The change points are consistently observed in the periods from December 2017 to April 2018. Following these findings, we propose to use time-varying transition probability Markov-switching GARCH (TV-MSGARCH) models incorporated with logarithmic trading volume and Google searches series respectively as the exogenous variables to model the volatility dynamics of Bitcoin, Ethereum, Ripple, Bitcoin Cash and EOS. Extensive comparisons are carried out to compare the modelling and forecasting performances of the proposed model with the benchmark volatility models, which are the GARCH, GJRGARCH, TGARCH and MSGARCH. All of the volatility models are incorporated with three different error distributions, namely, normal, Student-t and generalised error. Results reveal that, regardless of error distributions, TV-MSGARCH models always predominate other volatility models for in-sample model fitting which are compared based on Akaike information criteria. Also, the Filardo's weighted transition probabilities are also computed to assess the marginal contributions of time-varying transition probabilities of TV-MSGARCH models. Furthermore, it has been discovered that TV-MSGARCH model

generally offers the best out-of-sample forecast evaluated based on quasi-likelihood loss function and assessed by using Hansen's model confidence set. Lastly, different levels of long and short positions of value-at-risk for GARCH model, GJRGARCH model, TGARCH model, MSGARCH model and TV-MSGARCH models, all incorporated with Student-t distribution, are calculated and tested using several backtests.

Keywords: Change points, Cryptocurrency, GARCH model, Markov-switching, Time-varying transition probability, Volatility.

PEMODELAN KERUAPAN DINAMIK KRIPTOWANG DENGAN MODEL PENSUISAN-MARKOV KEBARANGKALIAN PERALIHAN MASA-BERBEZA

ABSTRAK

Didorong oleh turun naik harga yang besar dan keruapan berlebihan tercerap di pasaran kriptowang, penyelidikan ini bertujuan untuk memodel dan meramal dinamik keruapan kriptowang. Pertama, kami menerima pakai model titik perubahan berganda Bai dan Perron (2003) dengan menggabungkan pemboleh ubah eksogen untuk menentukan bilangan dan lokasi titik perubahan pada siri harga, siri pulangan dan siri pulangan terkuasa dua bagi *Cryptocurrency Index*, *Cryptocurrency Index 30* serta sepuluh kriptowang teratas diatur mengikuti permodalan pasaran. Hasil kajian menunjukkan bahawa titik perubahan berlaku sangat kerap pada siri harga, diikuti dengan siri pulangan terkuasa dua dan siri pulangan. Titik perubahan telah diperhatikan secara konsisten antara bulan Disember 2017 hingga April 2018. Berikutan penemuan ini, kami mencadangkan penggunaan model pensuisan-Markov GARCH kebarangkalian peralihan masa-berbeza (TV-MSGARCH) yang menggabungkan logaritma jumlah dagangan dan siri carian Google sebagai pemboleh ubah eksogen untuk memodel dinamik keruapan Bitcoin, Ethereum, Ripple, Bitcoin Cash dan EOS. Perbandingan secara meluas telah dilakukan untuk membandingkan prestasi pemodelan dan peramalan bagi model yang dicadangkan dengan model keruapan penanda aras, iaitu GARCH, GJRGARCH, TGARCH dan MSGARCH. Kesemua model keruapan digabungkan dengan taburan ralat berbeza, iaitu normal, Student-t dan ralat teritlak. Hasil kajian menunjukkan bahawa apabila taburan ralat berbeza dipertimbangkan, model TV-MSGARCH mendominasi model keruapan yang lain untuk model penyuaian dalam-sampel yang dibandingkan berdasarkan kriteria maklumat *Akaike*. Di samping itu, kebarangkalian peralihan berwajaran *Filardo* telah dihitung untuk menilai sumbangan sut kesan kebarangkalian peralihan masa-berbeza

pada model TV-MSGARCH. Tambahan pula, didapati bahawa model TV-MSGARCH menawarkan ramalan luar-sampel yang terbaik dinilaikan berdasarkan fungsi kerugian kuasi-kebolehjadian dan dibandingkan dengan menggunakan set keyakinan model *Hansen*. Akhirnya, pelbagai tahap kedudukan panjang dan pendek nilai-berisiko bagi model GARCH, model GJRGARCH, model TGARCH, model MSGARCH dan model TV-MSGARCH dengan menggabungkan taburan Student-t telah dihitung dan hasilnya telah diuji dengan beberapa ujian ke-belakang.

Kata kunci: Titik perubahan, Kriptowang, Model GARCH, Pensuisan-Markov, Kebarangkalian peralihan masa-berbeza, Keruapan.

ACKNOWLEDGEMENTS

First, I would like to express my deepest appreciation to my supervisors Associate Professor Dr. Ng Kok Haur and Dr. Koh You Beng for always being supportive. They consistently provided me with acute advice and comments so that I could finish this research on schedule. Their guidance along this journey even when I was in huge doubt had definitely inspired me to continue, not to mention the technical concepts and methods they had encouraged me to explore. On top of that, I would also like to thank their dedication in reading all of my work and gave me clear suggestion from time to time even during non-working hours and when they were abroad.

Last but not least, my gratitude is sent to my beloved family. Without their support and encouragement, this research would not be possible to complete. Their continuous strong support was my pillar of strength that helped me through all the hardship I encountered during this journey.

TABLE OF CONTENTS

LIST OF FIGURES

LIST OF TABLES

LIST OF SYMBOLS AND ABBREVIATIONS

P_t	:	Closing price at time t
b_t	:	Conditional mean at time t
σ_t^2	:	Conditional variance at time t
ε_t	:	Error term at time t
x_t	:	Exogenous variable at time t
a_t	:	Innovation component of return at time t
F_{t-1}	:	Past observed returns up to time $t-1$
s_t	:	Regime variable at time t
r_t	:	Return at time t
AIC	:	Akaike information criteria
AGARCH	:	Asymmetric GARCH
APGARCH	:	Asymmetric power GARCH
ARCH	:	Autoregressive conditional heteroscedasticity
BTC	:	Bitcoin
BCH	:	Bitcoin Cash
ADA	:	Cardano
CGARCH	:	Component GARCH
CMTGARCH	:	Component with multiple threshold GARCH
CC	:	Conditional coverage
CRIX	:	Cryptocurrency Index
CCI30	:	Cryptocurrency Index 30

DQ	:	Dynamic quantile
EPA	:	Equal predictive ability
ETH	:	Ethereum
EGARCH	:	Exponential GARCH
FIGARCH	:	Fractionally integrated GARCH
GARCH	:	Generalised autoregressive conditional heteroscedasticity
GED	:	Generalised error distribution
GJRGARCH	:	Glosten-Jagannathan-Runkle GARCH
IGARCH	:	Integrated GARCH
LTC	:	Litecoin
LL	:	Log-likelihood
MSGARCH	:	Markov-switching GARCH
MSE	:	Mean square error
MCS	:	Model confidence set
NORMD	:	Normal distribution
QLIKE	:	Quasi-likelihood
XRP	:	Ripple
SSM	:	Set of superior models
S&P 500	:	Standard & Poor 500
XLM	:	Stellar
STD	:	Student-t distribution

TVTP	:	Time-varying transition probability
TV-MSGARCH	:	Time-varying transition probability MSGARCH
TGARCH	:	Threshold GARCH
TRX	:	Tron
UC	:	Unconditional coverage
VaR	:	Value-at-risk
WTP	:	Weighted transition probability

LIST OF APPENDICES

CHAPTER 1 : INTRODUCTION

1.1 Background of study

Cryptocurrency market is a new investment opportunity that attracts tremendous public attention. Cryptocurrency represents a revolution of monetary system and is designed to work as a medium of exchange by encrypting the technique of cryptography to secure transactions without any third-party interference as opposed to central banking system. As the blockchain technology behind the cryptocurrency becomes more mature and receive widespread acceptance, we believe that cryptocurrency would develop as an appealing alternative to the existing monetary system which is inevitable in this digital era. Nevertheless, for cryptocurrency to be practically acceptable, the cryptocurrency regulations ought to be launched and studied sophisticatedly. Since the transactions of cryptocurrencies are anonymous, cryptocurrencies may be abused for money laundering activities, terrorism financing, human trafficking and other major social threats. Nonetheless, countries including Japan, Malaysia, Singapore, China, Spain, Germany, India, the Philippines, the United States and South Korea are actively working on cryptocurrency regulation establishments in order to provide a sustainable environment for the market participants.

The first cryptocurrency, Bitcoin (BTC), was launched in year 2009 by an individual or a group known as Satoshi Nakamoto, whose identity is still unknown to date (Nakamoto, 2008). The explosion of interest in BTC has induced the development of other cryptocurrencies, collectively known as “altcoins”, an abbreviation for “alternate coins”. There are more than two thousand cryptocurrencies circulating in the market at present (last checked on CoinMarketCap, 30 April 2018) with BTC marking a significant market capitalisation of 37.04% and the combined market capitalisation of the top five cryptocurrencies, namely BTC, Ethereum (ETH), Ripple (XRP), Bitcoin Cash (BCH) and

EOS is 69.56%. Fascinatingly, over the past few years, none of the altcoins ever jeopardise the dominance of BTC and BTC always remains as the largest and most popular cryptocurrencies of all. Nevertheless, altcoins have not garnered consistent interest levels for all time with their market rankings keep changing and portray high turnover rates (Elbahrawy et al., 2017).

Amid public interest on cryptocurrencies start to prominently emerge only when the market appears to portray radical and wild price dynamics with high-profit opportunities. A brief walk through on the prices of BTC over recent years calls attention to the highly volatile nature of cryptocurrencies. At the beginning of year 2017, the price of BTC was about 900 U.S. dollar which then surpassed 5000 U.S. dollar in October 2017. Few months later, BTC price skyrocketed to nearly 20000 U.S. dollar in January 2018. The sudden surge of interest and the high returns of BTC had undoubtedly drawn a great number of investors into the market. The entire cryptocurrency market capitalisation was approximated at 700 billion U.S. dollar in January 2018 with half of the capitals invested in BTC.

The massive growth in the cryptocurrency market however is accompanied by risks and huge uncertainty. No sooner than that, the entire market impulsively started to depreciate and overwhelmed by bearish episodes. The prices of BTC depreciated to around 9000 U.S. dollar at 30 April 2018 (our data end point) with the total market capitalisation of cryptocurrency dropped to nearly 400 billion U.S. dollar. The cryptocurrency market lost almost half of the capitals in only four months. In fact, cryptocurrency market has experienced instability since then, with bullish phases and bearish phases interchange invariably. Besides, the unique price dynamics seen in cryptocurrency market behave distinctly compared to other traditional financial markets. With that, cryptocurrencies are also known to be great investment tools for portfolio diversification which render potential benefits to the investors (Briere et al., 2015). Therefore, it is extremely vital to study the underlying risks bear by the investors and the dynamics of volatility in cryptocurrencies for both academic and practical purposes.

To our knowledge, the existing literatures on the topics of volatility focus mainly on the dominant cryptocurrency, BTC. Thus, this research aims to provide a comprehensive analysis on the volatility modelling of a class of cryptocurrencies which covers a wider selection of cryptocurrencies preferred based on their market capitalisation to gain in-depth knowledge on the cryptocurrency market.

1.2 Problem statement

The massive growth of cryptocurrency market has offered an alternative opportunity to investors. However, investors are also exposed to excessive risks due to its price unpredictability whereby the price direction and market dynamics are complex to comprehend resulting in high volatility features. Given the complexity of cryptocurrency market, modelling and forecasting the volatility of cryptocurrencies are therefore essential to foster a better understanding on the volatility dynamics for the purpose of risk management practices. A comprehensive study on the volatility of cryptocurrency market is undeniably a necessity to provide an analytical review for financial practitioners in all aspects given its potential in future monetary and banking system.

1.3 Objectives

This research comprises four objectives as listed in the following:

- To provide evidence of the existence of change points in price, return and squared return series of cryptocurrencies.

- To develop two-regime time-varying transition probability Markov-switching GARCH (TV-MSGARCH) model incorporated with exogenous variables to estimate and forecast the volatility of cryptocurrencies.
- To compare the cryptocurrencies volatility estimation and forecasting performances of the TV-MSGARCH model with Markov-switching GARCH (MSGARCH) model and GARCH-type models, by evaluating their performances using various criteria.
- To derive the value-at-risk (VaR) of the TV-MSGARCH models.

1.4 Dissertation outline

The structure of the dissertation is organised as follows. Chapter 2 provides a comprehensive literature on the volatility modelling of cryptocurrencies and briefs through the background of Markov-switching model. Then, the factors driving the prices of cryptocurrencies are also discussed. Chapter 3 introduces the cryptocurrency data used in this research and the descriptive statistics of the respective cryptocurrencies are provided. In Chapter 4, multiple change point model is used to detect the existence of change points in the price, return and squared return series of cryptocurrencies. The introduction of GARCH-type models and its extensions to MSGARCH model and TV-MSGARCH model are provided in Chapter 5 together with different distributions for errors, namely normal, Student-t and generalised error. Then, the formulations of VaR for the proposed model and the existing models are derived and the VaR estimates evaluated using various tests are discussed. Chapter 6 discusses and compares the in-sample model fitting performances of the various volatility models based on different criteria. The contribution of time-varying transition probabilities in TV-MSGARCH model is assessed via the computation of weighted transition probabilities. Chapter 7 compares the forecasting performances of various volatility models based on quasi-likelihood (QLIKE) loss function and then tested using model confidence set (MCS) procedure. VaR forecasts are also calculated and tested using several backtests. Chapter 8 provides conclusion and remarks for this research and offers recommendations for future researches.

CHAPTER 2 : LITERATURE REVIEW

2.1 Introduction

One of the interesting aspects of cryptocurrency market is the unpredictability indicated by its dramatic price changes and the high underlying volatility. It is reported that the volatility of BTC is seven times higher than that of gold, eight times higher than Standard and Poor 500 (S&P 500) index and eighteen times greater than the U.S. dollar (Williams, 2014). The volatility of BTC is also known to be larger than a set of foreign currencies in the U.S. dollar (Dwyer, 2015). Particularly, Chaim and Laurini (2018) recorded two high volatility periods of BTC, from late 2013 to early 2014 and in December 2017.

Statistically speaking, volatility is referred to as the conditional standard deviation of returns. It is commonly used in the financial strategies to calculate the uncertainty of any financial decisions. To provide a deeper understanding on the nature of volatility in the returns of cryptocurrencies, Philip et al. (2018) considered a vast selection of 224 cryptocurrencies in their studies and provided evidence of cryptocurrencies exhibiting unique properties such as long memory, leverage and are heavy-tailed. Besides, cryptocurrencies also appear to display volatility clustering property in which the conditional volatilities are significantly affected by both past shocks and past conditional volatilities (Katsiampa, 2019). The author also found leverage effect between good and bad news in BTC, ETH, XRP and Litecoin (LTC). By leverage effect, it means that the volatility increases more after bad news than after good news. In fact, volatility clustering and leverage effect are commonly seen in financial series and the most popular systematic framework for such volatility modelling mostly work on the basis of autoregressive conditional heteroscedasticity (ARCH) model by Engle (1982) and the generalised autoregressive conditional heteroscedasticity (GARCH) model by Bollerslev (1986).

2.2 Cryptocurrencies modelling and applications

In the most recent studies, various GARCH-type models have been widely employed in different research topics on cryptocurrencies. For instance, asymmetric GARCH (AGARCH) model is used to explore the financial ability of BTC to be used for hedging (Dyhrberg, 2016) and fractionally integrated GARCH (FIGARCH) model is used to study the long-range memory property in seven BTC markets (Lahmiri et al., 2018). In the attempt to study the volatility dynamics of cryptocurrencies returns, Katsiampa (2017) fitted six GARCH-type models to BTC return series and discovered that the component GARCH (CGARCH) model gave the best optimal fit. Chu et al. (2017) extended the work by considering twelve GARCH-type models with different error distributions to the return series of seven cryptocurrencies including BTC, XRP and LTC. Their work suggested integrated GARCH (IGARCH) model incorporated with normal error distribution is the best fitted volatility model for BTC and LTC; whereas standard GARCH model incorporated with normal error distribution is the best fitted volatility model for XRP. Nevertheless, it is known that IGARCH model might be biasedly chosen as the best volatility model when the change points found in return series are not accounted for which may give rise to false impression on high persistency in the return series (Caporale et al., 2003; Mikosch & Starica, 2004).

Change points are detected when the probability distribution of a stochastic time process experiences changes and can also be referred to as the unexpected change in the parameters of a regression model. Failure to recognise change points can lead to huge forecasting errors and the unreliability of the model. The central issue of change point detection is to ensure the stability of model coefficients for the entire sample periods. Discussed by Bariviera et al. (2017), it is observed that BTC return series experiences great swings during the period of their study which they then concluded to be the reason behind the feature of large volatility in BTC. In particular, previous studies have found prominent statistical changes in cryptocurrencies which further give hint on the presence of change points in cryptocurrencies. For instance, Bouoiyour and Selmi (2016) found a pronounced volatility change at January 2015, the period when the volatility of BTC began to decline at a rapid pace. To overcome this statistical change, they separated BTC return series at January 2015 and fitted nine GARCH-type models to the two segmented returns. The best fitted models are the component with multiple threshold GARCH (CMTGARCH) model for prior 2015 return segment and the asymmetric power GARCH (APGARCH) model for post 2015 return segment. Bouri et al. (2017), on the other hand, found evidence of change points around December 2013 (during the BTC price crash), detected by using Bai and Perron (2003) method. They utilised AGARCH model to test the asymmetric effect of shocks on BTC volatility for the periods before the price crash and after the price crash. It was discovered that the BTC return series portrayed inverse asymmetric (safe heaven) property in the pre-crash period and showed asymmetric property in the post-crash period. To investigate the stability of the return and volatility of BTC, Thies & Mólnar (2018) applied Bayesian change point model and recorded forty-eight change points in BTC return series. Furthermore, Bouri et al. (2019a) studied the impact of change points in the stagnancy of BTC price level and its volatility of two markets, namely Bitstamp and Coindesk, by using logarithmic price series, squared return series and absolute return series. By adopting Bai and Perron (2003) method but restricted to a maximum of five change points only, the authors reported four and five change points respectively in Bitstamp and Coindesk markets. In addition, Katsiampa (2019) also found that change points are present in the conditional volatility of BTC and LTC. Regardless, the complex underlying dynamics of cryptocurrencies due to its fast-changing and speculative nature are the motivations of this dissertation.

2.3 Markov-switching volatility models

It is well-known that traditional return-based models are prone to demonstrate high persistency in the conditional volatility (Hamilton & Susmel, 1994; Gray, 1996) which may indicate biasness if the series displays structural break (Bauwens et al., 2014b). Mensi et al. (2019) highlighted that the presence of change points in the mean and variance of BTC series can result in persistence overestimation if the change points are not accounted for. With that, Markov-switching models are suggested instead. Pioneered by Hamilton & Susmel (1994), Markov-switching GARCH (MSGARCH) model is ideally reported to be capable of accounting for the high persistency and poor forecasting performance problem when traditional single-regime GARCH-type models are employed. For instance, Ardia et al. (2019) showed that two-regime MSGARCH model outperforms single-regime GARCH model and single-regime Glosten-Jagannathan-Runkle GARCH (GJRGARCH) model in both in-sample and out-of-sample BTC volatility modelling. Caporale & Zekokh (2019) offered a similar conclusion such that the two-regime MSGARCH models provide better volatility forecasting estimates than those single-regime GARCH models for BTC, ETH, XRP and LTC. Nevertheless, it is worth noting that the extensive discussions of these results are focused mainly on the application of constant transition probability for the entire period. The plausibility of the transition probabilities that can be time-varying over time is not addressed and is still lacking in the previous literature.

The switch of conditional volatility between states or regimes for MSGARCH model is governed by transition probabilities which remain constant for all time t. Noteworthy, financial time series often undergoes series of alternating calm and turbulent periods. Diebold et al. (1994) and Filardo (1994) noted that the constant transition probability is too restrictive for some empirical settings which may not be appropriate to capture complex statistical features and suggested the use of time-varying transition probability

(TVTP) alternatively. The transition probability may evolve as either a logistic function or a probit function of a series of exogenous variables or lagged dependent variables which are time-varying. The use of time-varying transition probability MSGARCH (TV-MSGARCH) model is found to be capable of providing a better fit compared to MSGARCH model (Bazzi et al., 2017). In this respect, we are keen to answer the research question of whether by incorporating the drivers of cryptocurrencies price dynamics as the exogenous variables in TV-MSGARCH model would help to increase the model flexibility in explaining the volatility of cryptocurrencies.

2.4 Determinants of cryptocurrencies prices

Empirical studies have been put forward in an attempt to determine the drivers of cryptocurrencies price dynamics. The identified factors affecting BTC prices include fundamentals such as supply and demand of BTC; and speculation (Ciaian et al., 2016). The utility of BTC in trades and exchange activities contributes to the holdings of BTC resulting in its price appreciation in the long term (Bouoiyour & Selmi, 2015). Baek and Elbeck (2015) discovered the volatility of BTC is driven mainly by its buyers and sellers rather than by the fundamental economic factors. But without institutional support and backing, the fundamental value of BTC is simply zero (Cheah & Fry, 2015). Investor's attention is the direct contribution to the price dynamics of most financial assets and Google searches series, which are obtained directly from Google Trends, are reported to be the optimal indicator to measure such attention (Da et al., 2011). Discovered by Andrei and Hasler (2015), the volatility of returns and risk premium are directly related to investor's attention proxied by Google searches series. BTC price dynamics also appear to be particularly susceptible to the market sentiments, volume of transactions and public interests measured by the number of searches for "Bitcoin" from Google Trends (Kristoufek, 2015; Parino et al., 2018). Urquhart (2018) who utilised Google Trends as the proxy for BTC attention, realised that previous day volatility and trading volume are the significant drivers that attract investors to BTC. A similar conclusion was also drawn by Aalborg et al. (2019). The authors discovered that the trading volume can improve the volatility model for BTC when the trading volume is predicted from Google Trends. Additionally, Bouri et al. (2019b) studied the impact of trading volume to the returns and volatility of seven cryptocurrencies including BTC, ETH, XRP and LTC. Their work showed that trading volume has predictive power on the returns of cryptocurrencies at extreme events while trading volume can only be used to forecast volatility on selected cryptocurrencies when the volatility is low. Besides, Katsiampa (2019) noticed that cryptocurrencies volatility dynamics are responsive to major news. More specifically, Corbet et al. (2019) and Panagiotidis et al. (2019) provided a more comprehensive and systematic review of the cryptocurrency market on major academic research.

CHAPTER 3 : DATA SETS

This chapter discusses the data used in this research, starting with the introduction of cryptocurrency indices and the top five cryptocurrencies ranked according to market capitalisation. This chapter also discusses the cryptocurrencies trading volume data and Google searches series data. The trading volume and Google searches series are found to be the exogenous variables that can impact the cryptocurrency series.

3.1 Cryptocurrency indices

Financial market indices are often used as the tool or indicator to provide an insight to a specified market segment. Indices conventionally comprise a hypothetical constituent of securities that represents a particular market. With the increasing interest in cryptocurrency market, cryptocurrency indices are proposed to act as a benchmark index designed to monitor the overall market performance. In this respect, the following subsections introduce two types of cryptocurrency indices: Cryptocurrency Index (CRIX) and Cryptocurrency Index 30 (CCI30).

3.1.1 Cryptocurrency Index

Cryptocurrency Index (CRIX) was introduced by Trimborn and Härdle (2016). The number of constituents in the index are chosen in steps of five based on a lengthy time-varying selection method that relies on Akaike information criteria (AIC). The base number for CRIX is 1000 and the index is rebalanced every month and reconstituted every quarter. CRIX data which spans from 8 August 2014 to 30 April 2018, are retrieved from the official website on daily basis, http://crix.hu-berlin.de, resulting in 1362 observations.

3.1.2 Cryptocurrency Index 30

Cryptocurrency Index 30 (CCI30) was proposed by Rivin and Scevola (2018). Unlike CRIX, the constituents of CCI30 are always chosen to be the first 30 cryptocurrencies ranked according to the market capitalisation. The base number for CCI30 is 100 and similarly, the index is rebalanced every month and reconstituted every quarter. CCI30 data which starts from 9 January 2015 to 30 April 2018, are retrieved from the official website on daily basis, https://cci30.com, resulting in 1208 observations.

3.2 Top five cryptocurrencies

The top five cryptocurrencies are BTC, ETH, XRP, BCH and EOS ranked according to market capitalisation as at 30 April 2018 and contributed to a combined market share of 69.56% at the time. The historical data are retrieved from the most popular site for cryptocurrency information, CoinMarketCap (www.coinmarketcap.com). There are three financial time series used in this research, namely price series, return series (obtained by taking the difference of two consecutive log prices) and squared return series (computed by taking the square of return series). All data starts from the first day of availability and ends on 30 April 2018 as described in Table 3.1.

Table 3.1: Data counts for the cryptocurrency indices and cryptocurrencies.

Cryptocurrencies	Data starts from	Counts
CRIX	8/8/2014	1362
CCI30	9/1/2015	1209
BTC	1/8/2010	2830
ETH	13/8/2015	992
XRP	28/1/2015	1190
BCH	7/8/2017	267
EOS	5/7/2017	300

The daily returns summary statistics of the cryptocurrency indices and the top five cryptocurrencies are provided in Table 3.2. Noteworthy, CRIX and CCI30 display distinctive characteristic in the sense that CRIX shows positive skewness while CCI30 shows negative skewness. Besides, as indicated by the mean and median of the cryptocurrencies, it is discovered that cryptocurrencies will earn below its expected return more than 50% of the time, except CCI30. On average, the expected gain in EOS is the highest among all, followed by ETH and BCH. The turbulent behaviour of cryptocurrency market can also be examined from Table 3.2. For instance, BTC and XRP both show lucrative profit in which the highest return recorded in a single day is 147.44% and 102.80% respectively. However, the promising profits are also accompanied by severe potential losses such that the lowest return recorded in a single day for BTC and XRP is -84.88% and -99.73% respectively. Finally, all of the cryptocurrencies display features such as leptokurtic distribution with kurtosis higher than normal distribution and are positively-skewed.

Table 3.2: Summary statistics of daily returns of the cryptocurrency indices and cryptocurrencies.

Cryptocurrencies	Min	1st Q	Median	Mean	3rd Q	Max	Kurtosis	Skewness
CRIX	-0.1985	-0.0180	-0.0028	-0.0025	0.0101	0.2533	9.7044	0.7340
CCI30	-0.2643	-0.0103	0.0041	0.0039	0.0212	0.1783	8.8504	-0.7631
BTC	-0.8488	-0.0133	0.0020	0.0042	0.0230	1.4744	96.9268	3.0230
ETH	-0.3101	-0.0283	0.0000	0.0059	0.0372	0.3830	6.2779	0.1070
XRP	-0.9973	-0.0342	-0.0130	0.0033	0.0279	1.0280	22.5110	0.7420
BCH	-0.3068	-0.0518	-0.0082	0.0053	0.0521	0.4379	6.5221	0.8634
EOS	-0.3521	-0.0489	-0.0053	0.0063	0.0528	0.3598	4.9056	0.3915

Note: Min refers to the minimum of returns, 1st Q refers to the first quantile of returns, 3rd Q refers to the third quantile of returns and Max refers to the maximum of returns.

For illustration purpose, Figures 3.1 to 3.7 present the price, return and squared return series of the two cryptocurrency indices and the top five cryptocurrencies. The vertical dotted lines represent the location of the estimated change points while the red line is the fitted line estimated using Eq. (4.2) in the presence of change points which will be further discussed in Chapter 4.

The large fluctuation of cryptocurrency market can be observed by the strikingly sharp increment in price since year 2017, which was then quickly followed by an abrupt depreciation in year 2018 demonstrated by both CRIX and CCI30 indices and the other cryptocurrencies. Correspondingly, spikes are also noticed in return series and squared return series indicating a high volatility level for the cryptocurrency market.

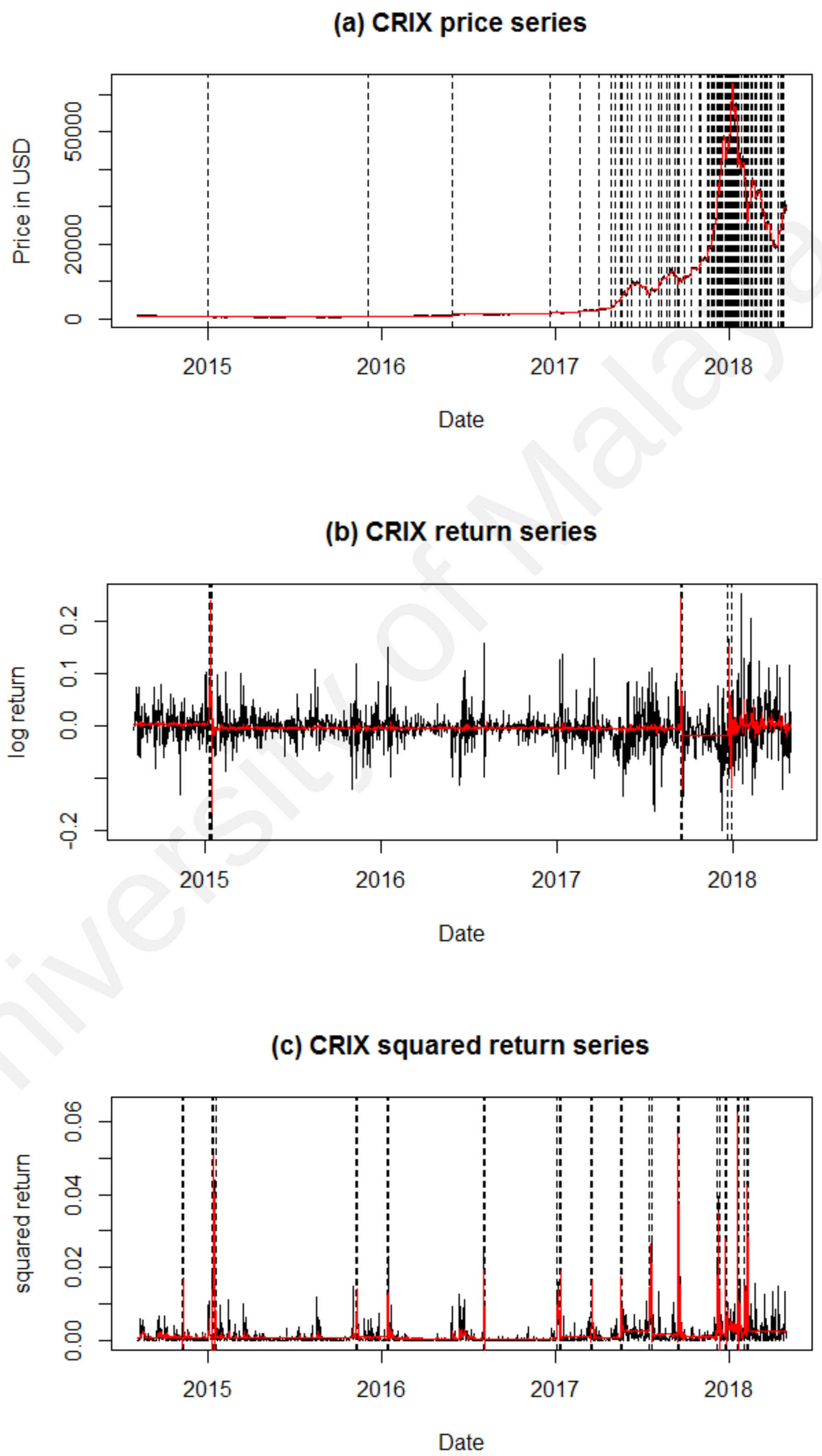

Figure 3.1: (a) CRIX price series, (b) CRIX return series and (c) CRIX squared return series.

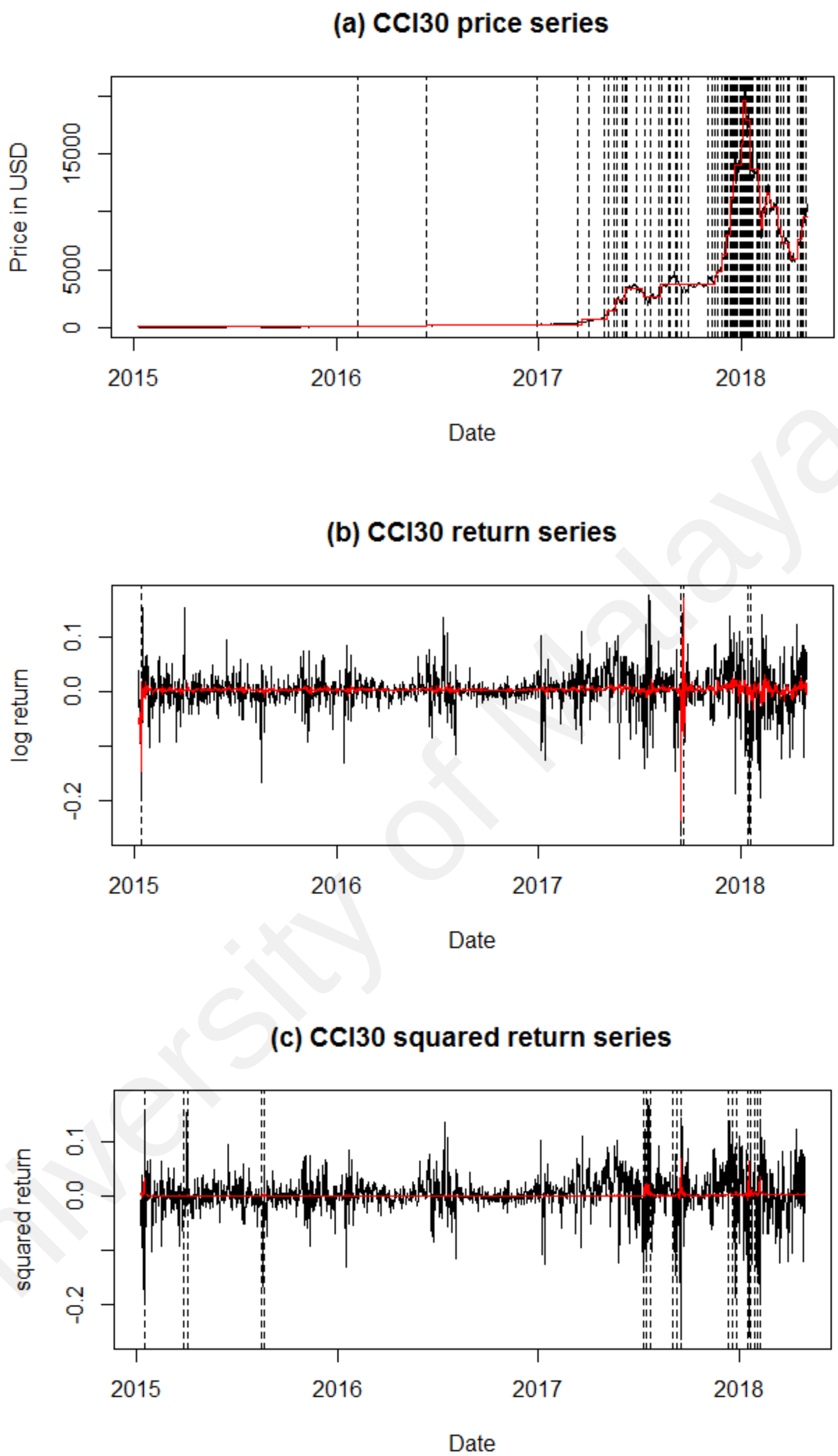

Figure 3.2: (a) CCI30 price series, (b) CCI30 return series and (c) CCI30 squared return series.

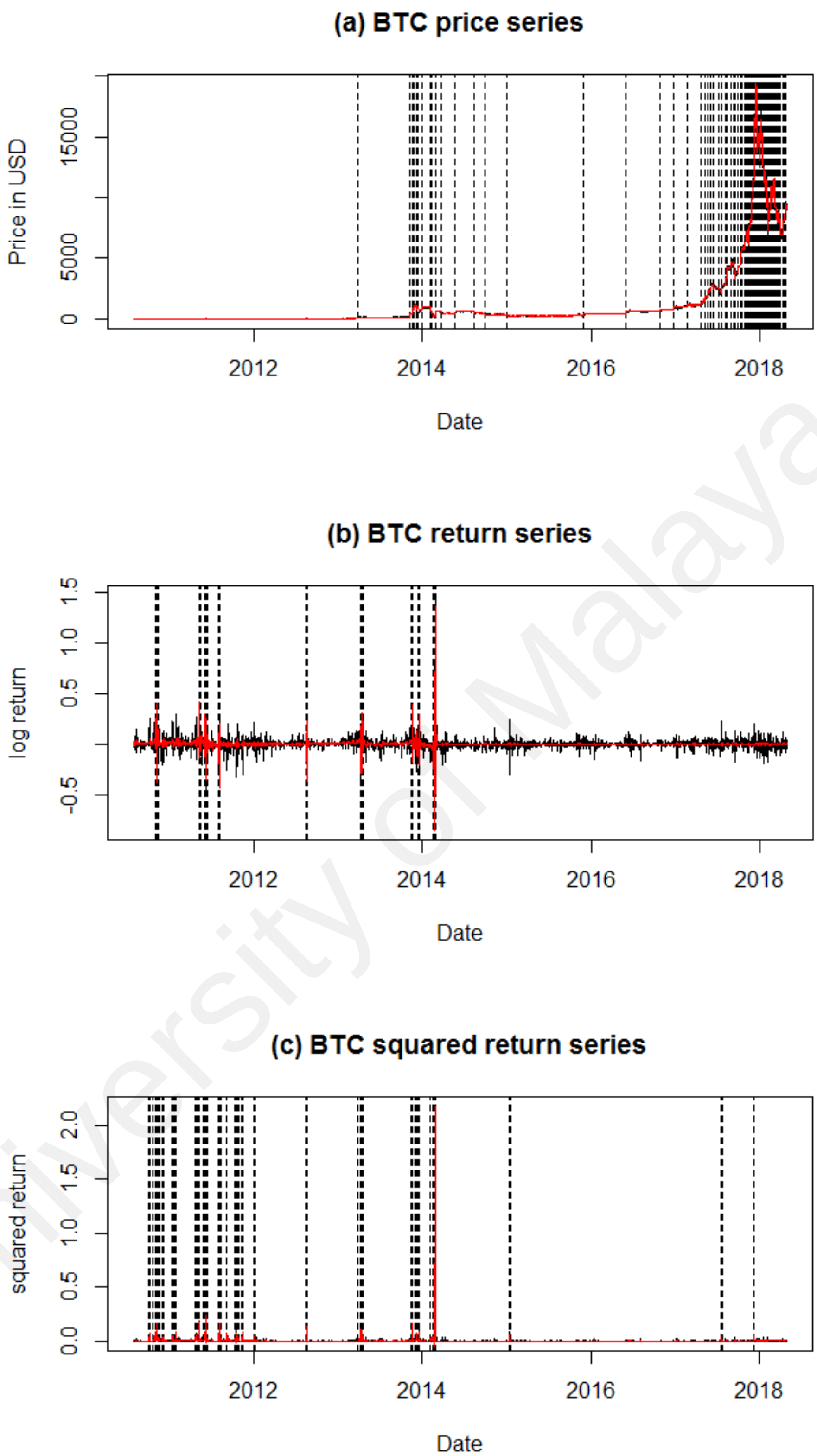

Figure 3.3: (a) BTC price series, (b) BTC return series and (c) BTC squared return series.

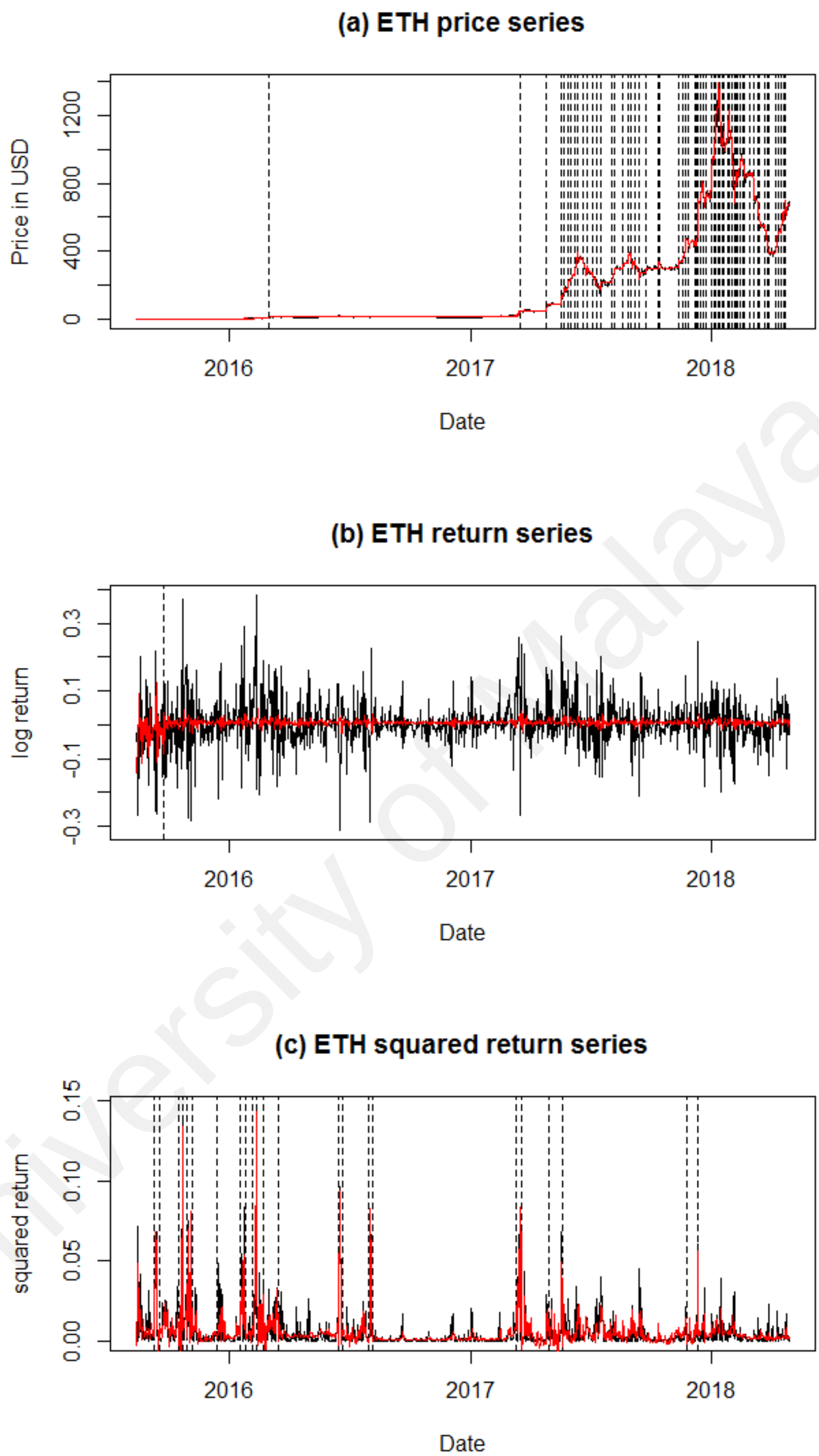

Figure 3.4: (a) ETH price series, (b) ETH return series and (c) ETH squared return series.

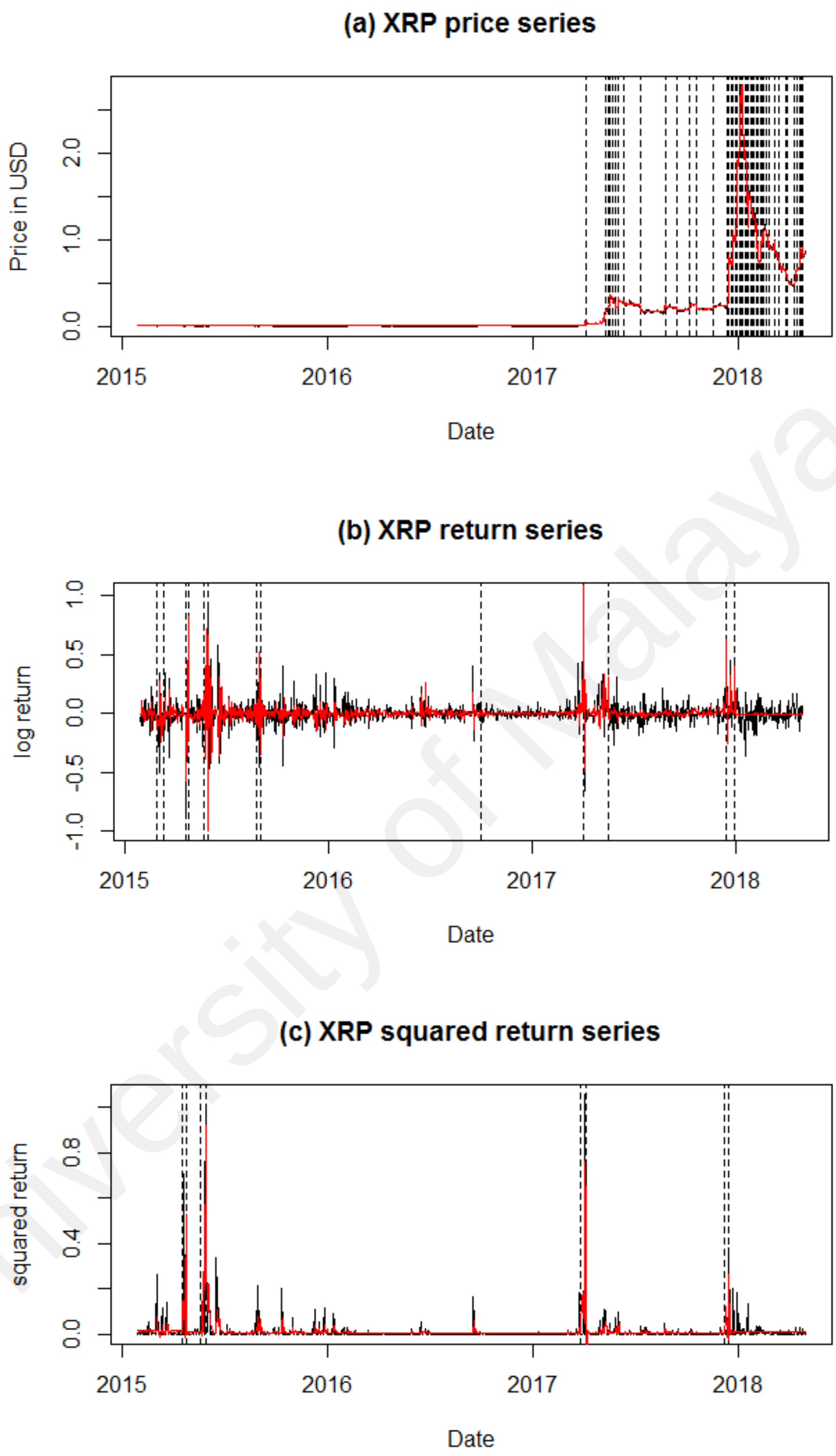

Figure 3.5: (a) XRP price series, (b) XRP return series and (c) XRP squared return series.

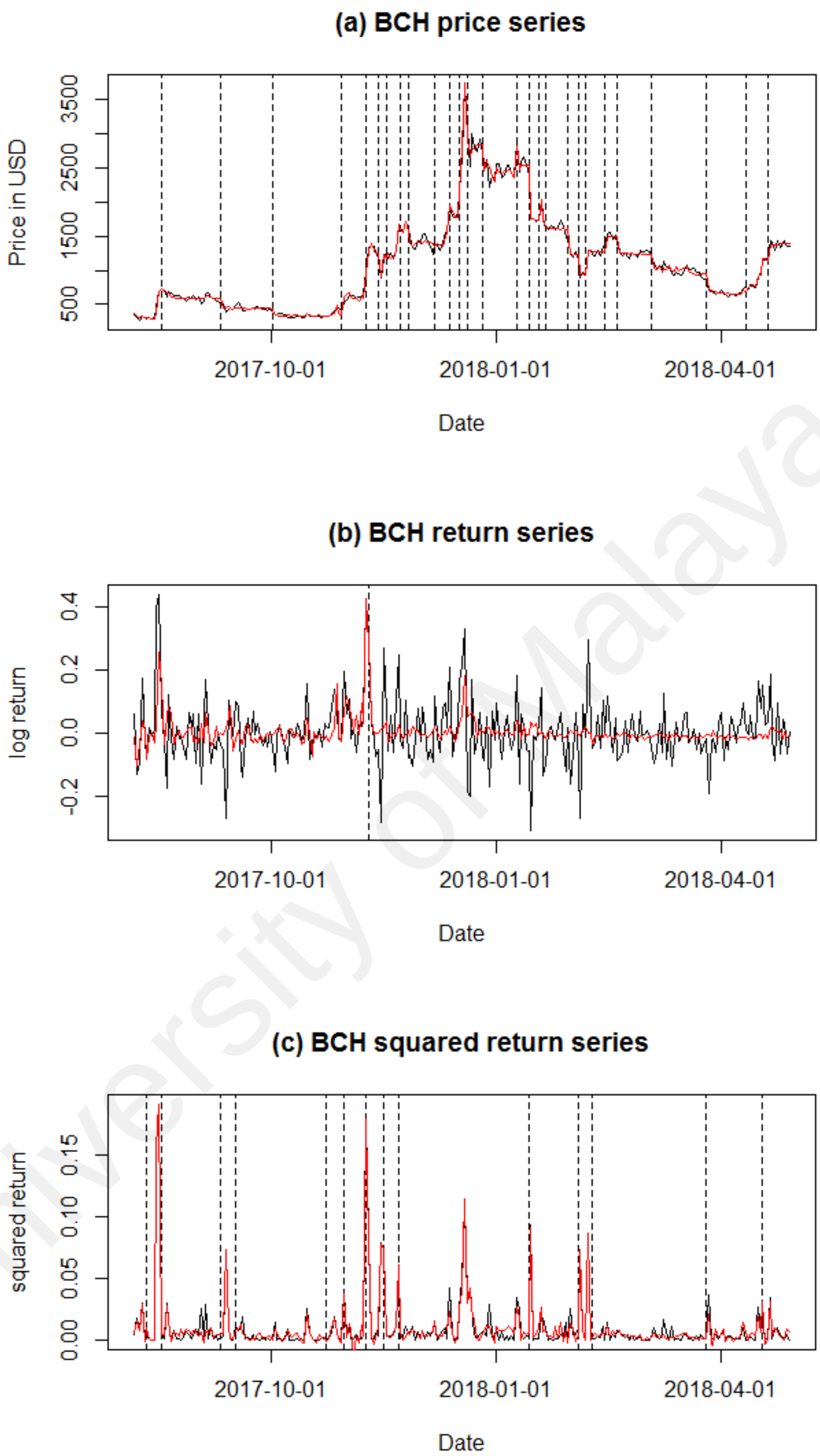

Figure 3.6: (a) BCH price series, (b) BCH return series and (c) BCH squared return series.

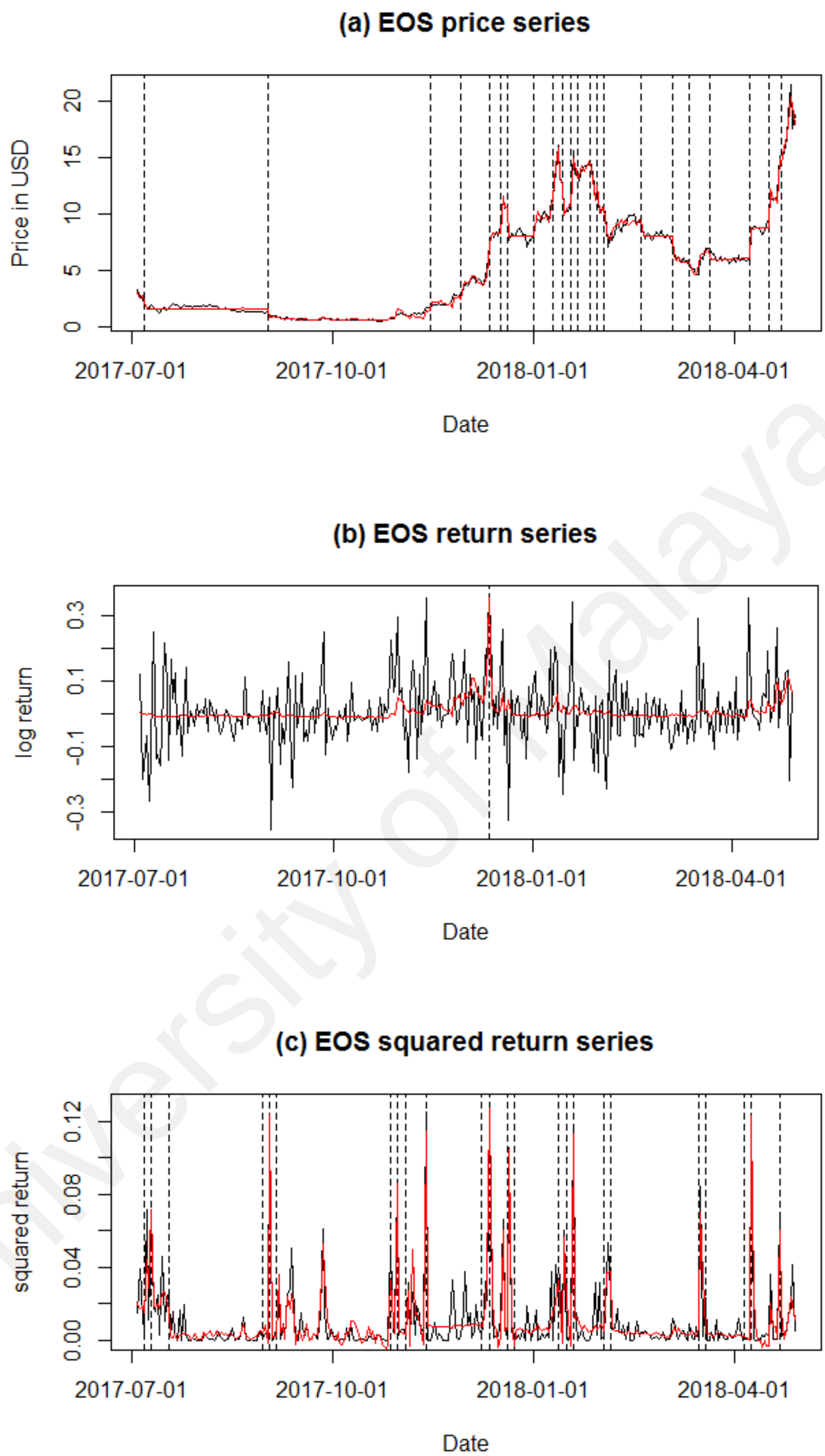

Figure 3.7: (a) EOS price series, (b) EOS return series and (c) EOS squared return series.

3.3 Trading volume

Existing literatures tend to relate the feature of high volatility of cryptocurrencies to their trading volume. Trading volume is the total number of cryptocurrencies traded over a specified period measured in terms of the current prices in U.S. dollar. An increase in the trading volume implies an increase of interest level in the cryptocurrencies, which may be influenced by either good or bad news. Bouri et al. (2019b) provided evidence such that the cryptocurrency trading volume contains useful information to predict returns but only on extreme market conditions. Our results in Chapter 4 also show that trading volume can be used to explain the dynamic of the price series, return series and squared return series of cryptocurrencies. With that, trading volume is incorporated as one of the exogenous variables for TV-MSGARCH model used in Eq. (5.13) in Chapter 5, to determine whether the trading volume can help to increase the flexibility of the traditional volatility models and thus, can better explain the volatility of cryptocurrencies.

The daily data of cryptocurrencies trading volume are collected from the same source where prices are retrieved, CoinMarketCap (www.coinmarketcap.com). The raw data of trading volume exhibits explosive exponential behaviour which might not be appropriate to be directly used in the modelling and forecasting application. Instead, natural logarithmic transformation is applied to the raw data of trading volume. Figures 3.8 to 3.12 illustrate the trading volume and log trading volume for the top five cryptocurrencies.

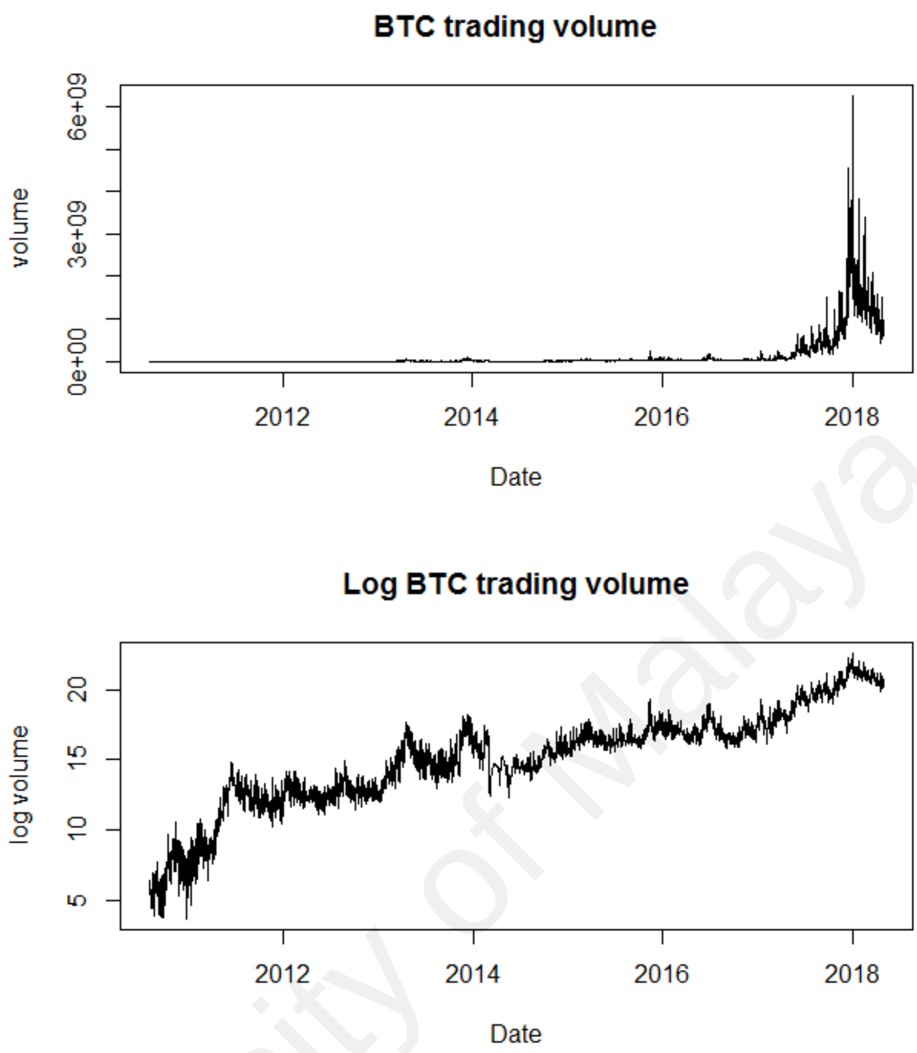

Figure 3.8: BTC trading volume and log BTC trading volume.

As shown in Figure 3.8, there was a prominent spike in BTC trading volume recorded at the turning of year 2017/2018. After the peak, there were another two peaks happened at January 2018 and February 2018. However, the trading volume of BTC appeared to be in a downtrend since year 2018. This might imply the investors started to reduce their holdings and lost their attention on BTC. Nevertheless, log BTC trading volume appeared to be in an upward trend.

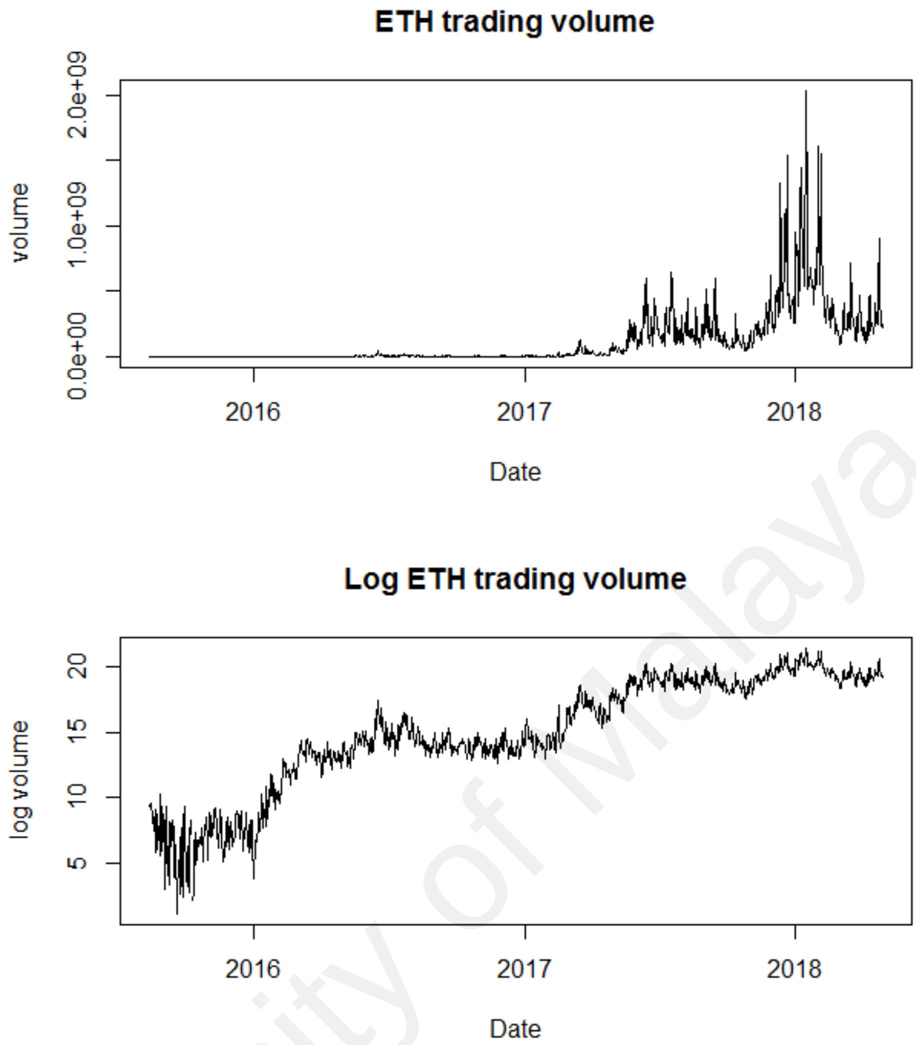

Figure 3.9: ETH trading volume and log ETH trading volume.

As shown in Figure 3.9, there were few spikes in ETH trading volume recorded in late 2017. The most prominent spike of ETH trading volume only occurred in year 2018. The trading volume of ETH marked a significant drop since the beginning of year 2018 which recovered slowly with a slight increasing trend thereafter. Nevertheless, log ETH trading volume remained in an upward trend at the time of research.

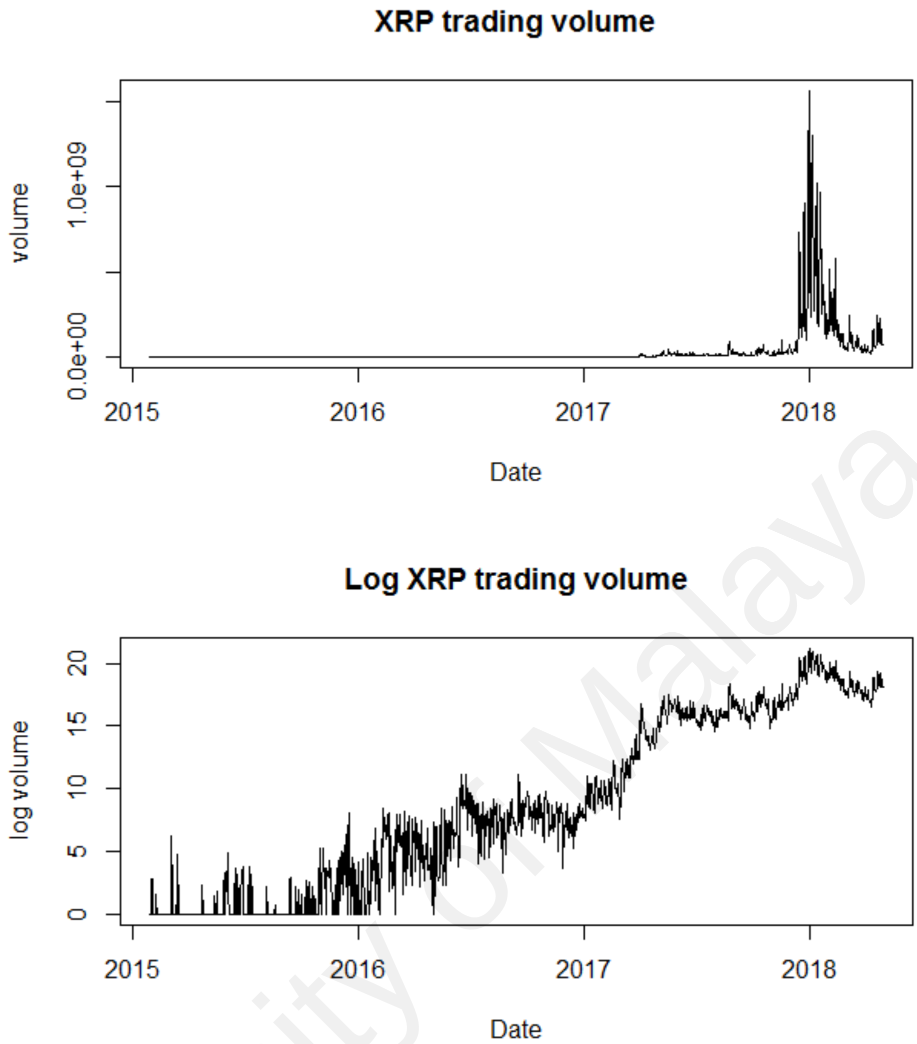

Figure 3.10: XRP trading volume and log XRP trading volume.

Figure 3.10 shows that the trading volume of XRP increased tremendously in the late of year 2017. The trading volume before the fourth quarter of year 2017 was minimal compared to the trading volume recorded after year 2018. Likewise, XRP trading volume started to reduce tremendously in year 2018 after the few prominent spikes recorded in the early of year 2018 while the log XRP trading volume displayed an increasing trend.

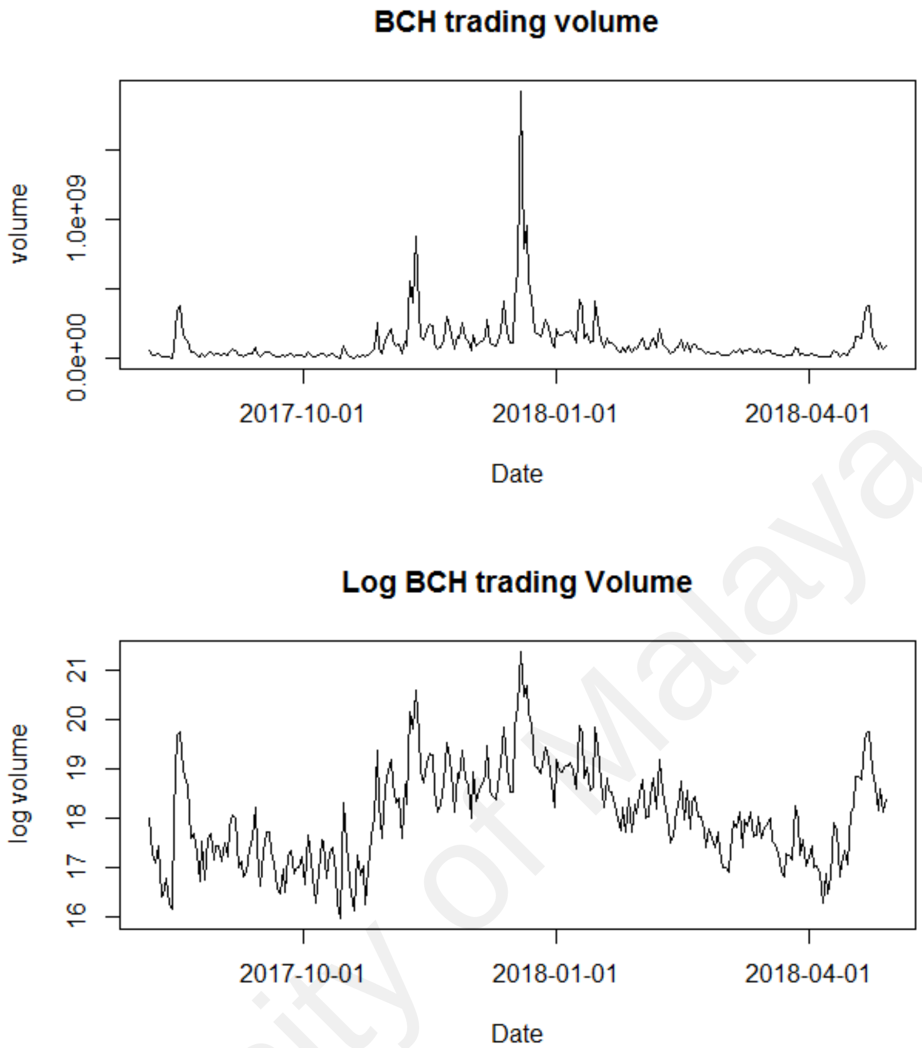

Figure 3.11: BCH trading volume and log BCH trading volume.

Figure 3.11 shows that the trading volume of BCH recorded the greatest spike at the end of year 2017 which however declined rapidly afterwards. The log trading volume of BCH was in a downward trend since the beginning of year 2018, which then started to recover since April 2018.

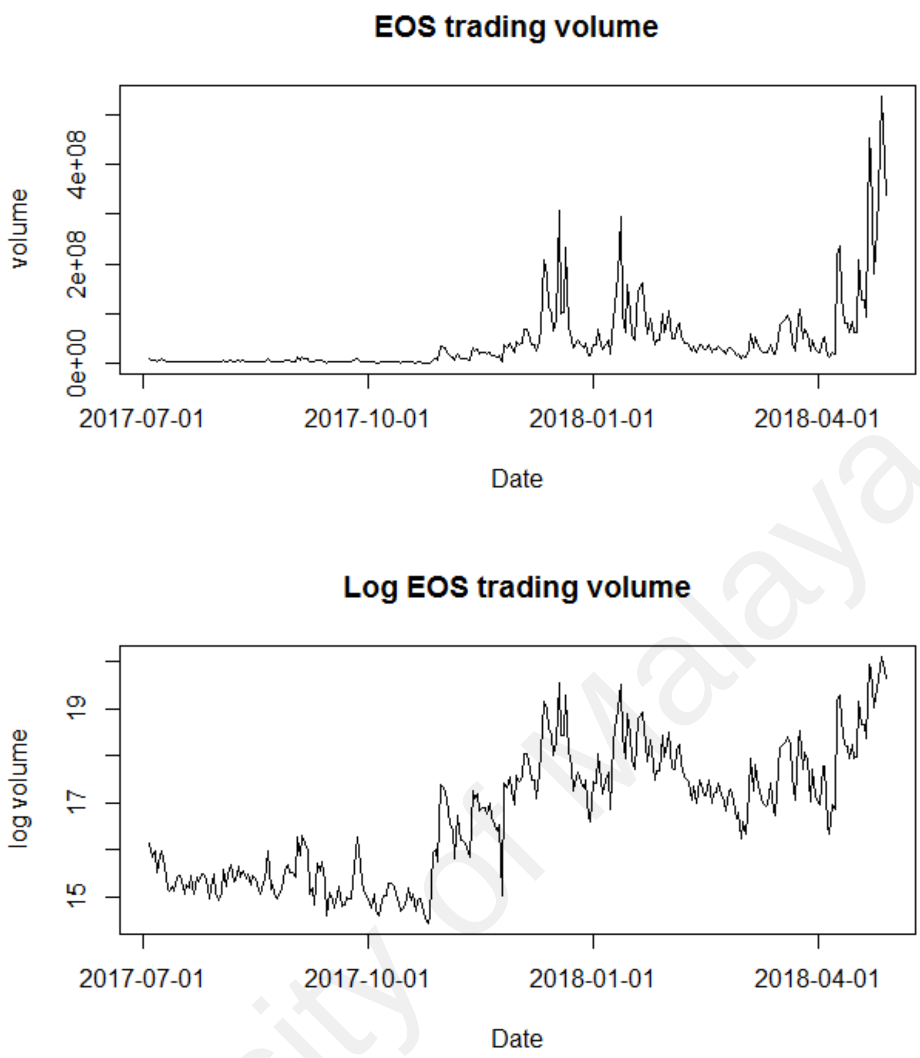

Figure 3.12: EOS trading volume and log EOS trading volume.

Figure 3.12 depicts the trading volume and log EOS trading volume. There were some frequent spikes in EOS trading volume observed since late year 2017, which were then accompanied by a short period of decrement at the beginning of year 2018. Nevertheless, the EOS trading volume started to increase tremendously since April 2018. The log EOS trading volume also appeared to be in an upward trend.

3.4 Google searches series

Google searches series measures the number of daily searches for a particular keyword on a worldwide basis obtained from Google Trends (https://trends.google.com). Existing literatures show close relationship of Google searches with the price dynamics of cryptocurrencies especially during episodes of explosive prices where the surge in the interest of cryptocurrencies drives the prices up while the rapid decline in public interest on cryptocurrencies pushes the prices down (Garcia et al., 2014; Kristoufek, 2015). Table 3.3 outlines the keywords used to extract Google searches series for various cryptocurrencies.

Table 3.3: Keywords used to extract Google searches series for various cryptocurrencies.

Cryptocurrencies	Keywords
BTC	Bitcoin
ETH	Ethereum
XRP	Ripple cryptocurrency
BCH	Bitcoin Cash
EOS	EOS cryptocurrency

Google Trends in nature does not provide the actual total number of searches. Instead, relative search interests within a certain time frame are provided. The scores for the relative interests are set to be in between 0 to 100. The highest search is scored at 100 and the searches of the other days within the time frame are then scored relatively. Google Trends has the limitation of 90 days for daily relative search interests. To obtain a longer period of data, we consider the technique proposed by Risteski and Davcev (2014). Firstly, both the relative monthly daily and daily search interests are downloaded over the whole sampled period. Then, the respective monthly adjustment factor is computed by dividing the monthly daily captured date value with the corresponding daily captured date value. Each of the monthly adjustment factors is then multiplied with the respective original daily search interests' values to obtain the adjusted daily Google searches series over the entire sampled period.

However, it is noticed that only those periods at the turning of year 2017/2018 show significant scores and if no adjustments are made, the impact of searches on the transition probabilities in TV-MSGARCH model (see Eq. (5.13)) may be biased to that particular periods. Hence, we would also want to consider the log difference of two consecutive Google searches that indicates the daily change of public interests in the cryptocurrencies. Figures 3.13 to 3.17 illustrate Google searches series and log difference of Google searches series for the top five cryptocurrencies.

Interestingly, figures of Google searches series for the top five cryptocurrencies resemble the figures of trading volume (Figures 3.8 to 3.12). The trends of Google searches series and the trends of trading volume are alike. Since trading volume and Google searches series can both reflect the demand on cryptocurrencies, the resemblance between the two data is expected. In fact, it is revealed that trading volume can also be predicted from Google Trends (Aalborg et al., 2019).

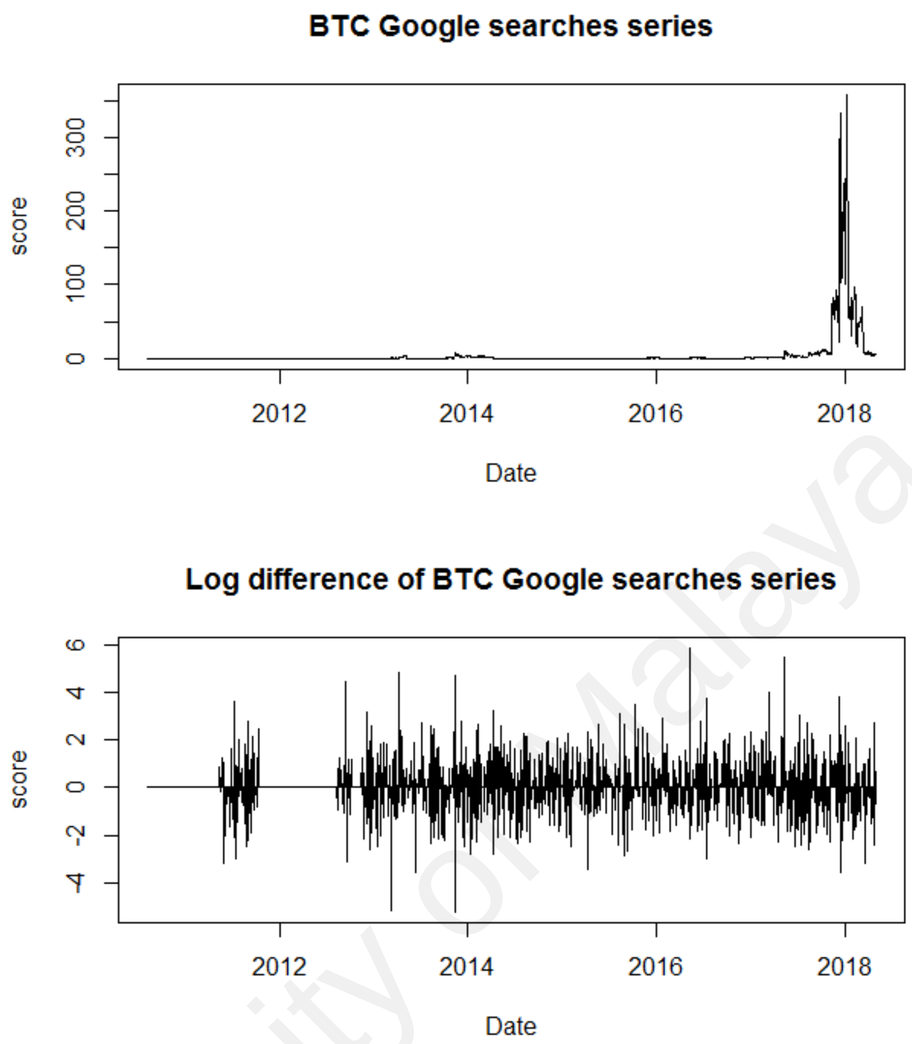

Figure 3.13: BTC Google searches series and log difference of BTC Google searches series.

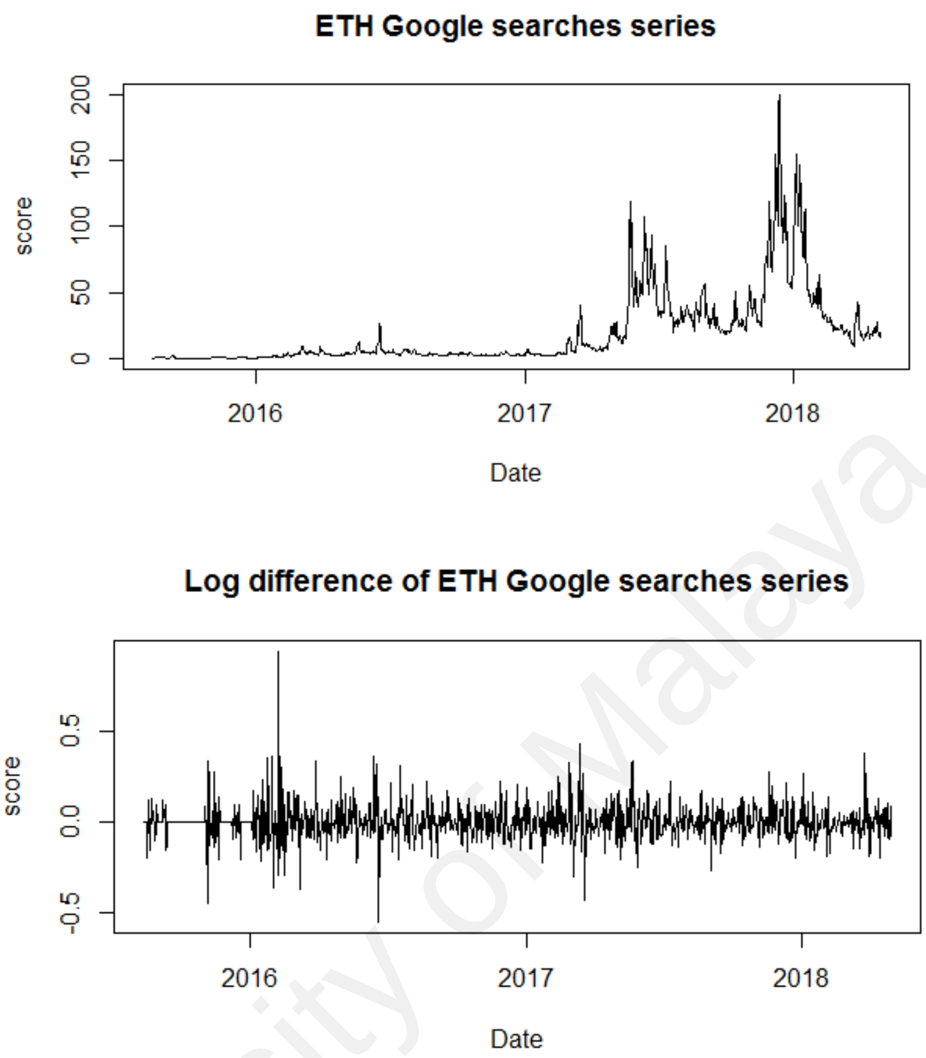

Figure 3.14: ETH Google searches series and log difference of ETH Google searches series.

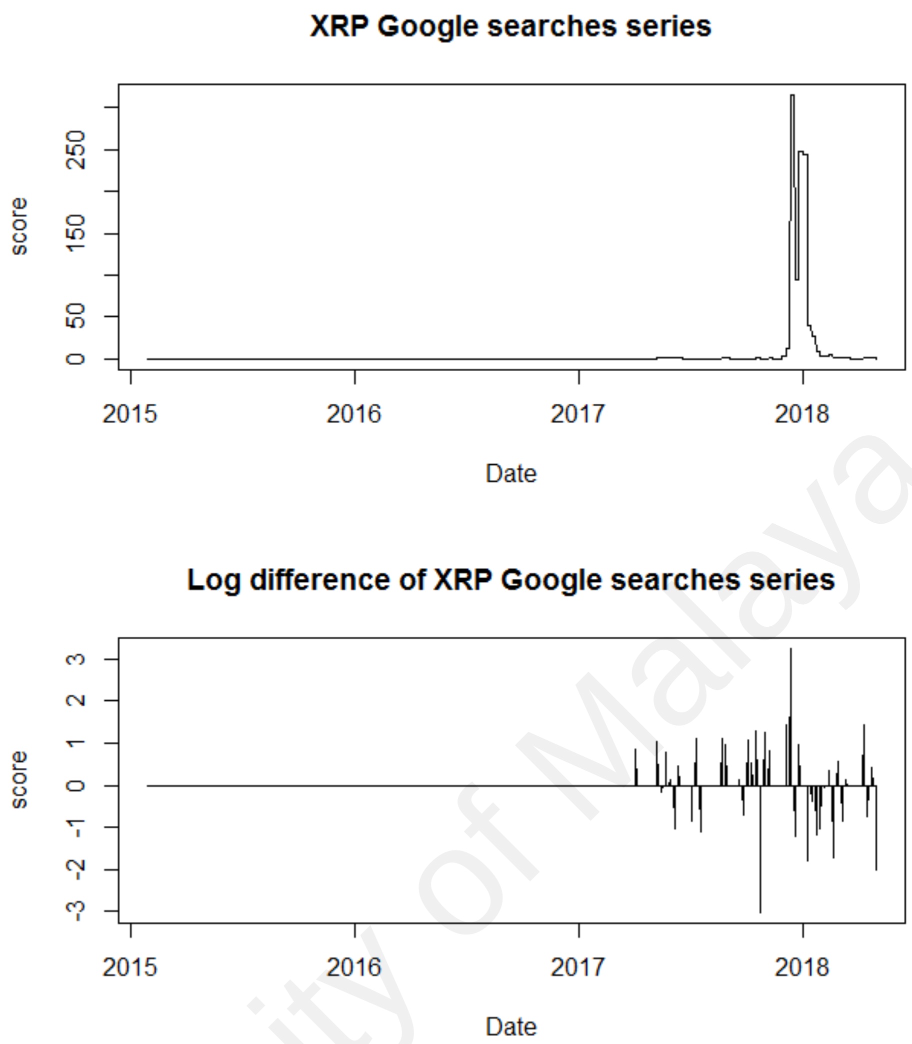

Figure 3.15: XRP Google searches series and log difference of XRP Google searches series.

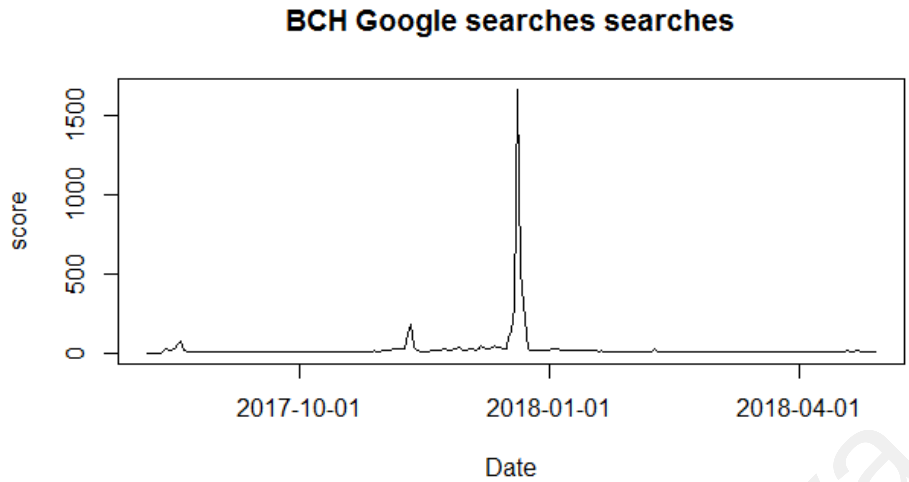

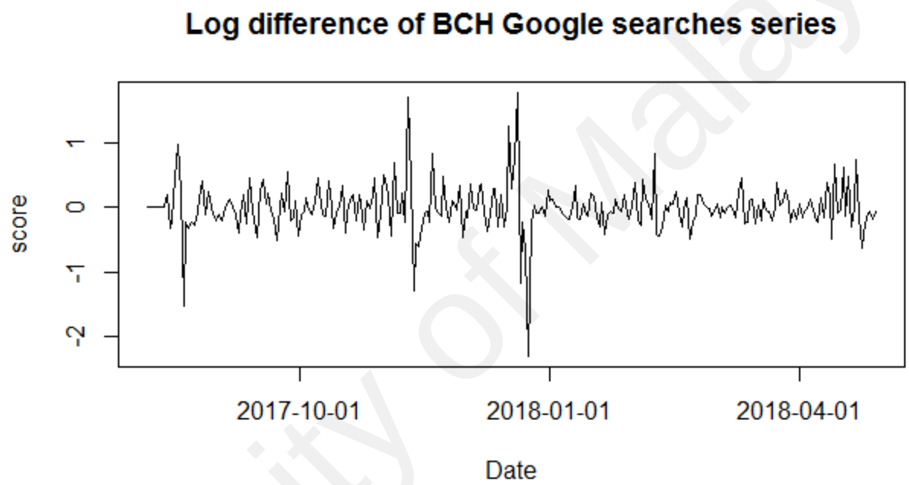

Figure 3.16: BCH Google searches series and log difference of BCH Google searches series.

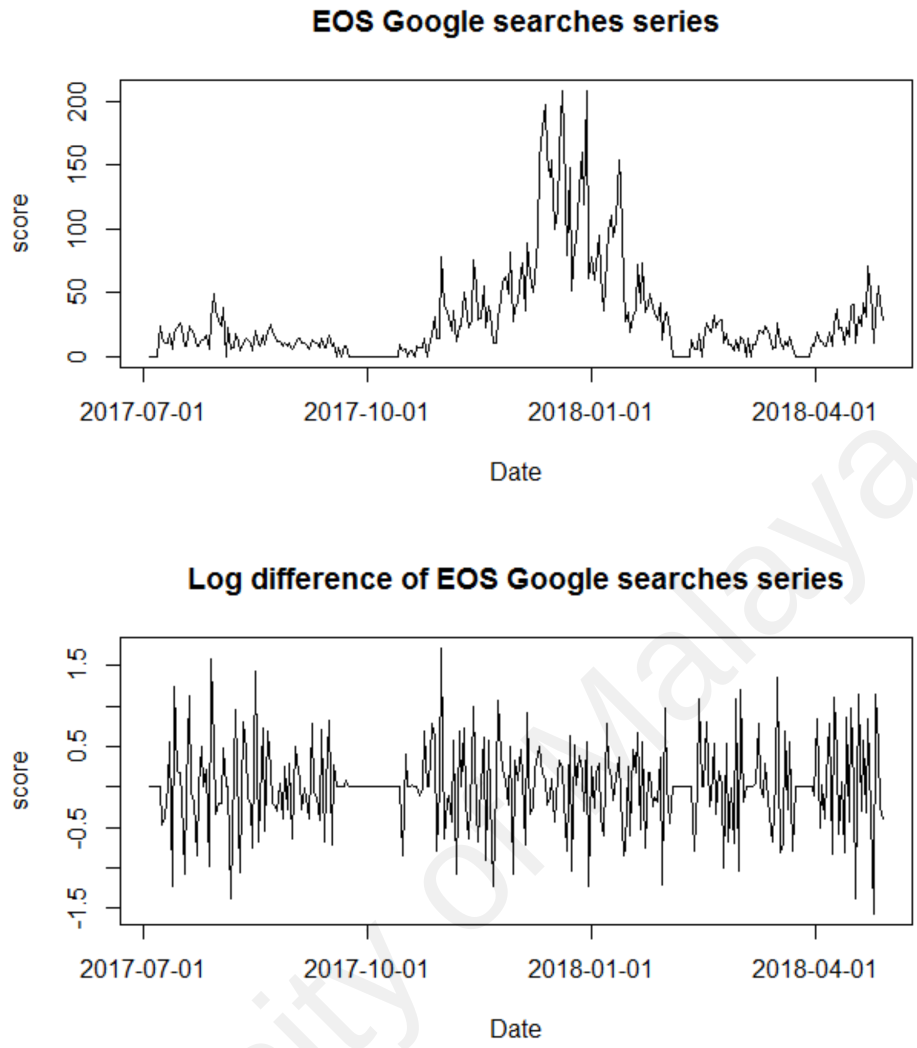

Figure 3.17: EOS Google searches series and log difference of EOS Google searches series.

CHAPTER 4 : CRYPTOCURRENCIES CHANGE POINT ESTIMATION

Change point statistically refers to the unexpected change in the parameters of a regression model whereby the instability of the coefficients over time may lead to huge forecasting error if not taken care of. With the prominent jumps and sudden shifts in cryptocurrency series, it is of the upmost interest to determine whether change points are present in cryptocurrency data. To provide an overall insight and to regard the entire cryptocurrency market as a whole, cryptocurrency indices such as CRIX and CCI30 are employed in this chapter. Cryptocurrency indices are designed specifically to act as a benchmark index for the entire market. To understand whether cryptocurrency indices are capable of representing the entire market, we decided to also include a larger market share of cryptocurrencies, comprising not only the top five cryptocurrencies (discussed in Chapter 3), but also the sixth until the tenth cryptocurrencies ranked according to market capitalisation, which are Cardano (ADA), LTC, Stellar (XLM), IOTA and Tron (TRX). With that, the top ten cryptocurrencies altogether contribute to 79% of the total market capitalisation as at 30 April 2018.

4.1 Exogenous variables impacting cryptocurrency series

Multiple change point model by Bai and Perron (2003) is applied to estimate the number and location of change points in price, return and squared return series of the two cryptocurrency indices and the top ten cryptocurrencies by incorporating the significant autoregressive variables and exogenous variable to the model. The autoregressive variables are the lagged values of the respective return series and squared return series whereas the exogenous variable refers to the trading volume.

To test the significance of these variables, we commence by fitting the three time series data, namely price, return, and squared return under different levels (constants), trading volume and autoregressive variables. We use levels (constants), trading volume and autoregressive variables to study which variables can explain the return series and squared return series of cryptocurrencies while for the case of price series, autoregressive variables are not considered as price series is statistically assumed to follow a random walk and are highly correlated. Table 4.1 provides the parameter estimates on various series and cryptocurrencies with values in parentheses are the standard errors of parameter estimates.

As shown in Table 4.1, it is perceived that trading volume has predictive power on cryptocurrencies price series as the coefficients of trading volume are significant. From practical perspective, trading volume reflects the demands and interest level from public and investors. According to Aalborg et al. (2019), the trading volume of BTC can be predicted from the Google searches on the term "Bitcoin" which is also the proxy of the public interest on BTC. Our results in Table 4.1 show that all of the cryptocurrencies have positive correlation between price series and trading volume.

For return series, it is discovered that trading volume has significant impact on the returns of XRP, BCH, EOS, ADA, LTC and XLM. Noteworthy, BTC return series is not affected by trading volume. This result can be further explained by the study of Balcilar et al. (2017). They concluded that the trading volume can be used to predict returns only when the market is fluctuating around the median but not viable during the periods when the market experiences extreme conditions. Besides, it is noticed that the lagged returns have different impact on the return series of cryptocurrencies. Take BTC for example, lag 1, lag 4 and lag 5 returns have positive impact on the current return while lag 2 return shows negative impact on the current return. Another example is demonstrated by ETH whereby the current return is negatively correlated with the past-day return but positively correlated with lag 3 return. Nevertheless, EOS, XLM and IOTA return series does not depend on their respective lagged returns.

Volatility wise, findings in Table 4.1 suggest that trading volume has positive impact on the squared return series for ETH, BCH, EOS, ADA, LTC, XLM and IOTA but not for BTC, XRP and TRX which is in line with the study by Balcilar et al. (2017), who showed that trading volume cannot be used to predict the volatility of BTC. Moreover, volatility is found to be correlated with past volatility. BTC volatility is significantly correlated to lag 2, lag 4 and lag 6 volatility. For the case of ETH, XRP, BCH, LTC and XLM, the relationship between today's and previous day's volatility is positive while ADA shows negative relationship between today's and previous day's volatility. On the other hand, EOS and IOTA volatilities are not affected by the lagged values.

Table 4.1: Parameter estimates on various series and cryptocurrencies with values in parentheses are the standard errors of parameter estimates.

	CRIX	CCI30	BTC	ETH	XRP	BCH	EOS	ADA	LTC	XLM	IOTA	TRX
	Price Series											
θ	0.0015	0.0018	0.0015	0.0035	0.003	0.012	0.012	0.010	0.002	0.008	0.010	0.020
Constant	6193.3* (307.9)	2070.2* (107.1)	398.3* (2.3610)	6.6930* (6.0350)	0.0959* (0.0071)	83.85* (4.150)	3.100* (0.2096)	0.2807* (0.0018)	1.8450* (1.0910)	0.0624* (0.0075)	0.9524* (0.0537)	0.0182* (0.0022)
Trading Volume	-----	-----	5.79×10^{-6}* (5.40×10^{-8})	9.81×10^{-7}* (2.35×10^{-8})	2.35×10^{-9}* (5.58×10^{-11})	2.29×10^{-6}* (1.99×10^{-7})	4.37×10^{-8}* (2.39×10^{-9})	5.87×10^{-11}* (4.29×10^{-10})	3.12×10^{-7}* (9.17×10^{-9})	1.63×10^{-8}* (9.60×10^{-10})	1.30×10^{-8}* (7.29×10^{-10})	1.07×10^{-8}* (6.07×10^{-10})
	Return Series											
θ	0.0025	0.0035	0.0022	0.005	0.005	0.017	0.010	0.020	0.004	0.008	0.0065	0.025
Constant	-0.0022* (0.0011)	0.0031* (0.0012)	0.0040* (0.0013)	0.0072* (0.0027)	0.0016 (0.0033)	-0.0127 (0.0073)	-0.0050 (0.0069)	-0.0007 (0.0093)	4.96×10^{-5} (0.0020)	-0.0026 (0.0063)	0.0046 (0.0066)	0.0037 (0.0134)
Trading Volume	-----	-----	-4.40×10^{-12} (3.01×10^{-12})	-1.08×10^{-11} (1.04×10^{-11})	8.50×10^{-11}* (2.64×10^{-11})	1.62×10^{-10}* (3.85×10^{-11})	2.49×10^{-10}* (8.52×10^{-11})	1.12×10^{-9}* (2.57×10^{-10})	7.63×10^{-11}* (1.74×10^{-11})	3.46×10^{-9}* (8.88×10^{-10})	-2.55×10^{-11} (9.54×10^{-11})	4.69×10^{-9} (3.92×10^{-9})
Lag 1	-0.0141 (0.0270)	-0.0065 (0.0286)	0.0462* (0.0188)	-0.0637* (0.0315)	-0.3281* (0.0291)	-0.0461 (0.0617)	-0.0410 (0.0589)	-0.1376 (0.0732)	-0.1280* (0.0247)	0.0026 (0.0048)	0.0591 (0.0573)	-0.0022 (0.0707)
Lag 2	-0.0160 (0.0270)	0.0200 (0.0286)	-0.1693* (0.0188)	0.0060 (0.0313)	0.0629* (0.0304)	-0.1400* (0.0620)	0.0106 (0.0581)	0.1669* (0.0680)	-0.0542* (0.0247)	-0.0064 (0.0467)	-0.0354 (0.0574)	0.1772* (0.0709)
Lag 3	0.0400 (0.0270)	0.0640* (0.0287)	0.0228 (0.0190)	0.0707* (0.0313)	-0.0211 (0.0304)	-0.0084 (0.0602)	0.0398 (0.0572)	0.0325 (0.0713)	0.0160 (0.0247)	-0.0027 (0.0463)	0.1107 (0.0578)	0.2051* (0.0709)
Lag 4	0.0095 (0.0271)	-0.0069 (0.0287)	0.0107* (0.0190)	-0.0151 (0.0312)	0.0191 (0.0304)	-0.1122 (0.0586)	-0.0576 (0.0494)	-0.0159 (0.0693)	0.0407 (0.0248)	-0.0778 (0.0456)	0.0057 (0.0572)	-0.1390* (0.0702)
Lag 5	0.0127 (0.0272)	0.0190 (0.0286)	0.0835* (0.0190)	0.0013 (0.0312)	-0.0435 (0.0304)	0.0201 (0.0575)	-0.0238 (0.0496)	-0.0929 (0.0681)	0.0032 (0.0247)	0.0788 (0.0463)	0.0188 (0.0555)	0.0179 (0.0697)
Lag 6	0.1055* (0.0272)	0.1205* (0.0286)	-0.0093 (0.0190)	-0.0009 (0.0293)	0.0492 (0.0289)	0.0154 (0.0571)	0.0602 (0.0493)	-0.0645 (0.0682)	0.0870* (0.0246)	0.0152 (0.0459)	0.0992 (0.0553)	-0.0370 (0.0695)

----- no data available; θ is the ratio of number of days in a segment over the total number of days (count).
*Significance at the 5% level.

Table 4.1, continued.

	CRIX	CCI30	BTC	ETH	XRP	BCH	EOS	ADA	LTC	XLM	IOTA	TRX
	Squared Return Series											
θ	0.003	0.005	0.002	0.008	0.008	0.025	0.012	0.030	0.004	0.010	0.010	0.015
Constant	0.0008* (0.0001)	0.0008* 0.0015)	0.0021* (0.0008)	0.0029* (0.0005)	0.0057* (0.0018)	0.0022* (0.0017)	0.0650* (0.0016)	0.0112* (0.0045)	0.0032* (0.0009)	0.0044* (0.0021)	0.0055* (0.0016)	0.0112 (0.0062)
Trading Volume	-----	-----	6.19×10^{-13} (1.96×10^{-12})	3.50×10^{-12}* (1.75×10^{-12})	1.76×10^{-11} (1.38×10^{-11})	6.61×10^{-11}* (8.31×10^{-12})	9.24×10^{-11}* (1.64×10^{-11})	9.64×10^{-10}* (1.27×10^{-10})	1.55×10^{-11}* (7.33×10^{-12})	1.26×10^{-9}* (2.69×10^{-10})	9.08×10^{-11}* (1.98×10^{-11})	2.70×10^{-9} (1.55×10^{-9})
Lag 1	0.2657* (0.0272)	0.1821* (0.0284)	0.0279 (0.0186)	0.2042* (0.0317)	0.4496* (0.0291)	0.1804* (0.0582)	-0.0648 (0.0570)	-0.1591* (0.0733)	0.5157* (0.0248)	0.3408* (0.0469)	0.1065 (0.0565)	0.0396 (0.0709)
Lag 2	0.0154 (0.0281)	0.0373 (0.0287)	0.1406* (0.0186)	0.0379 (0.0309)	-0.0275 (0.0318)	-0.2546* (0.0594)	-0.0562 (0.0559)	0.1658* (0.0636)	-0.2092* (0.0278)	0.0596 (0.0489)	-0.0262 (0.0568)	0.2049* (0.0710)
Lag 3	0.0001 (0.0281)	0.0613* (0.0286)	0.0087 (0.0183)	0.0747* (0.0308)	0.1375* (0.0318)	0.0258 (0.0580)	0.0003 (0.0056)	-0.1959* (0.0671)	0.0911* (0.0283)	0.0064 (0.0488)	0.0837 (0.0565)	0.1204 (0.0719)
Lag 4	0.1012* (0.0279)	0.1124* (0.0286)	0.2144* (0.0183)	0.0642* (0.0307)	-0.0519 (0.0318)	-0.0413 (0.0515)	0.0117 (0.0189)	-0.0191 (0.0647)	0.0085 (0.0283)	-0.0620 (0.0487)	0.0004 (0.0560)	0.0789 (0.0714)
Lag 5	0.0489 (0.0281)	0.0974* (0.0287)	-0.0070 (0.0186)	0.0519 (0.0300)	0.0827* (0.0318)	-0.0046 (0.0512)	0.0244 (0.0180)	-0.0699 (0.0633)	0.0019 (0.0278)	0.0877 (0.0488)	-0.0098 (0.0518)	-0.0766 (0.0700)
Lag 6	0.0118 (0.0282)	0.0375 (0.0283)	0.1664* (0.0186)	-0.0305* (0.0143)	-0.0238 (0.0291)	0.0950* (0.0477)	0.0116 (0.0178)	-0.1064 (0.0638)	0.0223 (0.0247)	-0.0779 (0.0455)	0.0332 (0.0511)	0.0354 (0.0700)

----- no data available; θ is the ratio of number of days in a segment over the total number of days (count).
*Significance at the 5% level.

4.2 Bai and Perron (2003) method in detecting change points

After the significant autoregressive variables and exogenous variables for price, return and squared return series are identified, these significant variables are incorporated to the multiple change point model.

Liu et al. (1997) first considered multiple change point model using least-squares method. They partitioned the data into m segments and then computed the sum of squared residuals for each segment. The change point estimators are regarded as the global minimisers of the sum of squared residuals. Bai and Perron (2003) extended their work by applying dynamic programming algorithm to estimate the global minimisers of the sum of squared residuals. The algorithm uses at most least-squares operations of order $O(T^2)$ for any number of m change points which appears to be a more efficient way of achieving a minimum global sum of squared residuals with T representing the length of data.

In this section, we applied the change point model of Bai and Perron (2003) by augmenting the significant exogenous variables into the model to determine the location and number of change points in price, return and squared return series of the two cryptocurrency indices and the top ten cryptocurrencies. In particular, consider a linear model as below with m changes ($m + 1$ segments):

$$y_t = \boldsymbol{x}_t'\boldsymbol{\beta} + \boldsymbol{z}_t'\boldsymbol{\delta}_j + u_t, \quad t = T_{j-1} + 1, T_{j-1} + 2, \ldots, T_j, \tag{4.1}$$

for $j = 1, 2, \ldots, m + 1$. In this model, y_t is the observed dependent variable at time t with dimension 1×1, $\boldsymbol{x}_t'$ is a $1 \times k$ vector of exogenous variables with k number of constant coefficients in vector $\boldsymbol{\beta}$ of dimension $k \times 1$, $\boldsymbol{z}_t'$ is a $1 \times n$ vector of exogenous variables as discussed in Section 4.1 with n number of corresponding coefficients that are subject to change in vector $\boldsymbol{\delta}_j$ of dimension $n \times 1$ and u_t is the disturbance at time t with dimension 1×1. The indices $(T_1, T_2, \dots, T_m)$ are the estimated change points treated as unknown with $T_0 = 0$ and $T_{m+1} = T$. In this research, we concentrate on pure change point model which allows all coefficients subjected to change by letting $\boldsymbol{\beta} = \mathbf{0}$ so that the shifts of all exogenous variables, if any, are considered. The above multiple linear regression system can then be expressed in its matrix form as below, where $\overline{\boldsymbol{Z}}$ is a diagonal matrix that partition $\boldsymbol{Z}_j$ at $(T_1, T_2, \dots, T_m)$:

$$\boldsymbol{Y} = \overline{\boldsymbol{Z}}\boldsymbol{\delta} + \boldsymbol{U}, \tag{4.2}$$

or

$$\begin{pmatrix} y_1 \\ y_2 \\ \vdots \\ y_T \end{pmatrix} = \begin{pmatrix} \boldsymbol{Z_1} & \mathbf{0} & \cdots & \mathbf{0} \\ \mathbf{0} & \boldsymbol{Z_2} & \cdots & \mathbf{0} \\ \vdots & \vdots & \ddots & \vdots \\ \mathbf{0} & \mathbf{0} & \cdots & \boldsymbol{Z_{m+1}} \end{pmatrix} \begin{pmatrix} \boldsymbol{\delta_1} \\ \boldsymbol{\delta_2} \\ \vdots \\ \boldsymbol{\delta_{m+1}} \end{pmatrix} + \begin{pmatrix} u_1 \\ u_2 \\ \vdots \\ u_T \end{pmatrix},$$

where

$$\boldsymbol{Z_j} = \begin{pmatrix} \boldsymbol{z}'_{T_{j-1}+1} \\ \boldsymbol{z}'_{T_{j-1}+2} \\ \vdots \\ \boldsymbol{z}'_{T_j} \end{pmatrix}, \qquad j = 1, 2, \dots, m+1.$$

The dimension for $\boldsymbol{Y}$ is $T \times 1$, $\overline{\boldsymbol{Z}}$ is $T \times n(m+1)$, $\boldsymbol{\delta}$ is $n(m+1) \times 1$ and $\boldsymbol{U}$ is $T \times 1$.

For each m-partition $(T_1, T_2, \dots, T_m)$ denoted by $\{T_j\}$, the estimates of $\boldsymbol{\delta}_j$ are evaluated by minimising the sum of squared residuals. Substituting the values into the objective function and denoting the resulting sum of squared residuals as $S_T(T_1, T_2, \dots, T_m)$, the estimated change points $(\hat{T}_1, \hat{T}_2, \dots, \hat{T}_m)$ are then determined by $(\hat{T}_1, \hat{T}_2, \dots, \hat{T}_m) = \operatorname{argmin}_{T_1,\dots,T_m} S_T(T_1, T_2, \dots, T_m)$ where the minimisation is taken over all partitions, $(T_1, T_2, \dots, T_m)$. Consequently, the change point estimators are the global minimisers of the objective function. The global sum of squared residuals for any of the m-partition

$(T_1, T_2, \ldots, T_m)$ and for any value of m, must be particular a linear combination of these $T(T+1)/2$ sums of squared residuals. The estimates of the change points, m-partition $(\hat{T}_1, \hat{T}_2, \ldots, \hat{T}_m)$, will correspond to this linear combination with a minimal value. The dynamic programming algorithm is regarded as a more efficient approach to contrast all possible combinations (corresponding to different m-partitions) in order to achieve a minimum global sum of squared residuals. The number of changes is controlled by the trimming error, θ, where θ is the ratio of number of days in a segment over the total number of days (count). In this research, we let θ to be the smallest possible value without limiting the number of change points as opposed to the study by Bouri et al. (2019a) who only allowed a maximum of five change points in their analysis. For estimation purposes, the number of days in a segment must be greater than the number of regressors in the model. The above algorithms to estimate the change points in cryptocurrencies are implemented using the R package strucchange and function breakpoints.

4.3 Discussion on change points detected

A large number of change points in price, return and squared return series of cryptocurrencies are detected. The detected change points are not totally consistent among the three financial time series but with more change points detected in price series, followed by squared return series and the least in return series. Table 4.2 summarises the total number of change points detected in various series and cryptocurrencies.

Table 4.2: Total number of change points detected in various series and cryptocurrencies.

Cryptocurrencies	Price series	Return series	Squared return series
CRIX	72	7	31
CCI30	68	5	19
BTC	72	22	56
ETH	62	1	23
XRP	45	13	8
BCH	27	1	14
EOS	22	1	24
ADA	26	3	9
LTC	66	14	14
XLM	31	4	20
IOTA	27	2	16
TRX	10	0	12

The primary causes to the abrupt change in the cryptocurrency market are hypothesised to be caused by the huge correction from sharp price appreciation, stricter regulations and government involvement, rumours and positive or negative news as well as other technological issues. In particular, announcements of macroeconomic news related to both unemployment rates and durable goods are found to affect the returns of BTC (Corbet et al., 2020). These are the influential factors that contribute to the instability dynamics of the cryptocurrency market. Investors and financial practitioners hence ought to be cautious to the risks attached in the market. Next, the change points detected in price, return and squared return series would be discussed in length.

4.3.1 Price series

Price series is greatly affected by the force of supply and demand as well as other external events. Price reacts sensitively to news and information in the market. When demand is greater than supply, the price will ascend and the market is bullish or vice versa. It is noticed that there are few consistent and significant change points detected in cryptocurrencies price series over time. Figure 4.1 depicts the monthly segmentation of price series, in which a change point is represented by a change in colour of the horizontal bar.

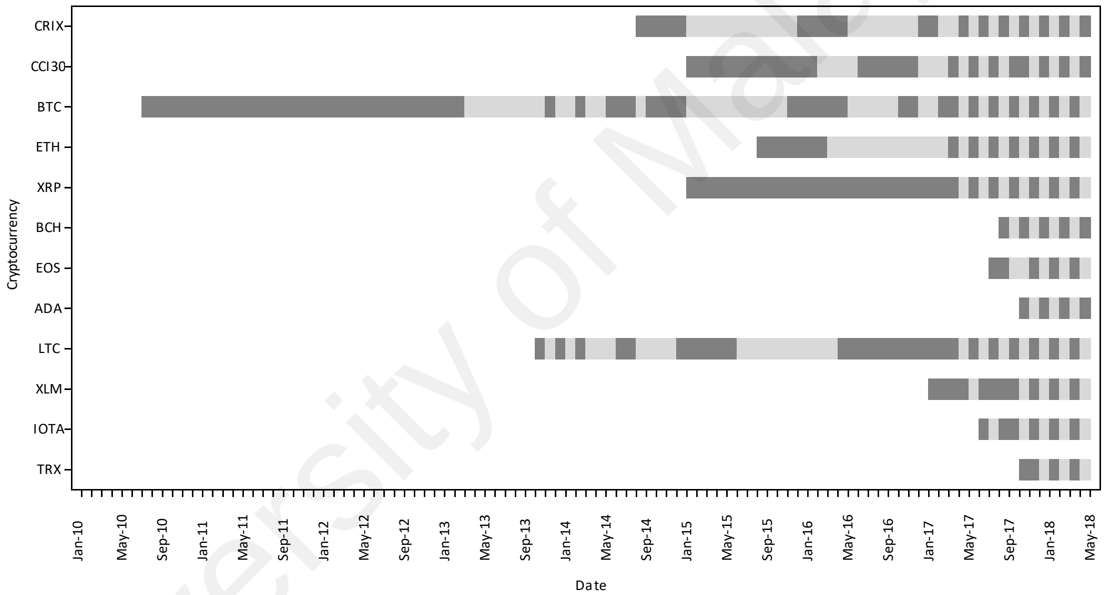

Figure 4.1: The monthly segmentation of cryptocurrencies price series by change points.

Figure 4.1 reveals that change points in price series are detected specifically at the turnings of year. Observing the longer data such as CRIX, CCI30, BTC and LTC, change points are detected at almost every end or beginning of year commencing from the year 2013 when cryptocurrency market began to gain its popularity. We hence postulate that the cryptocurrency market is subject to "year-end" effect as there are cyclical changes in price series at the turnings of year. Our results also provide evidence and justification to the study conducted by Bouri et al. (2017) who segmented BTC return series at December 2013 in their analysis. The presence of frequent change points detected approximately at every month of year 2017 further confirms that the cryptocurrency market indeed undergo unexpected high price fluctuations. To be more concrete, Appendix A provides the detailed number of change points detected in each of the particular month throughout the whole sample period for the price series.

4.3.2 Return series

Return is an important variable in finance as it measures the profit of an investment. High return will usually be accompanied by high risk, hence, in the event of high volatility, high return is also expected. Figure 4.2 illustrates the monthly segmentation of return series in which a change point is represented by a change in colour of the horizontal bar.

From Figure 4.2, there is no change point detected in BTC return series after the second quarter of year 2014. We also notice that the ETH return series is detected with only one change point located at September 2015 and none thereafter. On the other hand, TRX is not detected with any change points in the return series.

Among all of the change points detected in the return series, CRIX and CCI30 show the consistency of change points in January 2015 and September 2017. Surprisingly, only LTC is detected with change points at these two periods but none for the other cryptocurrencies. These estimated change points may be attributed to some unexpected events only occurred to a certain group of cryptocurrencies which were the constituents of CRIX and CCI30 at those particular times but not to the top ten cryptocurrencies chosen at the time of research since the rankings of cryptocurrencies are fast-changing (Elbahrawy et al., 2017). Besides, CRIX return series is detected with one change point at December 2017 while the change point of CCI30 return series appeared a bit later in

January 2018 during the abrupt market price depreciation. Both change points are in expectation since cryptocurrency market is subject to obvious change of trends at the turning of years 2017/2018, whereby most of the cryptocurrencies also show the existence of change points at this particular period. For better understanding, Appendix A provides the detailed number of change points detected in each of the particular month throughout the whole sample period for the return series.

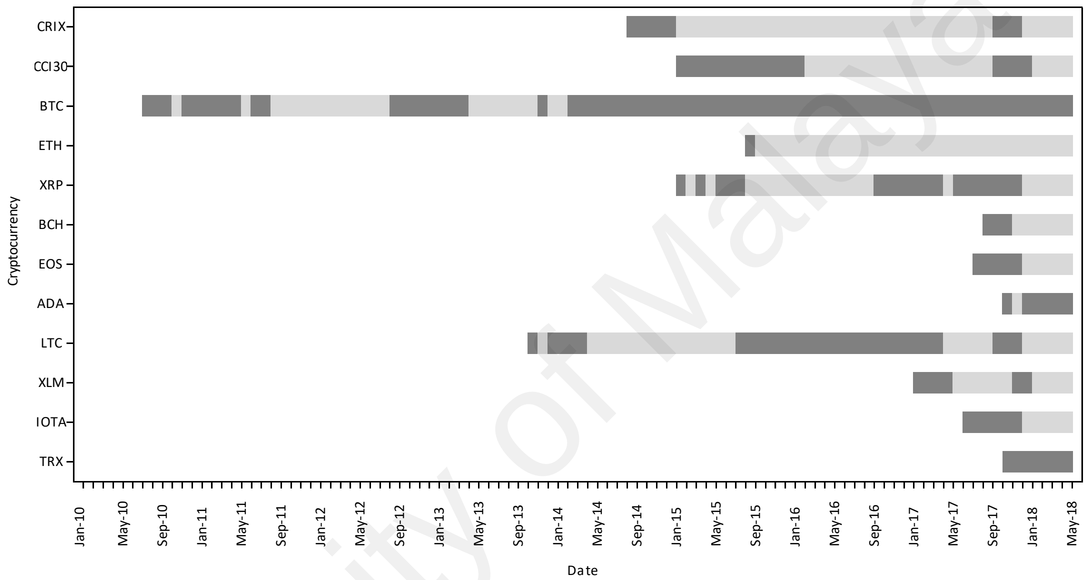

Figure 4.2: The monthly segmentation of cryptocurrencies return series by change points.

4.3.3 Squared return series

Squared return is commonly used to assess the uncertainty (or the risk) of the financial market. Since volatility is unobservable, we adopt the common practice of taking the square of the daily returns as proxy for volatilities. Figure 4.3 illustrates the monthly segmentation of squared return series in which a change point is represented by a change in colour of the horizontal bar.

As shown in Figure 4.3, there are more change points detected in squared return series as compared to return series especially for ETH, where there is only one change point detected in the return series, and yet, a total of twenty-three change points are detected in the squared return series throughout the period. BTC appears to experience more change points in the squared return series in year 2011 which then becomes lesser from year 2012 to year 2017 and no detected change point in year 2016. Our findings are in line with the selection of change point at the beginning of year 2015 by Bouoiyour and Selmi (2016) which further confirms the event of BTC volatility change at that specified period. Five change points are detected in ETH squared return series. Most cryptocurrencies show the presence of change points in the squared return series at July 2017, the last quarter of year 2017 and at January 2018. To compare, both indices display consistent signs of change at January 2015, July 2017, and at the turning of years 2017/2018. Appendix A provides the detailed number of change points detected in each of the particular month throughout the whole sample period for squared return series.

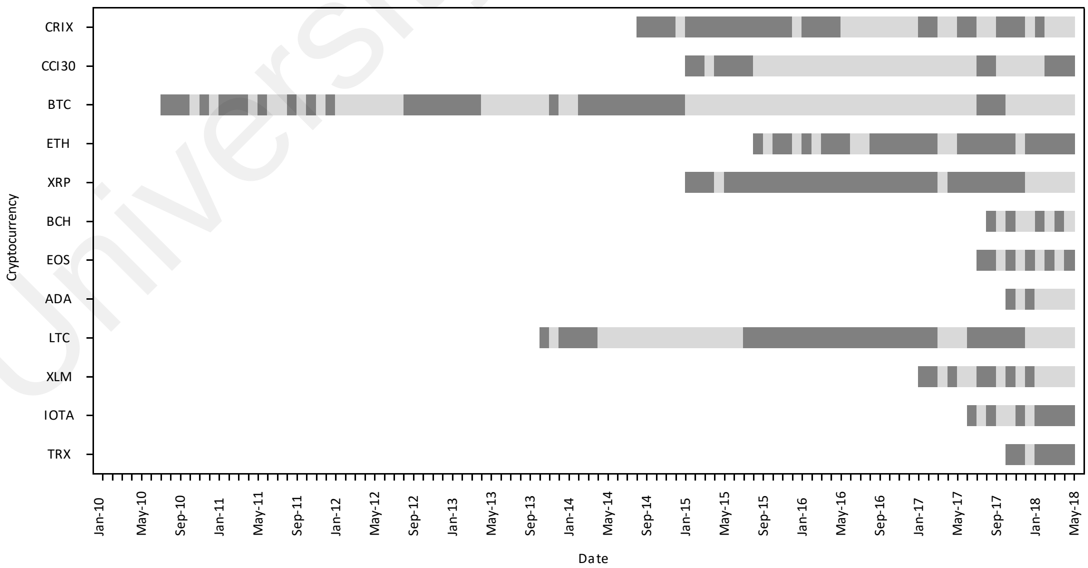

Figure 4.3: The monthly segmentation of cryptocurrencies squared return series by change points.

CHAPTER 5 : VOLATILITY MODELLING

5.1 Single-regime volatility models

Conditional heteroscedasticity models are frequently used in the work of financial volatility modelling and forecasting for the purpose of risk management. Financial time series commonly exhibits volatility clustering in which large changes in volatility are often followed by large changes while small changes in volatility tend to be followed by small changes. This behaviour is also formally known by econometrician and statistician as autoregressive conditional heteroscedasticity.

Consider the return series, r_t of a financial asset at time t for $t = 1, 2, \dots, T$, which can be calculated as $r_t = \ln P_t - \ln P_{t-1}$ where $\ln P_t$ is the natural logarithm of the daily closing price of a cryptocurrency at time t. The conditional mean and conditional variance of r_t of a volatility model given F_{t-1} are denoted as:

$$b_t = \mathbb{E}(r_t|F_{t-1}) \quad \text{and} \quad \sigma_t^2 = \mathrm{Var}(r_t|F_{t-1}) = \mathbb{E}[(r_t - b_t)^2|F_{t-1}], \tag{5.1}$$

where $F_{t-1} = \{r_{t-1}, r_{t-2}, \dots\}$ is the past observed returns up to time $t - 1$.

The r_t can be expressed as:

$$r_t = b_t + a_t, \quad t = 1,2, \dots, T, \tag{5.2}$$

where $a_t = \sigma_t \varepsilon_t$ is the innovation component (or shock) of return at time t with the volatility term σ_t, and ε_t representing the error term with zero mean and unit variance. To remove the serial dependence in return series, we use $b_t = \mu + \phi r_{t-1}$ where μ and ϕ are the model parameters to be estimated.

Combining Eq. (5.1) and Eq. (5.2), conditional variance can be expressed as:

$$\sigma_t^2 = \text{Var}(r_t|F_{t-1}) = \text{Var}(a_t|F_{t-1}), \quad t = 1, 2, \dots, T. \tag{5.3}$$

The following subsection discusses various model specifications for the conditional variance at time t, σ_t^2.

5.1.1 Autoregressive conditional heteroscedasticity model

The first model that provides systematic framework for the behaviour of volatility clustering is ARCH model by Engle (1982). The basic idea of ARCH model is to describe the conditional volatility by simple quadratic function of past shocks. The ARCH model with order q, ARCH(q) is given by:

$$\sigma_t^2 = \omega + \sum_{i=1}^{q} \alpha_i a_{t-i}^2, \quad t = 1, 2, \dots, T, \tag{5.4}$$

where ω and α_i are the model parameters with $\omega > 0$ and $\alpha_i \geq 0$ for $i = 1, 2, \dots, q$. For ARCH(1) model, the constraint of $0 < \alpha < 1$ must be satisfied to ensure the volatility is stationary. In applications, the condition of stationarity is required for one to perform forecasting and prediction on a time series.

5.1.2 Generalised autoregressive conditional heteroscedasticity model

ARCH model represents a simple approach to estimate the volatility. However, ARCH model contains weaknesses such that in many times, only high order of ARCH model is adequate to describe the volatility of an asset return. Due to this respect, Bollerslev (1986) introduced an extended model of ARCH, known as GARCH model. A low order of GARCH model is found to be effectively capturing the same effects as a high order ARCH model.

The GARCH model with orders p and q, GARCH(p, q) is expressed as:

$$\sigma_t^2 = \omega + \sum_{i=1}^{q} \alpha_i a_{t-i}^2 + \sum_{j=1}^{p} \beta_j \sigma_{t-j}^2, \quad t = 1, 2, \dots, T, \tag{5.5}$$

where ω, α_i and β_j are the model parameters with $\omega > 0$, $\alpha_i \geq 0$ for $i = 1, 2, \dots, q$, $\beta_j \geq 0$ for $j = 1, 2, \dots, p$ and $\sum_{i=1}^{\max(q,p)} (\alpha_i + \beta_i) < 1$. The latter constraint implies covariance stationarity to ensure the unconditional volatility of r_t is finite. From Eq. (5.5), a large a_{t-i}^2 or a large σ_{t-j}^2 gives rise to large σ_t^2 depicting volatility clustering behaviour.

5.1.3 Glosten-Jagannathan-Runkle GARCH model

One of the well-known properties displayed by financial time series is asymmetric effect, also known as leverage effect, which describes the different impact of positive and negative shocks on volatility. Practically, the volatility of a financial asset is known to be more responsive to negative shocks than positive shocks. To address asymmetric property, Glosten et al. (1993) proposed GJRGARCH model. The GJRGARCH model with orders p and q, GJRGARCH(p, q) is expressed as:

$$\sigma_t^2 = \omega + \sum_{i=1}^{q} (\alpha_i a_{t-i}^2 + \gamma_i \mathbb{I}\{a_{t-i} < 0\}) + \sum_{j=1}^{p} \beta_j \sigma_{t-j}^2, \quad t = 1, 2, \dots, T, \tag{5.6}$$

where ω, α_i, β_j and γ_i are the model parameters with $\omega > 0$, $\alpha_i \geq 0$ for $i = 1, 2, \dots, q$, $\beta_j \geq 0$ for $j = 1, 2, \dots, p$, $\mathbb{I}\{a_{t-i} < 0\}$ is an indicator variable such that $\mathbb{I}\{a_{t-i} < 0\} = 1$ if $a_{t-i} < 0$ for $i = 1, 2, \dots, q$ and zero otherwise; whereas γ_i is the asymmetric parameter that controls the degree of asymmetry effect corresponding to the past shock in the conditional variance. This implies that negative shock will result in higher conditional variance σ_t^2 when $\gamma_i > 0$. In some occasional circumstances, $\gamma_i < 0$, which means positive shocks have larger impact on conditional variance, also known as inverted asymmetric effect. For GJRGARCH(1,1) model to be weakly stationary, we have that $[\alpha_1 + \gamma_1 \mathbb{E}(\varepsilon_t^2 \mathbb{I}\{\varepsilon_t < 0\}) + \beta_1] < 1$.

5.1.4 Threshold GARCH model

Another model commonly used to handle asymmetric effect is threshold GARCH (TGARCH) model proposed by Zakoian (1994). Unlike GJRGARCH model, TGARCH model applies threshold to differ the impacts of positive and negative shocks on volatility. The TGARCH model with orders p and q, TGARCH(p, q) is given by:

$$\sigma_t = \omega + \sum_{i=1}^{q} \left\{ \alpha_i (\mathbb{I}\{a_{t-i} > 0\}) - \gamma_i \mathbb{I}\{a_{t-i} < 0\} \right\} a_{t-i} + \sum_{j=1}^{p} \beta_j \sigma_{t-j},\ t = 1, 2, \dots, T, \tag{5.7}$$

where ω, α_i, β_j and γ_i are the model parameters with $\omega > 0$, $\alpha_i \geq 0$ and $\gamma_i \geq 0$ for $i = 1, 2, \dots, q$, $\beta_j \geq 0$ for $j = 1, 2, \dots, p$ and $\mathbb{I}\{a_{t-i} < 0\} = 1$ if $a_{t-i} < 0$ and zero otherwise. TGARCH model is capable of capturing leverage effect governed by α_i and γ_i. In this setting, positive and negative shocks have a different impact on the conditional volatility where the impact of positive shock is governed by α_i and the impact of negative shock is governed by γ_i. Here, weakly stationary of TGARCH(1,1) model requires that $\mathbb{E}[(\alpha_1 a_t \mathbb{I}\{a_t > 0\} - \gamma_1 a_t \mathbb{I}\{a_t < 0\} + \beta_1)^2] < 1$ (Francq & Zakoian, 2019).

5.2 Regime-switching model

One potential weakness of these GARCH-type models is the implication of constant model parameters over time (single-regime volatility model). The structural forms of conditional mean and conditional variance are held fixed throughout the whole sample period. Practically speaking, financial time series often undergoes periods of expansion and recession hence is unreasonable to assume constant model parameters for all time.

Recall the findings from Chapter 4, change points are frequently detected in price, return and squared return series of cryptocurrencies. The frequent existence of change points affected by the underlying internal or external factors definitely alert the financial practitioners or researchers to realise about the possible instability of parameters which ought to be addressed in all aspects of cryptocurrency analysis and modelling process.

Therefore, single-regime volatility model is perceived to be inflexible in explaining the volatility of cryptocurrencies and the specification of single-regime GARCH-type models often gives rise to false impression of high persistency and poor forecasting performance (Caporale et al., 2003; Mikosch & Stărică, 2004).

5.2.1 Two-regime Markov-switching GARCH(1,1) model

The limitation of single-regime GARCH-type models can be resolved by applying MSGARCH model. MSGARCH model allows the model parameters to be different in every regime to account for the possibility that the return series may undergo a finite number of changes over period. Assuming a two-regime model specification, the model parameters are varying and dependent on a latent process, denoted by $s_t \in \{1, 2\}$ for $t = 1, 2, \dots, T$. The latent state process is assumed to be an irreducible and aperiodic Markov chain with stationary probability measure $\pi = (\pi_1, \pi_2)$, where $\pi_1 = \mathbb{P}(s_t = 1)$ and $\pi_2 = \mathbb{P}(s_t = 2)$. The variable s_t is known as state or regime variable.

Under the Markov-switching framework, it is assumed that r_t can be decomposed into two components subjected to Markov-switching process conditional on past observed returns up to time $t - 1$. For MSGARCH(1,1) model, the r_t can be expressed as:

$$r_t = b_t(s_{1:t}; F_{t-1}) + a_t, \quad t = 1, 2, \dots, T, \tag{5.8}$$

where $s_{1:t} = \{s_1, s_2, \dots, s_t\}$, F_{t-1} is the past observed returns up to time $t - 1$ and $a_t = \sigma_t(s_{1:t}; F_{t-1})\varepsilon_t$ is the innovation component at time t with the volatility term $\sigma_t(s_{1:t}; F_{t-1})$, while ε_t is the error term with zero mean and unit variance.

We define the conditional mean component, $b_t(s_{1:t}; F_{t-1})$ as the following:

$$b_t(s_{1:t}; F_{t-1}) = \mu_{s_t} + \phi_{s_t} r_{t-1}, \quad t = 1, 2, \dots, T. \tag{5.9}$$

The conditional variance $\sigma_t^2(s_{1:t}; F_{t-1})$ of MSGARCH(1,1) model at time t is formulated based on GARCH(1,1) model:

$$\sigma_t^2(s_{1:t}; F_{t-1}) = \omega_{s_t} + \alpha_{1s_t} a_{t-1}^2 + \beta_{1s_t} \sigma_{t-1}^2(s_{1:t-1}; F_{t-2}), \quad t = 1, 2, \dots, T, \tag{5.10}$$

where ω_{s_t}, α_{1s_t} and β_{1s_t} are the model parameters at the regime s_t. Even though the regimes are unobserved, probabilistic statement can be drafted over their likelihood of occurrence conditional on past observed returns up to time $t - 1$.

The regime variable, s_t is governed by constant transition probability such that:

$$p_{ij} = \mathbb{P}(s_t = j | s_{t-1} = i; F_{t-1}), \quad \text{for } i, j \in \{1, 2\}, \quad t = 1, 2, \dots, T, \tag{5.11}$$

where $0 < p_{ij} < 1$ and $\sum_{j=1}^{2} p_{ij} = 1$ for $i \in \{1, 2\}$.

In particular, the stationary probability of a constant transition probability model can be obtained by:

$$\pi_j = \mathbb{P}(s_t = j) = \frac{(1 - p_{ii})}{(2 - p_{ii} - p_{jj})}, \quad \text{for } i, j = 1, 2 \quad \text{and. } i \neq j. \tag{5.12}$$

See Hamilton and Susmel (1994) for details.

According to Bauwens et al. (2010), the stationarity of MSGARCH(1,1) model can be guaranteed even if not all of the regimes satisfy the stationary condition. However, this constraint must be satisfied on average with respect to the probability distribution of the regimes. This inference is made on the assumption that the stationary regime dominates the entire process such that the volatility process will revert back to the stationary state after a big shock occurs, which is described as the “relieving effect”.

In sum, MSGARCH(1,1) model is strictly stationary if the following conditions are met:

Assumption 1: The error term ε_t is independently and identically distributed (i.i.d) with continuous density on the whole real line which is centred on zero and $\mathbb{E}[\varepsilon_t^2]^\delta < \infty$ for some $\delta > 0$.

Assumption 2: $\alpha_{1i} > 0$, $\beta_{1i} > 0$ and $p_{ii} \in (0,1)$ for $i \in \{1,2\}$.

Assumption 3: $\sum_{i=1}^{2} \pi_i \mathbb{E}[\log(\alpha_{1i}\varepsilon_t^2 + \beta_{1i})] < 0$.

The first assumption is fulfilled for a wide range of distributions for the error terms, herein our research, normal distribution (NORMD), Student-t distribution (STD) and generalised error distribution (GED). The second assumption ensures that the Markov chain is discrete and ergodic. The third assumption implies that at least one of the regimes is stable and the strict stationarity conditions are not necessarily required in both of the regimes. With this, MSGARCH(1,1) model allows periods in which explosive regime takes place before collapsing to the stable regime. Further, the higher the probability of being in the stable regime, the higher the persistence level the non-stable regime can assume.

5.2.2 Time-varying transition probability MSGARCH(1,1) model

The specification of MSGARCH model employs constant transition probability which is too restrictive in some empirical settings (Diebold et al., 1994; Filardo, 1994). The assumption of constant transition probability could be relaxed in favour of time-varying transition probability (TVTP) to increase the flexibility of MSGARCH model. The specification of conditional mean and conditional volatility of TV-MSGARCH(1,1) model is the same as the MSGARCH model presented in Eq. (5.8) and Eq. (5.10). TVTP is assumed to evolve as a logistic function dependent on exogenous variable, x_t at every time t.

More specifically, the TVTP can be expressed as:

$$\mathbb{P}(s_t = i | s_{t-1} = i, x_{t-1}; F_{t-1}) = p_{ii,t} = \frac{\exp(c_i + d_i x_{t-1})}{1 + \exp(c_i + d_i x_{t-1})}, \quad \text{for } i = 1, 2, \tag{5.13}$$

where c_i is a constant and d_i is the coefficient of exogenous variable in regime i and $\mathbb{P}(s_t = j | s_{t-1} = i, x_{t-1}; F_{t-1}) = p_{ij,t} = 1 - p_{ii,t}$ for $i \neq j$. Note that when d_i is set to zero, the TVTP becomes constant at all times and TV-MSGARCH(1,1) model simply reduces to MSGARCH(1,1) model.

As discussed in Diebold et al. (1994), the steady-state or stationary probability of TVTP model is determined by the coefficient parameter of x_t and there is no analytical formula to calculate it. Motivated by Eq. (5.12), we assess the stationarity condition of TV-MSGARCH(1,1) by using the following formula:

$$\pi_j = \frac{(1 - \bar{p}_{ii})}{(2 - \bar{p}_{ii} - \bar{p}_{jj})} \quad \text{for } i, j = 1, 2 \quad \text{and} \quad i \neq j, \tag{5.14}$$

where $\bar{p}_{ii} = \frac{1}{T} \sum_{t=1}^{T} p_{ii,t}$ for $i = 1, 2$.

In this research, the exogenous variable, x_t employed in TV-MSGARCH(1,1) model is considered to be: (1) logarithmic trading volume; (2) Google searches series; and (3) log difference of Google searches series. Raw data of trading volume is not directly applied to TV-MSGARCH(1,1) model as the data is highly skewed. Instead, logarithmic trading volume is applied to TV-MSGARCH(1,1) model to ensure the advantage of using TVTP is interpretable. The motivation of using log transformation on the difference of Google searches series is to assess the impact of daily change in the public interest in cryptocurrencies to the volatility. By doing so, we can also avoid the biasness in cryptocurrencies volatility modelling and forecasting procedures since it was discovered that the data of Google searches series are protruding prominently at the turning of years 2017/2018 depicted in Figures 3.13 to 3.17. The discussion on the trading volume and Google searches series can be found in Chapter 3.

5.3 Estimation method

Parameter estimation is performed by maximising log-likelihood (LL) function using non-linear filter as proposed by Hamilton (1989) since s_t is not directly observed and evolves from a first-order Markov chain.

First, the joint density of r_t and the regime variables, s_t and s_{t-1} given the past observed returns up to time $t-1$, is estimated from the product of the conditional density of r_t and the conditional joint probability function of s_t and s_{t-1} as displayed in the following equation:

$$f(r_t, s_t, s_{t-1}|F_{t-1}) = f(r_t|s_t, s_{t-1}; F_{t-1})\mathbb{P}(s_t, s_{t-1}|F_{t-1}). \tag{5.15}$$

Secondly, to determine the conditional distribution of r_t, $f(r_t|F_{t-1})$, we integrate s_t and s_{t-1} from the joint density in Eq. (5.15) by summing up all the possible values of s_t and s_{t-1} as the following:

$$f(r_t|F_{t-1}) = \sum_{s_t=1}^{2}\sum_{s_{t-1}=1}^{2} f(r_t, s_t, s_{t-1}|F_{t-1})$$

$$= \sum_{s_t=1}^{2}\sum_{s_{t-1}=1}^{2} f(r_t|s_t, s_{t-1}; F_{t-1})\mathbb{P}(s_t, s_{t-1}|F_{t-1}), \quad (5.16)$$

where the conditional density function of r_t, $f(r_t|s_t, s_{t-1}; F_{t-1})$ is dependent on the distribution of error term, ε_t and can take different forms of distribution such as NORMD, STD and GED.

The LL function is then given by:

$$\text{LL}= \sum_{t=1}^{T} \ln\,[f(r_t|F_{t-1})]$$

$$= \sum_{t=1}^{T} \ln\left[\sum_{s_t=1}^{2}\sum_{s_{t-1}}^{2} f(r_t|s_t, s_{t-1}; F_{t-1})\mathbb{P}(s_t, s_{t-1}|F_{t-1})\right]. \quad (5.17)$$

To complete the above procedure, the conditional joint probability function of s_t and s_{t-1}, $\mathbb{P}(s_t = j, s_{t-1} = i|F_{t-1})$ for $i, j = 1, 2$ can be estimated from Hamilton filtering algorithm (Hamilton, 1989) which can be executed in the following two steps:

Step 1:

Given the conditional marginal probability $\mathbb{P}(s_{t-1} = i|F_{t-1})$ for $i = 1, 2$,the conditional joint probability function of s_t and s_{t-1}, can be calculated as:

$$\mathbb{P}(s_t = j, s_{t-1} = i|F_{t-1}) = \mathbb{P}(s_t = j|s_{t-1} = i; F_{t-1}) \times \mathbb{P}(s_{t-1} = i|F_{t-1}), \quad (5.18)$$

where $\mathbb{P}(s_t = j|s_{t-1} = i; F_{t-1})$ is the transition probability which is constant for all time t for MSGARCH model and time-varying for TV-MSGARCH model (see Eq. (5.13)).

Step 2:

At every t-th iteration when r_t is observed at the end of time t, the conditional joint probability calculated in Step 1 can be updated as follows:

$$\mathbb{P}(s_t = j, s_{t-1} = i|F_t) = \mathbb{P}(s_t = j, s_{t-1} = i|F_{t-1}, r_t)$$
$$= \frac{f(s_t = j, s_{t-1} = i, r_t|F_{t-1})}{f(r_t|F_{t-1})}$$
$$= \frac{f(r_t|s_t = j, s_{t-1} = i; F_{t-1})\mathbb{P}(s_t = j, s_{t-1} = i|F_{t-1})}{\sum_{j=1}^{2}\sum_{i=1}^{2} f(r_t, s_t = j, s_{t-1} = i|F_{t-1})}, \quad (5.19)$$

with

$$\mathbb{P}(s_t = j|F_t) = \sum_{i=1}^{2} \mathbb{P}(s_t = j, s_{t-1} = i|F_t). \quad (5.20)$$

The probability of being in regime j conditional up to observed returns at time t, $\mathbb{P}(s_t = j|F_t)$, also known as filtered probability, is inferred from the Hamilton filtering algorithm. To begin this iteration, steady-state probability or stationary probability are used for MSGARCH model (see Eq. (5.12)) and TV-MSGARCH model (see Eq. (5.14)).

One concern arises during parameter estimation of MSGARCH model as argued by both Cai (1994) and Hamilton and Susmel (1994). The specifications of MSGARCH model and TV-MSGARCH model suggest that conditional volatility is not only dependent on regime s_t but also indirectly dependent on the entire regime path up to time $t-1$, $\{s_{t-1}, s_{t-2}, \ldots\}$. A quick look at Eq. (5.10) implies that $\sigma_t^2(s_{1:t}; F_{t-1})$ at time t is dependent on $\sigma_{t-1}^2(s_{1:t-1}; F_{t-2})$ at time $t-1$ whereas $\sigma_{t-1}^2(s_{1:t-1}; F_{t-2})$ further depends on $\sigma_{t-2}^2(s_{1:t-2}; F_{t-3})$ at time $t-2$ and goes on. The realisation of LL function is hence intractable in R^T number of possibilities where R refers to the number of regimes and T refers to the length of data. This is also known as path dependence problem.

Several solutions are suggested to solve path dependence problem while in the meantime preserving the essential nature of GARCH volatility specification. The first attempt to eliminate path dependence problem was proposed by Gray (1996) who suggested to collapse the conditional volatility in each regime into a proxy at every time t so that the estimated volatility would not be dependent on the entire regime path. Other similar modified solutions to path dependence problem were also raised by Dueker (1997) and Klaassen (2002). Haas et al. (2004) assumed that conditional volatility of each regime is independent such that each regime is characterised by its own volatility within that regime. In addition, Elliot et al. (2012) utilised Viterbi algorithm to identify the current state of volatility before the estimation procedure takes place. Moreover, sequential Monte Carlo method can also be applied to approximate the LL function (see Augustyniak, et al., 2018; Bauwens et al., 2014a).

The method of parameter estimation is not the primary concern of this research and the ML method is used under Gray's technique due to its ease of implementation in the maximisation of LL function through `R` optimisation package. Gray's technique of estimating volatility suggested the use of collapsed conditional variance rather than the actual conditional variance by integrating out the historical regime path.

The shock a_t in Eq. (5.8) can be estimated by the following:

$$\begin{aligned} a_t &= r_t - \mathbb{E}[r_t|F_{t-1}] \\ &= r_t - \mathbb{E}[b_t(s_{1:t};F_{t-1}) + a_t(s_{1:t};F_{t-1})|F_{t-1}] \\ &= r_t - \mathbb{E}[b_t(s_{1:t};F_{t-1})|F_{t-1}] \\ &= r_t - \textstyle\sum_{j=1}^{2} b_t(s_t = j;F_{t-1}) \times \mathbb{P}(s_t = j|F_{t-1}). \end{aligned} \tag{5.21}$$

Similarly, the path dependent conditional variance, $\sigma_t^2(s_{1:t}; F_{t-1})$ of Eq. (5.10) is proxied by $\sigma_c^2(t; F_{t-1})$ and is estimated with the following equation:

$$\begin{aligned}\sigma_c^2(t; F_{t-1}) &= \mathbb{E}[r_t^2(s_{1:t}; F_{t-1})|F_{t-1}] - \{\mathbb{E}[r_t(s_{1:t}; F_{t-1})|F_{t-1}]\}^2 \\ &= \mathbb{E}[b_t^2(s_{1:t}; F_{t-1})|F_{t-1}] + \mathbb{E}[a_t^2|F_{t-1}] - \{\mathbb{E}[b_t(s_{1:t}; F_{t-1})|F_{t-1}]\}^2 \\ &= \textstyle\sum_{j=1}^2 [b_t^2(s_t = j; F_{t-1}) + \sigma_t^2(s_t = j; F_{t-1})] \times \mathbb{P}(s_t = j|F_{t-1}) \\ &\quad -\left[\textstyle\sum_{j=1}^2 b_t(s_t = j; F_{t-1}) \times \mathbb{P}(s_t = j|F_{t-1})\right]^2, \end{aligned} \tag{5.22}$$

with

$$b_t(s_t = j; F_{t-1}) = \mu_j + \phi_j r_{t-1},$$

and

$$\sigma_t^2(s_t = j; F_{t-1}) = \omega_j + \alpha_{1j} a_{t-1}^2 + \beta_{1j} \sigma_c^2(t-1; F_{t-2}).$$

It can be noticed that the collapsed conditional variance, $\sigma_c^2(t; F_{t-1})$ is calculated by aggregating the conditional variances from the two regimes. The path dependence has been effectively removed as $\sigma_c^2(t; F_{t-1})$ is now the weighted average of the regime dependent conditional variance, $\sigma_t^2(s_t = j; F_{t-1})$, weighted by the probability being in that particular regime conditional on past observed returns up to time $t-1$.

5.4 Distributions of return

In many occasion, financial time series is assumed to follow NORMD. In respect to the heavy-tailed properties displayed by cryptocurrencies (Philip et al., 2018), STD and GED are also considered in this research.

5.4.1 Normal distribution

Suppose that ε_t follows NORMD, then the following probability density function at time t applied:

$$f(\varepsilon_t) = \frac{1}{\sqrt{2\pi}} e^{\frac{-\varepsilon_t^2}{2}}, \quad -\infty < \varepsilon_t < \infty. \tag{5.23}$$

Recall Eq. (5.2), we obtain the conditional density function of r_t on past observed returns assuming NORMD as the follows:

$$f(r_t|F_{t-1}) = \frac{1}{\sqrt{2\pi\sigma_t^2}} e^{\frac{-(r_t-b_t)^2}{2\sigma_t^2}}, \quad -\infty < r_t < \infty. \tag{5.24}$$

5.4.2 Student-t distribution

Suppose that ε_t follows STD with τ degrees of freedom, then the following probability density function at time t applied:

$$f(\varepsilon_t) = \frac{\Gamma\left(\frac{\tau+1}{2}\right)}{\sqrt{\pi(\tau-2)}\Gamma\left(\frac{\tau}{2}\right)} \left(1 + \frac{\varepsilon_t^2}{(\tau-2)}\right)^{-\frac{\tau+1}{2}}, \quad -\infty < \varepsilon_t < \infty, \quad \tau > 2. \tag{5.25}$$

Recall Eq. (5.2), we obtain the conditional density function of r_t on past observed returns assuming STD as the follows:

$$f(r_t|F_{t-1}) = \frac{1}{\sigma_t} \frac{\Gamma\left(\frac{\tau+1}{2}\right)}{\sqrt{\pi(\tau-2)}\Gamma\left(\frac{\tau}{2}\right)} \left(1 + \frac{(r_t-b_t)^2}{\sigma_t^2(\tau-2)}\right)^{-\frac{\tau+1}{2}}, \quad -\infty < r_t < \infty, \quad \tau > 2, \tag{5.26}$$

where $\Gamma(\tau) = \int_0^\infty e^{-x} x^{\tau-1} dx$ is the gamma function. The parameter τ measures the tail thickness of the distribution which takes care of the heavy tail property of the financial time series. When $\tau \to \infty$, the distribution will converge to NORMD (Gosset, 1908).

5.4.3 Generalised error distribution

Finally, assume ε_t follows GED as the follows:

$$f(\varepsilon_t) = \frac{\tau \exp\left[-\left(\frac{1}{2}\right)\left|\frac{\varepsilon_t}{\lambda}\right|^{\tau}\right]}{\lambda 2^{1+\frac{1}{\tau}}\Gamma\left(\frac{1}{\tau}\right)}, \quad -\infty < \varepsilon_t < \infty, \quad \tau > 0, \tag{5.27}$$

where $\Gamma(\cdot)$ is the gamma function and $\lambda = \left[\frac{2^{-\left(\frac{2}{\tau}\right)}\Gamma\left(\frac{1}{\tau}\right)}{\Gamma\left(\frac{3}{\tau}\right)}\right]^{\frac{1}{2}}$.

Recall Eq. (5.2), we obtain the conditional density function of r_t on past observed returns assuming GED as the follows:

$$f(r_t|F_{t-1}) = \frac{1}{\sigma_t}\frac{\tau \exp\left[-\left(\frac{1}{2}\right)\left|\frac{r_t-b_t}{\sigma_t\lambda}\right|^{\tau}\right]}{\lambda 2^{1+\frac{1}{\tau}}\Gamma\left(\frac{1}{\tau}\right)}, \quad -\infty < r_t < \infty, \quad \tau > 0. \tag{5.28}$$

GED reduces to NORMD when $\tau = 2$ and has thicker tails than normal (Nelson, 1991).

5.5 Value-at-risk

Conventionally in finance, VaR is often used as an indicator to estimate the possible risk exposure for a given time horizon and risk level. VaR indicates the maximum potential loss of an investment which is vital in risk management practice. Analytically, the $100(\nu_2 - \nu_1)\%$ confidence limits for VaR forecast of single-regime GARCH-type models at time t is defined as:

$$\left(\mathrm{VaR}_{t,\nu_1}, \mathrm{VaR}_{t,\nu_2}\right) = \left[b_t + q_{\nu_1}\sigma_t, b_t + q_{\nu_2}\sigma_t\right], \tag{5.29}$$

where q_{ν_1} and q_{ν_2} respectively, are the corresponding critical values of the lower quantile, ν_1 and the upper quantile, ν_2 of the respective distribution.

As for Markov-switching models, i.e. MSGARCH(1,1) and TV-MSGARCH(1,1) models, we propose the use of collapsed conditional mean at time t, $b_c(t; F_{t-1})$, and collapsed conditional standard deviation at time t, $\sigma_c(t; F_{t-1})$, to calculate the forecast of VaR. The $100(\nu_2 - \nu_1)\%$ confidence limits for VaR forecast at time t is:

$$\left(\mathrm{VaR}_{t,\nu_1}, \mathrm{VaR}_{t,\nu_2}\right) = \left[b_c(t; F_{t-1}) + q_{\nu_1}\sigma_c(t; F_{t-1}), b_c(t; F_{t-1}) + q_{\nu_2}\sigma_c(t; F_{t-1})\right], \tag{5.30}$$

where

$$b_c(t; F_{t-1}) = \mathbb{E}[b_t(s_{1:t}; F_{t-1})|F_{t-1}] = \textstyle\sum_{j=1}^{2} b_t(s_t = j; F_{t-1}) \times \mathbb{P}(s_t = j|F_{t-1}).$$

The collapsed conditional standard deviation, $\sigma_c(t; F_{t-1})$ at time t can be obtained from Eq. (5.22).

Once VaR forecasts are computed for each model over the forecasting period, the accuracy of VaR forecasts is assessed via VaR backtests. The first test was proposed by Kupiec (1995), also known as unconditional coverage (UC) test, which was then extended by Christoffersen (1998) who introduced conditional coverage (CC) test. A more general VaR backtest procedure was provided by Engle and Manganelli (2004), also known as dynamic quantile (DQ) test, which is based on a linear regression model. UC test checks the correct VaR coverage of the marginal return distribution $f(r_t)$ while CC test deals with the conditional density on past observed returns up to time $t-1$, $f(r_t|F_{t-1})$.

5.5.1 Unconditional coverage test

Unconditional coverage (UC) test calculates the number of VaR violations (the number of losses exceeding VaR estimates). If the number of violations exceeds the expected number indicated by the confidence level, ν, the model underestimates risk and if vice versa, the model overestimates risk. Both situations may affect financial strategies such that for the former, negative return is expected and for the latter, additional capital is required to secure the investment. Let N_ν be the number of VaR violations and h is the total number of days using one-day ahead forecast. Then, N_ν follows binomial distribution with h trials and success probability ν.

The likelihood ratio statistic is:

$$\mathrm{LR_{UC}} = 2\ln\left[\left(1-\frac{N_\nu}{h}\right)^{h-N_\nu}\left(\frac{N_\nu}{h}\right)^{N_\nu}\right] - 2\ln[(1-\nu)^{h-N_\nu}\,\nu^{N_\nu}], \tag{5.31}$$

where $\mathrm{LR_{UC}}$ is an asymptotically distributed chi-square with one degree of freedom.

5.5.2 Conditional coverage test

One of the drawbacks of UC test happens when the clustered VaR violations are not accounted for. In order to reject concentrated VaR violations, CC test jointly tests the independence of the "hit sequence" and the unconditional coverage of the VaR forecasts. First, define an indicator variable $\mathbb{I}_t$, which takes value of one if VaR is violated and takes value of zero if no violation occurs. Then, define a first-order Markov process with n_{ij} as the number of days with condition i on the previous day and j on the current day.

To provide better understanding, the 2×2 contingency table is as follows:

Table 5.1: Contingency table for CC test.

	$\mathbb{I}_t = 0$	$\mathbb{I}_t = 1$	Total
$\mathbb{I}_{t-1} = 0$	n_{00}	n_{01}	$n_{00} + n_{01}$
$\mathbb{I}_{t-1} = 1$	n_{10}	n_{11}	$n_{10} + n_{11}$

Let κ represents the probability of VaR violations and κ_i denotes the probability of VaR violations given the condition of being in regime i in the previous day, then the following applies:

$$\kappa_0 = \frac{n_{01}}{n_{00}+n_{01}}, \quad \kappa_1 = \frac{n_{11}}{n_{10}+n_{11}} \quad \text{and} \quad \kappa = \frac{n_{01}+n_{11}}{n_{00}+n_{01}+n_{10}+n_{11}}. \tag{5.32}$$

The null hypothesis of the independence test suggests that $\kappa_0 = \kappa_1 = \kappa$. In other words, the "hit sequence" should not be time dependent whereby the occurrence of VaR violation should not be dependent on whether there is a VaR violation occurrence on previous day. It is important to test whether the "hit sequence" is independent and the average number of violations is correct. The likelihood test statistic is defined as follows:

$$\mathrm{LR_{ind}} = 2\ln\left[(1-\kappa_0)^{n_{00}}\kappa_0^{n_{01}}(1-\kappa_1)^{n_{10}}\kappa_1^{n_{11}}\right] - 2\ln\left[(1-\kappa)^{n_{00}+n_{10}}\kappa^{n_{01}+n_{11}}\right], \tag{5.33}$$

where $\mathrm{LR_{ind}}$ is an asymptotically distributed chi-square with one degree of freedom.

CC test jointly tests the correct failure rate and the independence of VaR violations and the likelihood test statistic is carried out as:

$$\mathrm{LR_{CC}} = \mathrm{LR_{UC}} + \mathrm{LR_{ind}}, \tag{5.34}$$

where $\mathrm{LR_{CC}}$ is an asymptotically distributed chi-square with two degrees of freedom.

5.5.3 Dynamic quantile test

Dynamic quantile (DQ) test is based on a linear regression model where the dependent variable on VaR violation, known as "hit variable", is linked to a set of explanatory variables including a constant, lagged values of the hit variable and any useful information from the past. Denote hit variable at time t on confidence level ν as

$Hit_t(\nu) = \mathbb{I}_t(\nu) - \nu$ and under the correct model specification, the following moment conditions for the hit variables are satisfied:

$$\mathbb{E}[Hit_t(\nu)] = 0, \mathbb{E}[Hit_t(\nu)\mathbb{I}_{t-1}(\nu)] = 0 \text{ and } \mathbb{E}[Hit_t(\nu)Hit_{\grave{t}}(\nu)] = 0 \quad \text{for } t \neq \grave{t}. \tag{5.35}$$

The linear regression is defined as the follows:

$$Hit_t(\nu) = \delta + \sum_{k=1}^{K} \beta_k Hit_{t-k}(\nu) + \sum_{k=1}^{K} \gamma_k g(\, Hit_{t-k}(\nu), Hit_{t-k-1}(\nu), \dots) + \varepsilon_t, \tag{5.36}$$

where $g(.)$ is a function of past information. The null hypothesis of DQ test is to test whether the coefficients are jointly equal to zero such that:

$$\mathrm{H}_0: \delta = \beta_1 = \beta_2 = \cdots = \beta_K = \gamma_1 = \cdots = \gamma_K = 0 \tag{5.37}$$

5.5.4 Model confidence set

To further assess the forecasting performance of the models, MCS procedure by Hansen et al. (2011) was employed. MCS procedure consists of a sequence of statistical tests for constructing a set of superior models (SSM) where the null hypothesis of equal predictive ability (EPA) will not be rejected at certain confidence level. At each iteration, MCS procedure eliminates the worst model until the hypothesis of EPA is accepted for SSM. The SSM are then used to forecast future volatility level of cryptocurrencies. To sum up, MCS procedure accounts for the forecasting performance for a set of models rather than comparing relatively over a benchmark model for instance, Diebold-Mariano test (Diebold & Mariano, 1995) and superior predictive ability test (Hansen, 2005).

Consider a set of models M of dimension m encompassing of m models described in Sections 5.1 and 5.2. Let the loss function calculated for model i at time t denoted as $L_{i,t}$. The loss differential of two models i and j at time t, defined as $d_{ij,t}$, is calculated as follows:

$$d_{ij,t} = L_{i,t} - L_{j,t}, \quad i,j = 1,2,\dots,m, \quad i \neq j \quad \text{and} \quad t = 1,2,\dots,h. \tag{5.38}$$

Next, let

$$d_{i\cdot,t} = \frac{1}{m-1}\sum_{j=1}^{m} d_{ij,t}, \quad i = 1,2,\dots,m, \quad i \neq j, \tag{5.39}$$

where $d_{i\cdot,t}$ is the simple loss of model i relative to any other model j at time t.

The hypothesis for EPA is formulated as:

$$\mathrm{H}_0\colon \mu_{i\cdot} = 0 \quad \text{for all } i = 1,2,\dots,m,$$

$$\mathrm{H}_1\colon \mu_{i\cdot} \neq 0 \quad \text{for some } i = 1,2,\dots,m, \tag{5.40}$$

where $\mu_{i\cdot} = \mathbb{E}(d_{i\cdot})$ is assumed to be finite and not time dependent.

In order to test the null hypothesis mentioned in Eq. (5.40), the following test statistic is constructed:

$$t_{i\cdot} = \frac{\bar{d}_{i\cdot}}{\sqrt{\widehat{\mathrm{Var}}(\bar{d}_{i\cdot})}} \quad \text{for } i \in M, \tag{5.41}$$

where $\bar{d}_{i\cdot} = \frac{1}{m-1}\sum_{j=1}^{m} \bar{d}_{ij}$ is the estimated loss for model i relative to the averages losses in the set of models M and $\bar{d}_{ij} = \frac{1}{h}\sum_{t=1}^{h} d_{ij,t}$ while $\widehat{\mathrm{Var}}(\bar{d}_{i\cdot})$ is the bootstrapped estimate of the variance, $\mathrm{Var}(\bar{d}_{i\cdot})$. Finally, the test statistic above can be naturally mapped into the following test statistic:

$$T_M = \max_{i \in M} t_{i\cdot}. \tag{5.42}$$

Note that the asymptotic distribution of T_M is non-standard and the relevant distributions are estimated using bootstrap procedure similar to the method for estimating $\mathrm{Var}(\bar{d}_{i\cdot})$.

Since MCS procedure is a sequential process which eliminates the worst model at each iteration as mentioned before, the elimination procedure consists of three steps.

Step 1: Set $M = M^0$ where M^0 represents the set of initial models.

Step 2: Test for EPA hypothesis and if EPA is accepted, the algorithm is terminated and the models belong to SSM, otherwise, eliminates the worst model.

Step 3: Remove the worst model in Eq. (5.43) and go back to Step 2.

$$e_M = \arg\max_i \left\{ \frac{\bar{d}_{i\cdot}}{\sqrt{\widehat{\mathrm{Var}}(\bar{d}_{i\cdot})}} \right\}. \tag{5.43}$$

CHAPTER 6 : MODEL FITTING

This chapter discusses the empirical results obtained from the volatility estimation of the top five cryptocurrencies which commences with the comparison of the model fitting performances based on several criteria. Next, a diagnostic analysis is performed on the standardised residuals to check the model capability in capturing the serial dependence of the return series of cryptocurrencies. Lastly, the contribution of time-varying transition probability (TVTP) for the volatility modelling of TV-MSGARCH models is assessed by calculating the weighted transition probability (WTP).

6.1 Model selection

To determine the best fitted volatility model for the returns of BTC, ETH, XRP, BCH and EOS, these cryptocurrencies are fitted with GARCH(1,1) model, TGARCH(1,1) model, GJRGARCH(1,1) model, MSGARCH(1,1) model and three TV-MSGARCH(1,1) models, all incorporated with three different error distributions: NORMD, STD and GED. The exogenous variables embedded in the TVTP of TV-MSGARCH(1,1) models are: (1) Google searches series, denoted by TV-MSGARCH$_{S}$(1,1); (2) log difference Google searches series, denoted by TV-MSGARCH$_{ldS}$(1,1); (iii) log trading volume, denoted by TV-MSGARCH$_{lnV}$(1,1). With that, a total of 105 volatility models are constructed and the parameter estimates for all these fitted models together with their standard errors in parentheses of various cryptocurrencies are provided in Appendix B.

The selection of the best fitted model for each of the cryptocurrencies is based on a specification test known as AIC, proposed by Akaike (1974), which can be calculated as follows:

$$\text{AIC} = 2k - 2\text{LL}, \tag{6.1}$$

where k represents the number of parameters. AIC measures the loss of information caused by likelihood estimation. The smaller the value of AIC, the better the model to be used for in-sample volatility estimation. The values of AIC and LL for various volatility models and cryptocurrencies with different error distributions are reported in Table 6.1.

Table 6.1: LL and AIC values for the fitted volatility models with different error distributions under various cryptocurrencies.

BTC	**Distribution**					
Models	NORMD		STD		GED	
	LL	AIC	LL	AIC	LL	AIC
GARCH(1,1)	4787.84	-9565.68	5241.58	-10471.16	5244.25	-10476.50
GJRGARCH(1,1)	4789.34	-9566.68	5242.11	-10470.22	5245.50	-10477.00
TGARCH(1,1)	4804.05	-9596.10	5255.86	-10497.72	5258.76	-10503.52
MSGARCH(1,1)	5247.03	-10470.06	5294.47	-10560.94	5294.46	-10560.92
TV-MSGARCH$_{S}$(1,1)	5249.30	-10470.60	5299.54	-10567.08	**5300.61**	**-10569.22**
TV-MSGARCH$_{lds}$(1,1)	5247.24	-10466.48	5298.70	-10565.40	5294.75	-10557.50
TV-MSGARCH$_{lnV}$(1,1)	5248.11	-10468.22	5296.66	-10561.32	5299.46	-10566.92
ETH	**Distribution**					
Models	NORMD		STD		GED	
	LL	AIC	LL	AIC	LL	AIC
GARCH(1,1)	1273.22	-2536.44	1337.41	-2662.82	1349.54	-2687.08
GJRGARCH(1,1)	1273.24	-2534.48	1337.44	-2660.88	1349.65	-2685.30
TGARCH(1,1)	1278.64	-2545.28	1337.45	-2660.90	1351.84	-2689.68
MSGARCH(1,1)	1357.54	-2691.08	1361.45	-2694.90	1365.55	-2703.10
TV-MSGARCH$_{S}$(1,1)	1357.62	-2687.24	1365.97	-2699.94	**1368.69**	**-2705.38**
TV-MSGARCH$_{lds}$(1,1)	1358.79	-2689.58	1362.70	-2693.40	1366.25	-2700.50
TV-MSGARCH$_{lnV}$(1,1)	1359.04	-2690.08	1363.93	-2695.86	1366.55	-2701.10

Table 6.1, continued.

XRP	Distribution					
Models	NORMD		STD		GED	
	LL	AIC	LL	AIC	LL	AIC
GARCH(1,1)	1138.64	-2267.28	1511.92	-3011.84	1486.61	-2961.22
GJRGARCH(1,1)	1165.37	-2318.74	1514.11	-3014.22	1488.22	-2962.44
TGARCH(1,1)	1154.41	-2296.82	1514.92	-3015.84	1487.08	-2960.16
MSGARCH(1,1)	1489.11	-2954.22	1544.48	-3060.96	1514.45	-3000.90
TV-MSGARCH$_{S}$(1,1)	1495.62	-2963.24	1546.41	-3060.82	1523.51	-3015.02
TV-MSGARCH$_{ldS}$(1,1)	1500.21	-2972.42	1545.38	-3058.76	1526.26	-3020.52
TV-MSGARCH$_{lnV}$(1,1)	1494.90	-2961.80	**1566.40**	**-3100.80**	1533.38	-3034.76
BCH	**Distribution**					
Models	NORMD		STD		GED	
	LL	AIC	LL	AIC	LL	AIC
GARCH(1,1)	242.46	-474.92	265.72	-519.44	266.27	-520.54
GJRGARCH(1,1)	243.26	-474.52	266.28	-518.56	266.88	-519.76
TGARCH(1,1)	244.29	-476.58	266.39	-518.78	267.01	-520.02
MSGARCH(1,1)	270.78	-517.56	289.68	-551.36	297.25	-566.50
TV-MSGARCH$_{S}$(1,1)	274.67	-521.34	302.23	-572.46	303.46	-574.92
TV-MSGARCH$_{ldS}$(1,1)	289.01	-550.02	296.35	-560.70	**307.29**	**-582.58**
TV-MSGARCH$_{lnV}$(1,1)	291.95	-555.90	299.21	-566.42	300.10	-568.20
EOS	**Distribution**					
Models	NORMD		STD		GED	
	LL	AIC	LL	AIC	LL	AIC
GARCH(1,1)	259.88	-509.76	276.49	-540.98	259.04	-506.08
GJRGARCH(1,1)	259.92	-507.84	276.80	-539.60	265.75	-517.50
TGARCH(1,1)	263.93	-515.86	278.00	-542.00	269.20	-524.40
MSGARCH(1,1)	288.75	-553.50	298.61	-569.22	290.26	-552.52
TV-MSGARCH$_{S}$(1,1)	292.82	-557.64	302.19	-572.38	311.51	-591.02
TV-MSGARCH$_{ldS}$(1,1)	291.72	-555.44	318.59	-605.18	299.61	-567.22
TV-MSGARCH$_{lnV}$(1,1)	293.39	-558.78	**320.71**	**-609.42**	299.43	-566.86

The volatility model with the lowest value of AIC and the highest value of LL is chosen to be the best fitted model amongst others. The best fitted volatility model for BTC, ETH, XRP, BCH and EOS are presented in bold in Table 6.1. Interestingly to know, TV-MSGARCH models gave the best volatility fit for all cryptocurrencies which, in overall, also give smaller AIC values compared to other volatility models. Among all, the best fitted volatility model for BTC and ETH is TV-MSGARCH$_{S}$(1,1) model with GED, the best fitted volatility model for BCH is TV-MSGARCH$_{ldS}$(1,1) model with GED and the best fitted volatility model for XRP and EOS is TV-MSGARCH$_{lnV}$(1,1) model with STD. In addition, it is discovered that Google searches series are more preferred for BTC, ETH and BCH while trading volume is more preferred for XRP and EOS to be incorporated into the TVTP for the respective TV-MSGARCH(1,1) model. For better understanding, the best fitted volatility models for BTC, ETH, XRP, BCH and EOS are also tabulated in Table 6.2 and the following analysis and discussions are based on the respective best fitted volatility model for each of the cryptocurrencies.

Table 6.2: The best fitted volatility models for BTC, ETH, XRP, BCH and EOS.

Cryptocurrencies	**Fitted volatility models**
BTC	TV-MSGARCH$_{S}$(1,1)-GED
ETH	TV-MSGARCH$_{S}$(1,1)-GED
XRP	TV-MSGARCH$_{lnV}$(1,1)-STD
BCH	TV-MSGARCH$_{ldS}$(1,1)-GED
EOS	TV-MSGARCH$_{lnV}$(1,1)-STD

The parameter estimates reported in Appendix B show that the best fitted model for BTC, ETH, BCH and EOS display evidence of "mean-reverting" effect particularly in the low volatility regime (regime 1) in which today's return relates negatively to yesterday's return. On the contrary, XRP fitted model displays "mean-reverting" effect in both of the regimes. The "mean-reverting" effect gradually causes the return series to move towards its average value in the long run. When the returns in the low volatility regime are below the average value, the fitted model pushes the returns back up towards its average value which often happens after the market recession. Similarly, when the returns in the high volatility regime are above the average value, the fitted model pushes the returns down towards its average value to avoid continuing explosive volatility. In addition, all of the best volatility models for BTC, ETH, XRP, BCH and EOS fulfil the stationary condition as discussed by Bauwens et al. (2010).

Next, with the employment of TV-MSGARCH model, we notice that the exogenous variables embedded in the TVTP contribute differently on the two regimes. Note that, negative (positive) values of regime 1 coefficients d_1 imply that, on average, a positive change in the respective exogenous variables increases (decreases) the likelihood function from regime 1 to regime 2. The same is also assumed for regime 2 whereby the negative (positive) values of regime 2 coefficients d_2 imply that, on average, a positive change in the respective exogenous variables increases (decreases) the likelihood function from regime 2 to regime 1. Following this, it is discovered that the probability of BTC and BCH staying in the same regime increases when the Google searches series on the respective cryptocurrencies increases. However, for ETH, an increase in ETH Google searches series decreases the probability of the returns to stay in the same regime and increases the probability of regime transition from either regime 1 (low volatility regime) to regime 2 (high volatility regime) or the other way round. Moreover, the returns of XRP are more likely to stay in the same regime when XRP trading volume increases. In contrast, returns of EOS tends to move from regime 2 (high volatility regime) to regime 1 (low volatility regime) and stay in the low volatility regime when EOS trading volume increases. Despite both Google searches series and trading volume are the direct measure of public interest, it is noticed that the two variables have different impact on different cryptocurrencies. These behaviours are important to facilitate and induce the flexibility of TV-MSGARCH models so that the jumps in the returns of cryptocurrencies can be accounted for at various phases of economic expansion and depression.

To provide in-depth understanding on the adequacy of the best fitted models in capturing the ARCH effects, Ljung-Box test is carried out on the standardised residuals and squared standardised residuals discussed in the following section.

6.2 Ljung-Box test on standardised residuals of fitted models

Ljung-Box test statistics are computed on the standardised residuals and the squared standardised residuals to examine if the conditional heteroscedasticity still exists after the model fitting on the mean and volatility of cryptocurrencies. The null hypothesis of

Ljung-Box test suggests zero serial correlation in the residuals. After model fitting, the squared standardised residuals should not display any serial correlation. With that, the fitted model is perceived to be capable of capturing the ARCH effects in the returns of the cryptocurrencies. The standardised residuals are calculated as the follows:

$$\tilde{a}_t = \frac{a_t}{\sqrt{\sigma_t^2}}, \quad \text{for } t = 1, 2, \ldots T, \tag{6.2}$$

where $\{\tilde{a}_t\}$ is the series of standardised residuals that forms a sequence of i.i.d random variables if the volatility model is properly specified and estimated.

Ljung-Box test is carried out on the standardised residuals and the squared standardised residuals of the best fitted model for BTC, ETH, XRP, BCH and EOS and the p-values for Ljung-Box test are reported in Table 6.3.

Table 6.3: P-values for Ljung-Box test of the best fitted models for various cryptocurrencies.

Ljung-Box test statistic	Cryptocurrencies				
	BTC	ETH	XRP	BCH	EOS
$Q(5)$	1.4×10^{-9}*	0.0517	0.4559	0.4271	0.3185
$Q(10)$	2.9×10^{-11}*	0.0720	0.3501	0.7314	0.3224
$Q^2(10)$	0.6694	0.8985	0.9999	0.4878	0.9791

*Significance at the 5% level.
Note: $Q(m)$ and $Q^2(m)$ are the test statistics for the Ljung-Box test of lag m for standardised residuals and squared standardised residuals respectively.

There are some points worth making about Table 6.3. It is noticeable that the best fitted models are adequate in fitting the mean and the conditional variance of the respective cryptocurrencies. Based on the standardised residuals, we have the p-values of $Q(5)$ and $Q(10)$ all are not significant at the 5% significance level for ETH, XRP, BCH and EOS. The Markov-switching specification in the mean equation adequately removes the serial dependence in the return series described by μ_{s_t} and ϕ_{s_t} (see Eq. (5.9)). These findings underscore the importance of integrating the Markov-switching specification in the return series in the process of volatility modelling and this manoeuvre is often lacking in the previous literature. However, the p-values of $Q(5)$ and $Q(10)$ on BTC standardised residuals both are significant at the 5% significance level. Future study may consider additional lags in the Markov-switching mean equation to curb with the remaining serial correlation left in the BTC standardised residuals. Nevertheless, all of the fitted volatility models for BTC, ETH, XRP, BCH and EOS are able to capture the ARCH effects. For model checking in capturing the ARCH effects, we have the p-values of $Q^2(10)$ on the squared standardised residuals are not significant at the 5% significance level for all BTC, ETH, XRP, BCH and EOS. The volatility clustering in the returns of cryptocurrencies have been well-captured by the respective model at the 5% significance level.

6.3 Marginal contributions of TV-MSGARCH models

As discussed in the previous sections, TV-MSGARCH models shows superiority in volatility estimation over other volatility models for BTC, ETH, XRP, BCH and EOS. To further evaluate the improvement of TVTP in TV-MSGARCH model against constant transition probabilities in MSGARCH model, we utilise the approach from Filardo (1994) to assess the marginal contributions of TVTP.

Weighted transition probability (WTP) is calculated for regime 1 and regime 2 for every time t, denoted as $\mathrm{WTP}(p_{11t})$ and $\mathrm{WTP}(p_{22t})$, by taking the difference between the transition probabilities at time t and the average of transition probabilities over time, then weighted by the filtered probabilities $\mathbb{P}(s_t = j|F_t)$ where $j = 1, 2$ and F_t represents the past observed returns up to time t.

The respective formulas for WTP(p_{11t}) and WTP(p_{22t}) are given as follows:

$$\mathrm{WTP}(p_{11t}) = (p_{11t} - \bar{p}_1) \times \mathbb{P}(s_t = 1|F_t), \tag{6.3}$$

and

$$\mathrm{WTP}(p_{22t}) = (p_{22t} - \bar{p}_2) \times \mathbb{P}(s_t = 2|F_t), \tag{6.4}$$

where $\bar{p}_i$ is the mean of $p_{ii,t}$ such that $\bar{p}_i = \frac{1}{T}\sum_{t=1}^{T} p_{ii,t}$ for $i = 1, 2$ and T is the length of data. As indicated by Filardo (1994), the marginal contributions can be examined by their deviations from zero based on Eq. (6.3) and Eq. (6.4).

The marginal contributions of TVTP in TV-MSGARCH models for BTC, ETH, XRP, BCH and EOS are illustrated in Figures 6.1 to 6.5. It is pronounced that TVTP does provide additional information to the TV-MSGARCH models. It is observed that BTC Google searches series shows significant contribution to the flexibility in the transition probabilities of TV-MSGARCH model around the turning of years 2013/2014 which is also the BTC historical incident, popularly known as BTC price crash 2013. Besides, the spikes of WTP in year 2018 correspond strongly for p_{22t} and less for p_{11t} for BTC. By comparing the WTP(p_{11t}) and WTP(p_{22t}) of ETH, we notice the ETH Google searches series appears to have similar impact on p_{11t} and p_{22t} in the mid-year of 2017 and also at the turning of year 2017/2018. As for XRP, the contribution of XRP trading volume on the transition probabilities can be clearly seen starting from the mid-year of 2017 when the WTP(p_{11t}) and WTP(p_{22t}) of XRP show significant deviations from zero. For BCH, there are three periods in year 2017 that BCH trading volume has strong contribution on the transition probabilities. Besides, the WTP (p_{11t}) and WTP (p_{22t}) of EOS are distinctive in the sense that the marginal contribution of TVTP for regime 1 affected by

EOS trading volume are more prominently observed while the marginal contribution of TVTP for regime 2 are minimal.

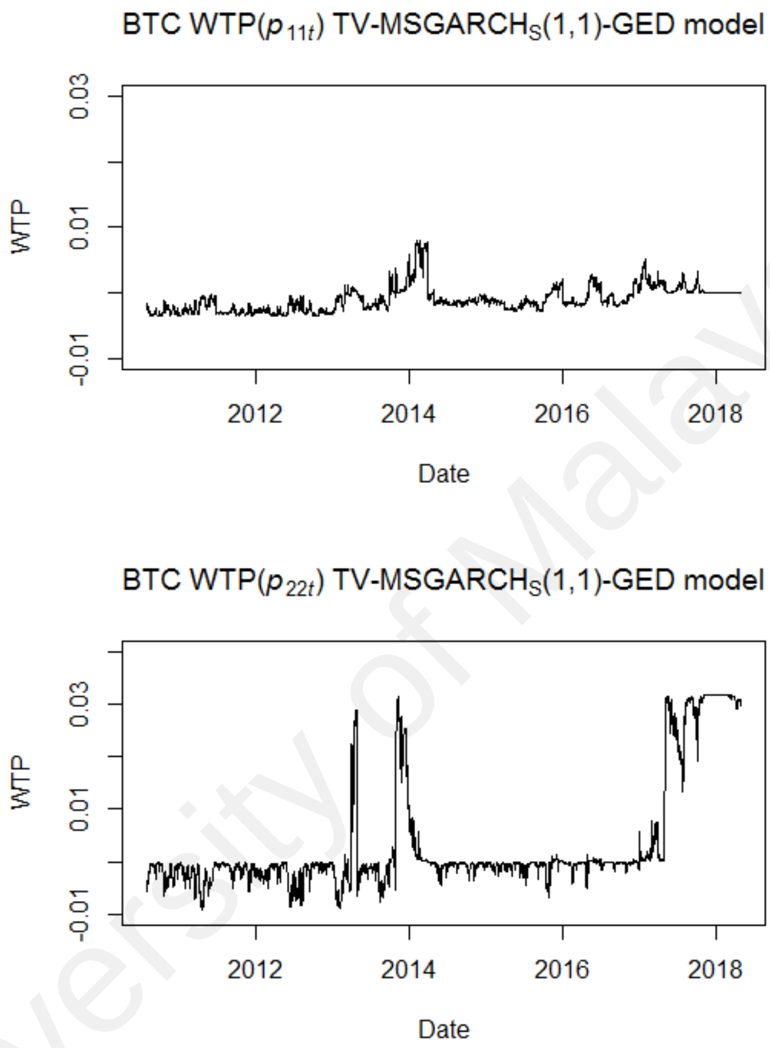

Figure 6.1: Marginal contributions of TVTP for TV-MSGARCH$_S$(1,1)-GED model for BTC.

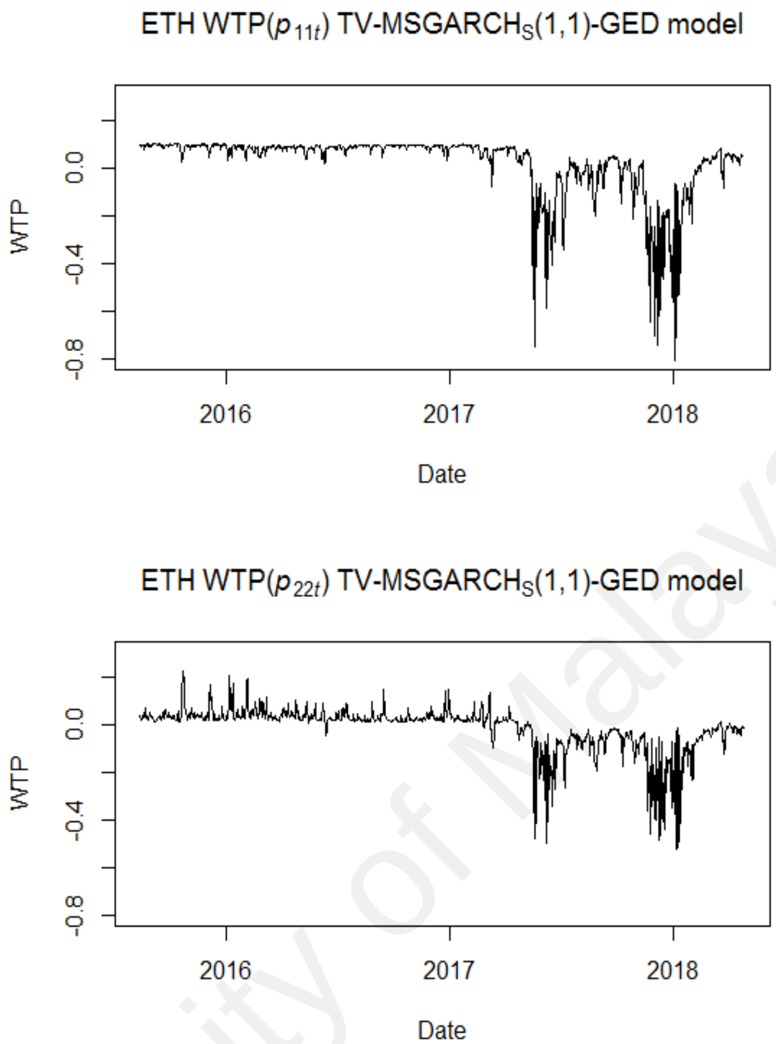

Figure 6.2: Marginal contributions of TVTP for TV-MSGARCH$_S$(1,1)-GED model for ETH.

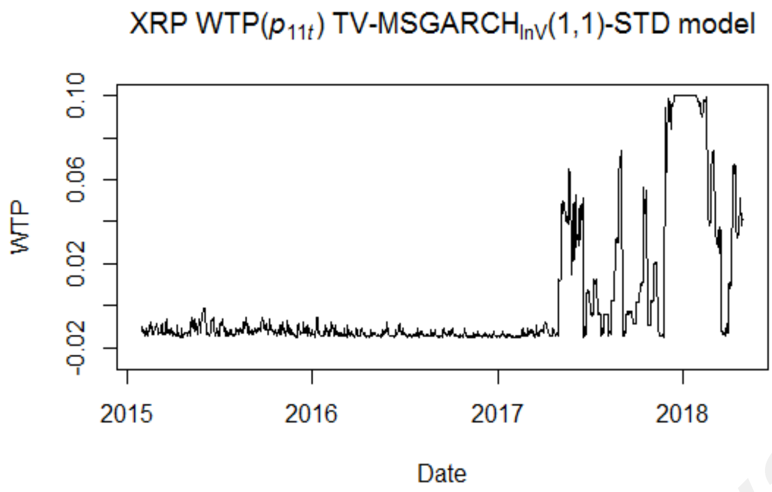

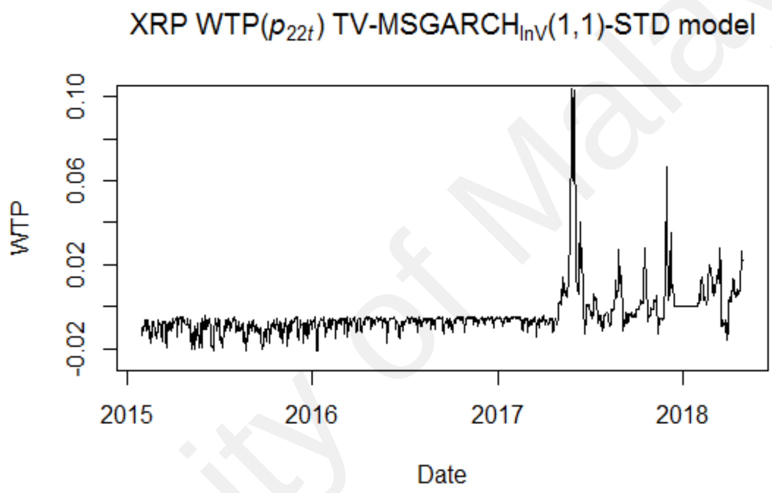

Figure 6.3: Marginal contributions of TVTP for TV-MSGARCH$_{lnV}$(1,1)-STD model for XRP.

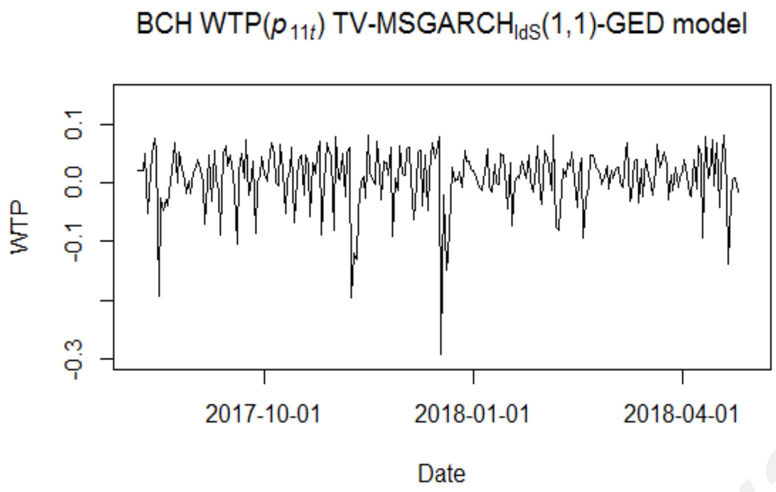

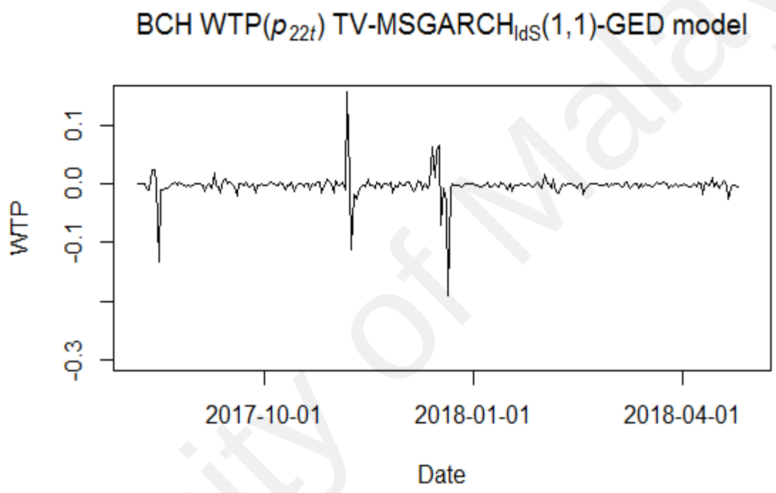

Figure 6.4: Marginal contributions of TVTP for TV-MSGARCH$_{IdS}$(1,1)-GED model for BCH.

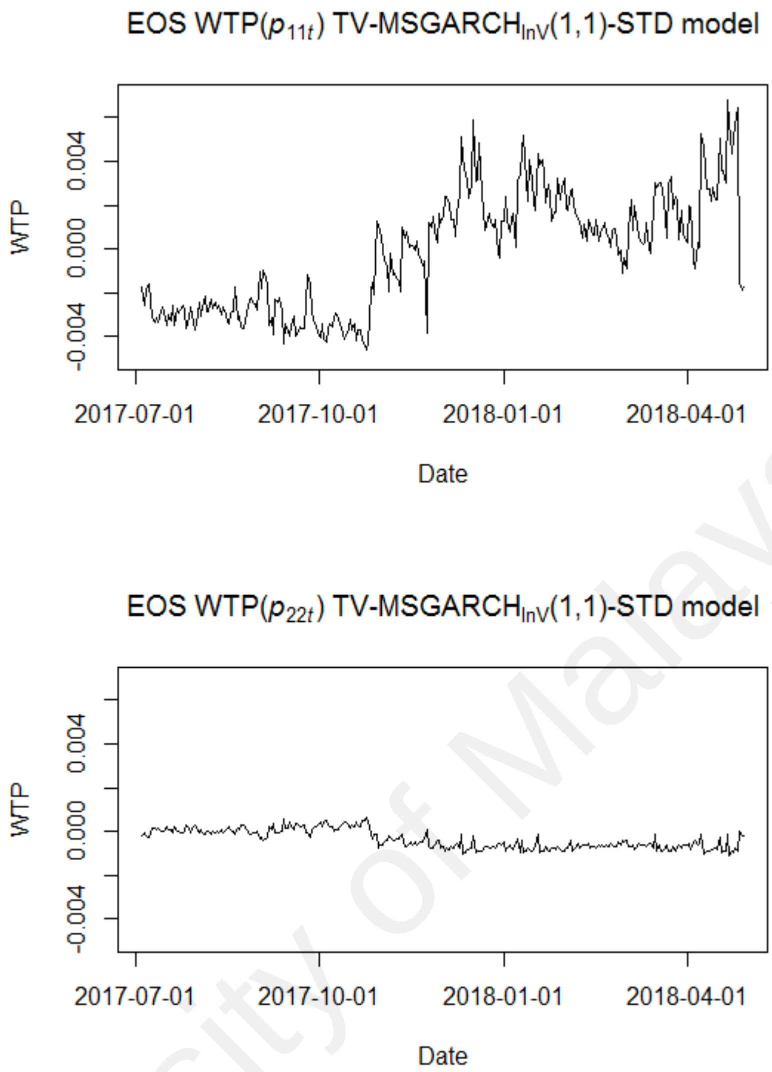

Figure 6.5: Marginal contributions of TVTP for TV-MSGARCH$_{lnV}$(1,1)-STD model for EOS.

CHAPTER 7 : FORECASTING AND APPLICATIONS

Volatility forecasting performance is important to finance researchers from both academia and financial industry. These forecasts will form the basis of risk management decision making as the forecasts represent the future dynamics of financial time series and the foreseeable undertaking risks. With that, this chapter computes one-day ahead volatility forecasts from 1 May 2018 to 31 July 2018, resulting in $h = 92$ forecasting points for BTC, ETH, XRP, BCH and EOS. One-day ahead rolling window technique with window size T (subject to the data length of each cryptocurrency tabulated in Table 3.1) was used to predict the volatility of cryptocurrencies.

Philip et al. (2018) investigated 224 cryptocurrencies and found out that the returns of most of the cryptocurrencies are heavy-tailed and the error distributions follow STD. Hence, the volatility models used in the forecasting application for BTC, ETH, XRP, BCH and EOS are incorporated with STD, denoted as GARCH(1,1)-STD model, TGARCH(1,1)-STD model GJRGARCH(1,1)-STD model, MSGARCH(1,1)-STD model, TV-MSGARCH$_{S}$(1,1)-STD model, TV-MSGARCH$_{ldS}$(1,1)-STD model and TV-MSGARCH$_{lnV}$(1,1)-STD model.

7.1 Loss functions and model confidence set procedure

The performances of forecasts are assessed by deriving the loss functions. Patton (2011) studied the properties of nine loss functions and suggested that only mean square error (MSE) and quasi-likelihood (QLIKE) are robust to the noise of volatility proxy.

The formulas for MSE and QLIKE are given below:

$$\text{MSE} = h^{-1} \sum_{t=T+1}^{T+h} \left\{\hat{a}_t^2 - \hat{\sigma}_t^2\right\}^2, \tag{7.1}$$

and

$$\text{QLIKE} = h^{-1} \sum_{t=T+1}^{T+h} \left\{\frac{\hat{a}_t^2}{\hat{\sigma}_t^2} - \log\left(\frac{\hat{a}_t^2}{\hat{\sigma}_t^2}\right) - 1\right\}, \tag{7.2}$$

where $\hat{a}_t$ is the proxy volatility and $\hat{\sigma}_t^2$ is the predicted volatility. $\hat{a}_t$ is estimated from Eq. (5.2) for single-regime GARCH-type models while $\hat{a}_t$ is estimated from Eq. (5.21) for MSGARCH(1,1) model and TV-MSGARCH(1,1) model. Table 7.1 shows the forecast errors obtained by MSE and QLIKE where the volatility model with the least forecast errors recorded in bold.

Table 7.1: Comparison of forecast errors using MSE and QLIKE for the fitted volatility models under various cryptocurrencies.

BTC		
Model	**MSE**	**QLIKE**
GARCH(1,1)-STD	5.56×10^{-6}	1.8222
GJRGARCH(1,1)-STD	5.87×10^{-6}	1.8416
TGARCH(1,1)-STD	1.36×10^{-5}	2.0013
MSGARCH(1,1)-STD	**5.51×10^{-6}**	1.7747
TV-MSGARCH$_{S}$(1,1)-STD	7.47×10^{-6}	1.7791
TV-MSGARCH$_{lds}$(1,1)-STD	6.13×10^{-6}	**1.7664**
TV-MSGARCH$_{lnV}$(1,1)-STD	6.17×10^{-6}	1.8021
ETH		
Model	**MSE**	**QLIKE**
GARCH(1,1)-STD	1.95×10^{-5}	2.0931
GJRGARCH(1,1)-STD	2.01×10^{-5}	2.0451
TGARCH(1,1)-STD	1.81×10^{-5}	2.1077
MSGARCH(1,1)-STD	3.70×10^{-5}	2.1167
TV-MSGARCH$_{S}$(1,1)-STD	1.61×10^{-5}	1.9105
TV-MSGARCH$_{lds}$(1,1)-STD	1.53×10^{-5}	1.9102
TV-MSGARCH$_{lnV}$(1,1)-STD	**1.50×10^{-5}**	**1.8418**

Table 7.1, continued.

XRP		
Model	**MSE**	**QLIKE**
GARCH(1,1)-STD	1.95×10^{-5}	2.1641
GJRGARCH(1,1)-STD	2.01×10^{-5}	**1.7127**
TGARCH(1,1)-STD	1.81×10^{-5}	2.0669
MSGARCH(1,1)-STD	3.70×10^{-5}	2.0142
TV-MSGARCH$_{S}$(1,1)-STD	1.61×10^{-5}	1.8456
TV-MSGARCH$_{Ids}$(1,1)-STD	1.53×10^{-5}	1.8453
TV-MSGARCH$_{InV}$(1,1)-STD	$\mathbf{1.50\times10^{-5}}$	1.7863
BCH		
Model	**MSE**	**QLIKE**
GARCH(1,1)-STD	7.10×10^{-5}	1.9256
GJRGARCH(1,1)-STD	8.48×10^{-5}	1.9746
TGARCH(1,1)-STD	7.20×10^{-5}	1.9126
MSGARCH(1,1)-STD	3.84×10^{-5}	1.7178
TV-MSGARCH$_{S}$(1,1)-STD	$\mathbf{2.76\times10^{-5}}$	**1.5596**
TV-MSGARCH$_{Ids}$(1,1)-STD	5.21×10^{-5}	1.9122
TV-MSGARCH$_{InV}$(1,1)-STD	5.51×10^{-5}	2.0518
EOS		
Model	**MSE**	**QLIKE**
GARCH(1,1)-STD	1.69×10^{-4}	2.2082
GJRGARCH(1,1)-STD	1.11×10^{-4}	2.2495
TGARCH(1,1)-STD	1.63×10^{-4}	2.1478
MSGARCH(1,1)-STD	1.02×10^{-4}	2.1784
TV-MSGARCH$_{S}$(1,1)-STD	1.11×10^{-4}	2.1260
TV-MSGARCH$_{Ids}$(1,1)-STD	$\mathbf{9.70\times10^{-5}}$	2.0604
TV-MSGARCH$_{InV}$(1,1)-STD	1.26×10^{-4}	**1.8777**

Results from Table 7.1 report that both MSE and QLIKE suggest the best volatility models for forecasting application is TV-MSGARCH$_{InV}$(1,1)-STD model for ETH and TV-MSGARCH$_{S}$(1,1)-STD model for BCH. However, in the case of BTC, XRP and EOS, MSE and QLIKE imply contradict results. Although MSE and QLIKE are both popular loss functions used very often, their formulations are different. MSE is a loss function based on forecast error, $\hat{a}_t^2 - \hat{\sigma}_t^2$ whereas QLIKE is a loss function based on standardised forecast error, $\frac{\hat{a}_t^2}{\hat{\sigma}_t^2}$. Due to this reasoning, Patton (2011) was motivated to use QLIKE rather than MSE in volatility forecasting application especially when extreme observations are observed since MSE is sensitive to extreme observations and the level of volatility return.

With the prominent fluctuations in cryptocurrencies returns, it is believed that QLIKE behaves as a better indicator to select the best forecasting model. To sum up, we are in the view that TV-MSGARCH$_{\mathrm{ldS}}$(1,1)-STD model gives the best forecasting performance for BTC with lowest QLIKE value and similarly, GJRGARCH(1,1)-STD model for XRP and TV-MSGARCH$_{\mathrm{lnV}}$(1,1)-STD model for EOS.

To further assess the forecasting performance of the respective volatility models, MCS procedure by Hansen et al. (2011) is employed. The forecasting performance for the volatility models is evaluated based on EPA with QLIKE. The ranks of the volatility models are reported in Table 7.2 below.

Table 7.2: Comparison of forecasting performance on MCS procedure for the fitted volatility models under various cryptocurrencies.

BTC			
Model eliminated: None			
Models	**Rank**	**Test statistic**	**P-value**
GARCH(1,1)-STD	5	-0.0736	1.0000
GJRGARCH(1,1)-STD	6	0.2309	0.9932
TGARCH(1,1)-STD	7	2.0267	0.1176
MSGARCH(1,1)-STD	1	-1.0892	1.0000
TV-MSGARCH$_{\mathrm{S}}$(1,1)-STD	4	-0.5894	1.0000
TV-MSGARCH$_{\mathrm{ldS}}$(1,1)-STD	2	-1.0277	1.0000
TV-MSGARCH$_{\mathrm{lnV}}$(1,1)-STD	3	-0.7557	1.0000
ETH			
Model eliminated: None			
Models	**Rank**	**Test statistic**	**P-value**
GARCH(1,1)-STD	6	1.2147	0.4878
GJRGARCH(1,1)-STD	4	0.6591	0.8636
TGARCH(1,1)-STD	7	1.3852	0.3816
MSGARCH(1,1)-STD	5	0.7397	0.8146
TV-MSGARCH$_{\mathrm{S}}$(1,1)-STD	2	-1.3630	1.0000
TV-MSGARCH$_{\mathrm{ldS}}$(1,1)-STD	3	-1.0033	1.0000
TV-MSGARCH$_{\mathrm{lnV}}$(1,1)-STD	1	-2.3782	1.0000
XRP			
Model eliminated: GARCH(1,1)-STD, TGARCH(1,1)-STD, MSGARCH(1,1)-STD			
Models	**Rank**	**Test statistic**	**P-value**
GJRGARCH(1,1)-STD	1	-1.4012	1.0000
TV-MSGARCH$_{\mathrm{S}}$(1,1)-STD	4	1.3622	0.3392
TV-MSGARCH$_{\mathrm{ldS}}$(1,1)-STD	3	1.1629	0.4646
TV-MSGARCH$_{\mathrm{lnV}}$(1,1)-STD	2	-0.1789	1.0000

Table 7.2, continued.

BCH			
Model eliminated: None			
Models	**Rank**	**Test statistic**	**P-value**
GARCH(1,1)-STD	5	0.9818	0.7702
GJRGARCH(1,1)-STD	6	1.2168	0.6084
TGARCH(1,1)-STD	4	0.7247	0.9126
MSGARCH(1,1)-STD	2	-1.2142	1.0000
TV-MSGARCH$_S$(1,1)-STD	1	-6.2041	1.0000
TV-MSGARCH$_{ldS}$(1,1)-STD	3	0.4491	0.9872
TV-MSGARCH$_{lnV}$(1,1)-STD	7	1.2979	0.5498
EOS			
Model eliminated: None			
Models	**Rank**	**Test statistic**	**P-value**
GARCH(1,1)-STD	6	1.3241	0.4856
GJRGARCH(1,1)-STD	7	2.1438	0.1058
TGARCH(1,1)-STD	4	0.3047	0.9984
MSGARCH(1,1)-STD	5	0.4851	0.9762
TV-MSGARCH$_S$(1,1)-STD	3	0.0616	1.0000
TV-MSGARCH$_{ldS}$(1,1)-STD	2	-0.8378	1.0000
TV-MSGARCH$_{lnV}$(1,1)-STD	1	-2.0613	1.0000

The implementation of MCS procedure is completed via R package MCS and evaluated using 5000 bootstrap replications tested at the 5% significance level. The corresponding forecasting performance is ranked in column 2 of Table 7.2 in such a way that the lower the value of test statistic, the higher the rank. The best volatility model for forecasting application evaluated on MCS procedure is MSGARCH(1,1)-STD model for BTC, TV-MSGARCH$_{lnV}$(1,1)-STD model for ETH, GJRGARCH(1,1)-STD model for XRP, TV-MSGARCH$_S$(1,1)-STD model for BCH and TV-MSGARCH$_{lnV}$(1,1)-STD for EOS. In addition, all of the TV-MSGARCH(1,1) models appear to be belonging to SSM. The forecasting superiority of TV-MSGARCH(1,1) models over single-regime GARCH-type models is again confirmed based on the rankings of these models. It is also observed that TV-MSGARCH models always occupy the first few ranks according to MCS procedure while GARCH-type models are often ranked the last, mostly due to their restricted volatility specifications which are not flexible to account for the volatility of cryptocurrencies.

7.2 Value-at-risk backtests

The accuracy of VaR forecasts are evaluated based on UC test, CC test and DQ test which can be implemented via `R` package `GAS`. Optimal volatility forecasting models should provide an accurate VaR coverage with minimum percentage of VaR violations. The p-values for UC test, CC test and DQ test are given in Table 7.3 on various confidence limits.

Table 7.3: Comparison of VaR backtest results for different confidence limits for the fitted volatility models under various cryptocurrencies.

BTC	**Lower confidence limit, ν_1**			**Upper confidence limit, ν_2**		
Model	**0.05**	**0.025**	**0.005**	**0.95**	**0.975**	**0.995**
GARCH(1,1)-STD						
UC test	0.2847	0.3033	0.0928	0.4150	0.0843	0.1739
CC test	0.4654	0.4898	0.2329	0.1270	0.0399*	0.3967
DQ test	0.0286*	0.0435*	0.0003*	0.2500	0.0000*	0.9964
GJRGARCH(1,1)-STD						
UC test	0.5215	0.3033	0.0928	0.4150	0.6550	0.3369
CC test	0.5329	0.4898	0.2329	0.1270	0.1602	0.6306
DQ test	0.1429	0.0607	0.0009*	0.2620	0.0196*	0.9996
TGARCH(1,1)-STD						
UC test	0.4150	0.8377	0.3369	0.0021*	0.0309*	0.3369
CC test	0.6476	0.9362	0.6306	0.0089*	0.0974	0.6306
DQ test	0.8703	0.9493	0.9996	0.7048	0.9443	0.9996
MSGARCH(1,1)-STD						
UC test	0.8502	0.6550	0.0928	0.4150	0.3290	0.3369
CC test	0.7344	0.8170	0.2329	0.1270	0.6141	0.6306
DQ test	0.3428	0.1619	0.1768	0.2469	0.9443	0.9996
TV-MSGARCH$_{S}$(1,1)-STD						
UC test	0.4150	0.8377	0.3369	0.4150	0.3290	0.3369
CC test	0.6476	0.9362	0.6306	0.1155	0.6141	0.6306
DQ test	0.9348	0.8575	0.9996	0.8988	0.9443	0.9996
TV-MSGARCH$_{ldS}$(1,1)-STD						
UC test	0.7693	0.6550	0.4901	0.4150	0.3290	0.3369
CC test	0.7969	0.8170	0.7794	0.1270	0.6141	0.6306
DQ test	0.5719	0.1742	0.1030	0.2404	0.9443	0.9996
TV-MSGARCH$_{lnV}$(1,1)-STD						
UC test	0.8502	0.6550	0.4901	0.4150	0.3290	0.3369
CC test	0.7344	0.8170	0.7794	0.1270	0.6141	0.6306
DQ test	0.4402	0.2850	0.3198	0.2746	0.9443	0.9996

*Significance at the 5% level.

Table 7.3, continued.

ETH	Lower confidence limit, ν_1			Upper confidence limit, ν_2		
Model	**0.05**	**0.025**	**0.005**	**0.95**	**0.975**	**0.995**
GARCH(1,1)-STD						
UC test	0.5215	0.6550	0.4901	0.0382*	0.9341	0.1739
CC test	0.5497	0.8170	0.7794	0.1155	0.9856	0.3967
DQ test	0.0758	0.3088	0.4027	0.7048	0.9964	0.9964
GJRGARCH(1,1)-STD						
UC test	0.5215	0.6550	0.4901	0.0382*	0.3290	0.3369
CC test	0.5497	0.8170	0.7794	0.1155	0.6141	0.6306
DQ test	0.0853	0.3240	0.4191	0.7048	0.9443	0.9996
TGARCH(1,1)-STD						
UC test	0.5215	0.6550	0.4901	0.0382*	0.3290	0.3369
CC test	0.5497	0.8170	0.7794	0.1155	0.6141	0.6306
DQ test	0.0547	0.1094	0.1197	0.7048	0.9443	0.9996
MSGARCH(1,1)-STD						
UC test	0.7693	0.8377	0.3369	0.0382*	0.3290	0.3369
CC test	0.7969	0.9362	0.6306	0.1155	0.6141	0.6306
DQ test	0.3069	0.8605	0.9996	0.7048	0.9443	0.9996
TV-MSGARCH$_S$(1,1)-STD						
UC test	0.5215	0.3033	0.4901	0.0382*	0.3290	0.3369
CC test	0.5497	0.4898	0.7794	0.1155	0.6141	0.6306
DQ test	0.1041	0.2227	0.4186	0.7048	0.9443	0.9996
TV-MSGARCH$_{ldS}$(1,1)-STD						
UC test	0.2847	0.3033	0.4901	0.0382*	0.3290	0.3369
CC test	0.4237	0.4898	0.7794	0.1155	0.6141	0.6306
DQ test	0.1041	0.2330	0.3829	0.7048	0.9443	0.9996
TV-MSGARCH$_{lnV}$(1,1)-STD						
UC test	0.5215	0.3033	0.4901	0.0382*	0.3290	0.3369
CC test	0.5497	0.4898	0.7794	0.1155	0.6141	0.6306
DQ test	0.0762	0.1810	0.2658	0.7048	0.9443	0.9996

*Significance at the 5% level.

Table 7.3, continued.

XRP	Lower confidence limit, ν_1			Upper confidence limit, ν_2		
Model	**0.05**	**0.025**	**0.005**	**0.95**	**0.975**	**0.995**
GARCH(1,1)-STD						
UC test	0.1696	0.3364	0.3395	0.0022*	0.1762	0.1762
CC test	0.3720	0.6229	0.6337	0.0094	0.4007	0.4007
DQ test	0.8671	0.9642	0.9996	0.7112	0.9966	0.9966
GJRGARCH(1,1)-STD						
UC test	0.8312	0.6423	0.4847	0.0401*	0.3364	0.3395
CC test	0.7283	0.8095	0.7747	0.1203	0.6229	0.6337
DQ test	0.3014	0.3592	0.1220	0.8818	0.9891	0.9996
TGARCH(1,1)-STD						
UC test	0.1696	0.3364	0.3395	0.0401*	0.0318	0.3395
CC test	0.3720	0.6229	0.6337	0.1203	0.0999	0.6337
DQ test	0.8484	0.9626	0.9996	0.8765	0.9460	0.9996
MSGARCH(1,1)-STD						
UC test	0.4279	0.3364	0.3395	0.0401*	0.3364	0.3395
CC test	0.6585	0.6229	0.6337	0.1203	0.6229	0.6337
DQ test	0.8717	0.9626	0.9996	0.8917	0.9938	0.9996
TV-MSGARCH$_S$(1,1)-STD						
UC test	0.4279	0.8505	0.3395	0.0401*	0.3364	0.3395
CC test	0.6585	0.9387	0.6337	0.1203	0.6229	0.6337
DQ test	0.7437	0.6286	0.9996	0.8701	0.9819	0.9996
TV-MSGARCH$_{ldS}$(1,1)-STD						
UC test	0.7873	0.8505	0.3395	0.0401*	0.3364	0.3395
CC test	0.8005	0.9387	0.6337	0.1203	0.6229	0.6337
DQ test	0.8683	0.8028	0.9996	0.8668	0.9938	0.9996
TV-MSGARCH$_{lnV}$(1,1)-STD						
UC test	0.7873	0.8505	0.3395	0.0022*	0.3364	0.3395
CC test	0.8005	0.0999	0.6337	0.0094*	0.0999	0.6337
DQ test	0.9666	0.9460	0.9996	0.7112	0.9460	0.9996

*Significance at the 5% level.

Table 7.3, continued.

BCH	Lower confidence limit, ν_1			Upper confidence limit, ν_2		
Model	**0.05**	**0.025**	**0.005**	**0.95**	**0.975**	**0.995**
GARCH(1,1)-STD						
UC test	0.1696	0.3364	0.3395	0.0022*	0.1762	0.1762
CC test	0.3720	0.6229	0.6337	0.0094*	0.4007	0.4007
DQ test	0.8671	0.9642	0.9996	0.7112	0.9966	0.9966
GJRGARCH(1,1)-STD						
UC test	0.8312	0.6423	0.4847	0.0401*	0.3364	0.3395
CC test	0.7283	0.8095	0.7747	0.1203*	0.6229	0.6337
DQ test	0.3014	0.3592	0.1220	0.8818	0.9891	0.9996
TGARCH(1,1)-STD						
UC test	0.1696	0.3364	0.3395	0.0401*	0.0318	0.3395
CC test	0.3720	0.6229	0.6337	0.1203	0.0999	0.6337
DQ test	0.8484	0.9626	0.9996	0.8765	0.9460	0.9996
MSGARCH(1,1)-STD						
UC test	0.4279	0.3364	0.3395	0.0401*	0.3364	0.3395
CC test	0.6585	0.6229	0.6337	0.1203	0.6229	0.6337
DQ test	0.8717	0.9626	0.9996	0.8917	0.9938	0.9996
TV-MSGARCH$_S$(1,1)-STD						
UC test	0.4279	0.8505	0.3395	0.0401*	0.3364	0.3395
CC test	0.6585	0.9387	0.6337	0.1203	0.6229	0.6337
DQ test	0.7437	0.6286	0.9996	0.8701	0.9819	0.9996
TV-MSGARCH$_{ldS}$(1,1)-STD						
UC test	0.7873	0.8505	0.3395	0.0401*	0.3364	0.3395
CC test	0.8005	0.9387	0.6337	0.1203	0.6229	0.6337
DQ test	0.8683	0.8028	0.9996	0.8668	0.9938	0.9996
TV-MSGARCH$_{lnV}$(1,1)-STD						
UC test	0.7873	0.0318	0.3395	0.0022*	0.0318	0.3395
CC test	0.8005	0.0999	0.6337	0.0094*	0.0999	0.6337
DQ test	0.9666	0.9460	0.9996	0.7112	0.9460	0.9996

* Significance at the 5% level.

Table 7.3, continued.

EOS	Lower confidence limit, ν_1			Upper confidence limit, ν_2		
Model	**0.05**	**0.025**	**0.005**	**0.95**	**0.975**	**0.995**
GARCH(1,1)-STD						
UC test	0.4150	0.3289	0.3369	0.0382*	0.9341	0.1739
CC test	0.6476	0.6141	0.6306	0.1155	0.9856	0.3967
DQ test	0.6739	0.9884	0.9996	0.8413	0.8579	0.9964
GJRGARCH(1,1)-STD						
UC test	0.4150	0.6550	0.3369	0.0382*	0.3290	0.3369
CC test	0.6476	0.8170	0.6306	0.1155	0.6141	0.6306
DQ test	0.5375	0.0885	0.9996	0.8596	0.9770	0.9996
TGARCH(1,1)-STD						
UC test	0.4150	0.6550	0.3369	0.0382*	0.3290	0.3369
CC test	0.6476	0.8170	0.6306	0.1155	0.6141	0.6306
DQ test	0.6668	0.2400	0.9996	0.8674	0.9828	0.9996
MSGARCH(1,1)-STD						
UC test	0.4150	0.6550	0.3369	0.0382	0.3290	0.3369
CC test	0.6476	0.8170	0.6306	0.1155	0.6141	0.6306
DQ test	0.7870	0.4080	0.9996	0.8618	0.9787	0.9996
TV-MSGARCH$_{S}$(1,1)-STD						
UC test	0.4150	0.6550	0.3369	0.0382*	0.3290	0.3369
CC test	0.6476	0.8170	0.6306	0.1155	0.6141	0.6306
DQ test	0.7870	0.3679	0.9996	0.8958	0.9963	0.9996
TV-MSGARCH$_{ldS}$(1,1)-STD						
UC test	0.4150	0.6550	0.3369	0.0382*	0.3290	0.3369
CC test	0.6476	0.8170	0.6306	0.1155	0.6141	0.6306
DQ test	0.7905	0.3679	0.9996	0.8422	0.9612	0.9996
TV-MSGARCH$_{lnV}$(1,1)-STD						
UC test	0.1613	0.3289	0.3369	0.0382*	0.3290	0.3369
CC test	0.3615	0.6141	0.6306	0.1155	0.6141	0.6306
DQ test	0.9708	0.9970	0.9996	0.8892	0.9942	0.9996

* Significance at the 5% level.

Results in Table 7.3 show that all volatility models do not reject null hypothesis of correct VaR forecasting for all volatility models at the 95% and 99% confidence limits with the exception of BTC. It is discovered that for BTC, the p-values are significant for GARCH(1,1)-STD model, GJRGARCH(1,1)-STD model and TGARCH(1,1)-STD model for the respective backtests. Besides, the single-regime GARCH-type models do not forecast VaR accurately even at the 99% confidence limits. On the other hand, MSGARCH(1,1) model and TV-MSGARCH(1,1) models are capable of providing reliable VaR estimates. Noteworthy, the results obtained from UC test and CC test vary from the results obtained from DQ test. More exactly, for most of the time, UC test and CC test indicate poor volatility forecasting performance at the 90% confidence limits while DQ test suggests that the VaR forecasts estimated are reliable at the 90%, 95% and 99% confidence limits. This may be due to the length of forecasting sample size is not adequate to relatively evaluate the number of exceedance or VaR violations at the 90% confidence limit. Nevertheless, UC test and CC test imply correct VaR forecasts at the 95% and 99% confidence limits. For illustration purpose, Figures 7.1 to 7.5 display the VaR plot for the best volatility model chosen from MCS procedure.

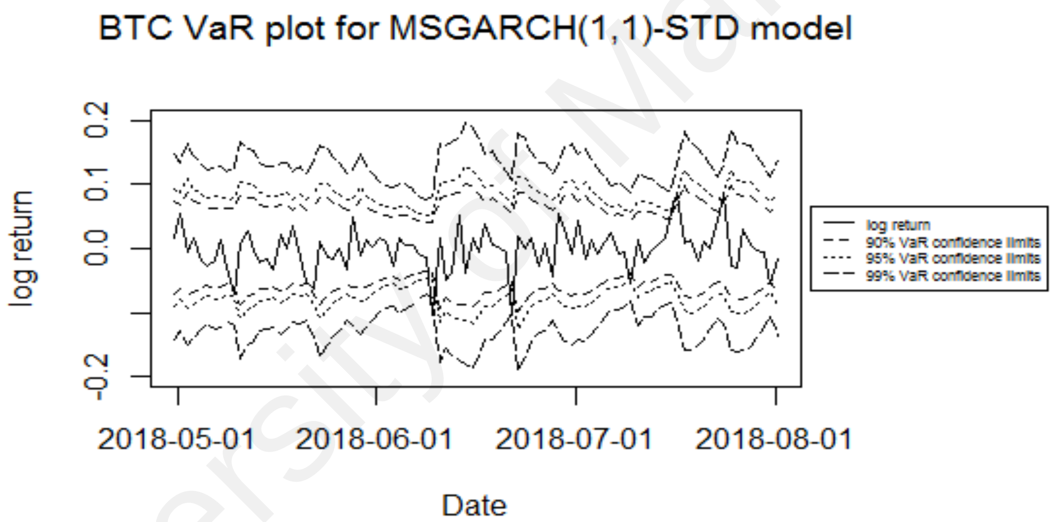

Figure 7.1: VaR plot for BTC of MSGARCH(1,1)-STD model.

The rankings of MCS procedure suggest that MSGARCH(1,1)-STD model is the best volatility model for forecasting application of BTC. However, it is also noticed that TV-MSGARCH$_{lds}$(1,1)-STD model, which has the lowest QLIKE value among other volatility models, is ranked as the second in MCS procedure. As both QLIKE and MCS procedure can be used to assess the volatility forecasting performance of a time series, the VaR plot for TV-MSGARCH$_{ldS}$(1,1)-STD model is also presented in Figure 7.6 for comparison purpose.

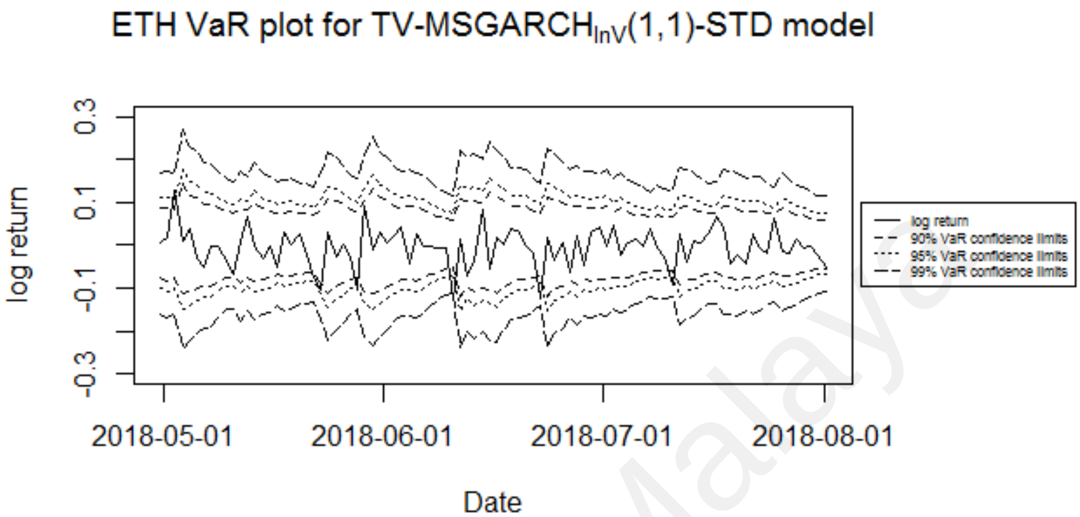

Figure 7.2: VaR plot for ETH of TV-MSGARCH$_{lnV}$(1,1)-STD model.

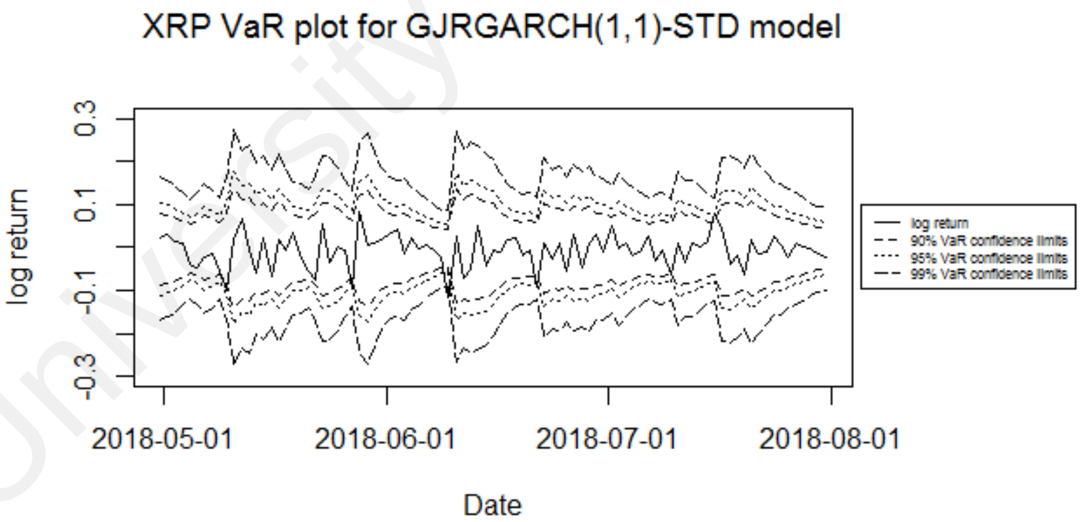

Figure 7.3: VaR plot for XRP of GJRGARCH(1,1)-STD model.

In the case of XRP, MCS procedure categorises GJRGARCH(1,1)-STD model and all TV-MSGARCH(1,1)-STD models as SSM while eliminates GARCH(1,1)-STD model, TGARCH(1,1)-STD model and MSGARCH(1,1)-STD model during the iteration process. To further evaluate the forecasting performance of TV-MSGARCH(1,1)-STD models on the volatility of XRP, the VaR plot for TV-MSGARCH$_{lnV}$(1,1)-STD model, which is also ranked as the second in MCS procedure, is provided in Figure 7.7.

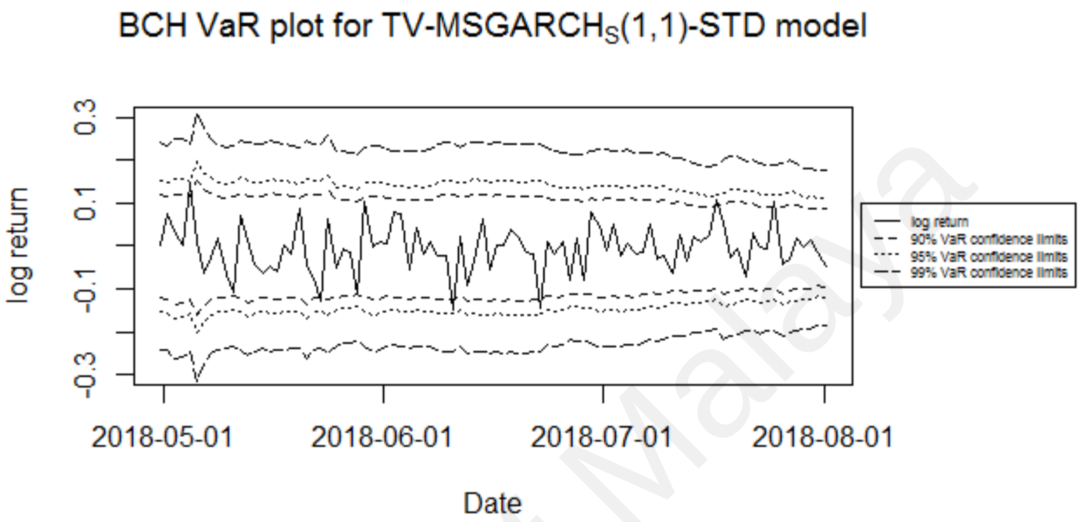

Figure 7.4: VaR plot for BCH of TV-MSGARCH$_S$(1,1)-STD model.

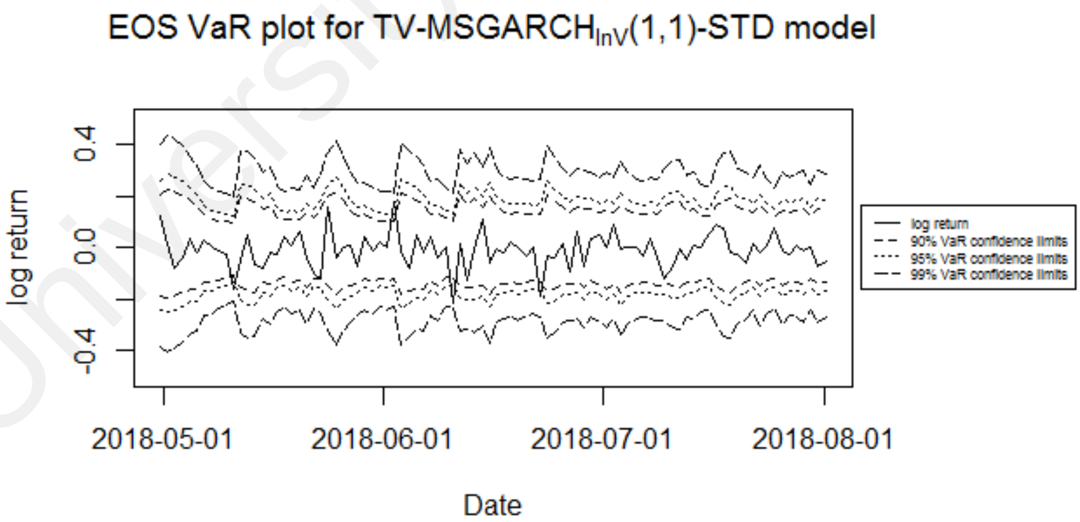

Figure 7.5: VaR plot for EOS of TV-MSGARCH$_{lnV}$(1,1)-STD model.

By comparing Figure 7.1 and Figure 7.6, we see that TV-MSGARCH$_{ldS}$(1,1)-STD model yields more conservative VaR forecasts compared to MSGARCH(1,1)-STD model for BTC. Similarly, TV-MSGARCH$_{lnV}$(1,1)-STD model also produces more conservative VaR forecasts compared to GJRGARCH(1,1)-STD model for XRP as portrayed by Figure 7.3 and Figure 7.7.

Both of the TV-MSGARCH(1,1) models appear to be overestimating the risk which would result in additional capital requirement in order to secure a particular investment. The exogenous variables incorporated in the TV-MSGARCH(1,1)-STD models for BTC and XRP do not effectively provide additional information to the volatility specifications. Nevertheless, the risk management strategy is subject to whether the decision maker is risk averse or risk taker.

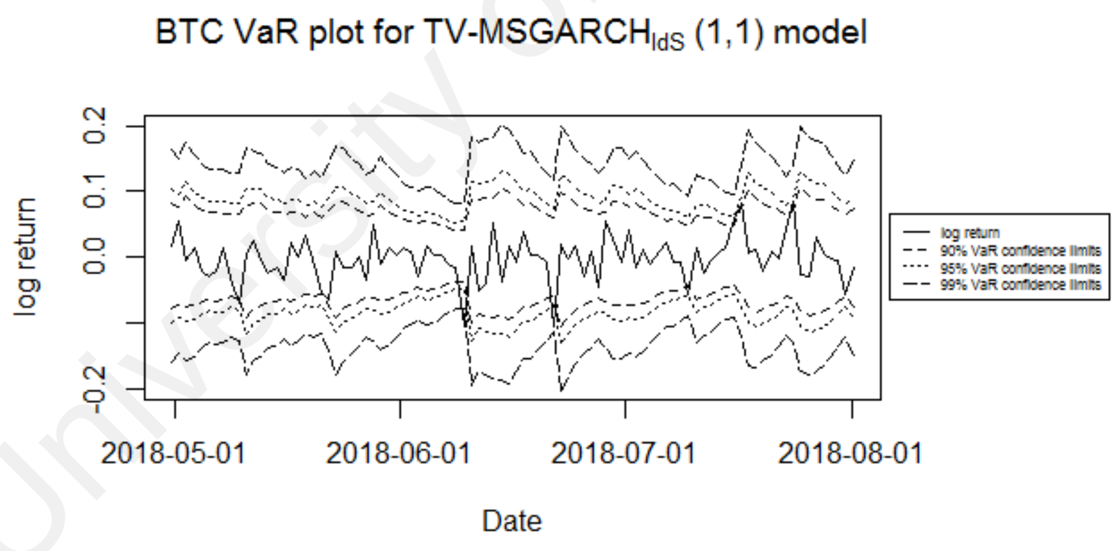

Figure 7.6: VaR plot for BTC of TV-MSGARCH$_{ldS}$(1,1)-STD model.

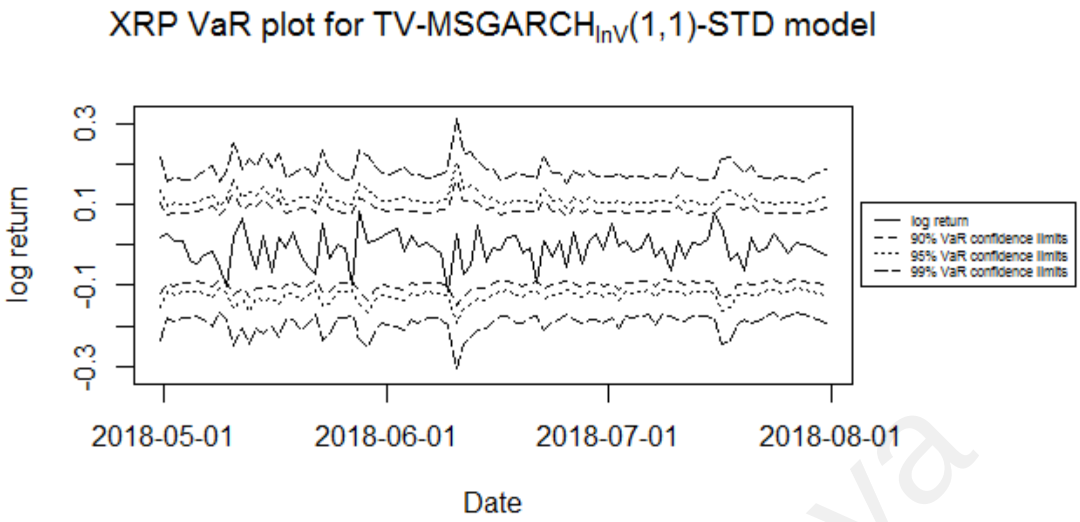

Figure 7.7: VaR plot for XRP of TV-MSGARCH$_{lnV}$(1,1)-STD model.

CHAPTER 8 : CONCLUSION AND DISCUSSIONS

In this research, the empirical findings signify the existence of change points in price, return and squared return series of cryptocurrencies data which made a suggestive point of view for financial practitioners and researchers to consider the probable instability of parameters in all aspects of cryptocurrency analysis especially for the study of volatility modelling. Frequent change points are recorded for all cryptocurrency series affected by either the underlying internal factors or external factors, for instance, trading volume and Google searches series retrieved from Google Trends. Besides, the cryptocurrency indices, namely CRIX and CCI30, both consist of a moderate number of cryptocurrencies based on their respective selection method, appear to be inappropriate to be used directly to compare and contrast with the cryptocurrencies in the practical applications within a presumed period since the turnover rates of cryptocurrencies based on their rankings of market capitalisation are high. The location and number of change points detected in CRIX and CCI30 series are not closely consistent with the results detected in the top ten cryptocurrencies ranked according to market capitalisation which, at the data collection date, contributed a large combined market share of 79%. This might partly be due to the fast-changing position nature of cryptocurrency market.

Following the study, the returns of the top five cryptocurrencies ranked according to total market capitalisation are fitted with various volatility models. Given the wild price fluctuations and excessive volatility observed in cryptocurrency market, TV-MSGARCH model which integrates with the drivers of cryptocurrencies prices, namely trading volume and Google searches series retrieved from Google Trends, are proposed. For empirical comparison purpose, the volatility models considered in this research includes GARCH(1,1) model, TGARCH(1,1) model, GJRGARCH(1,1) model, MSGARCH(1,1) model and three TV-MSGARCH(1,1) models, all incorporated with three different error distributions: NORMD, STD and GED. The exogenous variables considered for the three TV-MSGARCH(1,1) respectively are: (1) Google searches series, denoted by TV-MSGARCH$_S$(1,1); (2) log difference Google searches series, denoted by TV-MSGARCH$_{ldS}$(1,1); (iii) log trading volume, denoted by TV-MSGARCH$_{lnV}$(1,1). The in-sample estimations of all volatility models are contrasted based on AIC while the out-of-sample performance are contrasted and tested using MCS procedure on QLIKE loss function and by using several VaR backtests.

Based on the model selection criteria of LL and AIC, TV-MSGARCH$_S$(1,1)-GED model gave the best fit for BTC and ETH, TV-MSGARCH$_{ldS}$(1,1)-GED model gave the best fit for BCH; and TV-MSGARCH$_{lnV}$(1,1)-STD model gave the best fit for XRP and EOS. Ljung-Box test further confirms that these fitted model for the respective cryptocurrencies are adequate in capturing ARCH effects for which there is no serial correlation exists in the squared standardised residuals. The volatility clustering behaviours are well-captured by the respective optimal volatility models.

Moreover, volatility forecasting is one of the common risk management approach in which one-day ahead forecasts are computed to provide an insight on the underlying risk. The best volatility model for forecasting application evaluated using MCS procedure on QLIKE is MSGARCH(1,1)-STD model for BTC; TV-MSGARCH$_{lnV}$(1,1)-STD model for ETH; GJRGARCH(1,1)-STD model for XRP; TV-MSGARCH$_S$(1,1)-STD model for BCH; and TV-MSGARCH$_{lnV}$(1,1)-STD model for EOS. VaR backtests such as UC test, CC test and DQ test are carried out on the volatility models to adopt the understanding on the capabilities of these models in providing close estimation between actual volatility and volatility forecasts at the 90%, 95% and 99% confidence limits.

Despite the encouraging results in this research as to the positive effect in the modelling and forecasting process, future work might usefully be extended to explore other exogenous variables as well as multi-regime in the presence of dynamic changes of the cryptocurrencies prices. In so doing, it seeks to contribute to our growing understanding of how the approach can be employed in financial strategic planning.

REFERENCES

Aalborg, H. A., Mólnar, P. & de Vries, J. E. (2019). What can explain the price, volatility and trading volume of Bitcoin? *Finance Research Letters*, 29, 255-265.

Akaike, H. (1974). A new look at the statistical model identification. *IEEE Transactions on Automatic Control*, 19(6), 716-723.

Andrei, D. & Hasler, M. (2015). Investor attention and stock market volatility. *Review of Financial Studies*, 28(1), 33-72.

Ardia, D., Bluteau, K. & Rüede, M. (2019). Regime changes in Bitcoin GARCH volatility dynamics. *Finance Research Letters*, 29, 266-271.

Augustyniak, M., Boudreault, M. & Morales, M. (2018). Maximum likelihood estimation of the Markov-switching GARCH model based on a general collapsing procedure. *Methodology and Computing in Applied Probability*, 20(1), 165-188.

Baek, C. & Elbeck, M. (2015). Bitcoins as an investment or speculative vehicle? A first look. *Applied Economics Letters*, 22(1), 30-34.

Bai, J. & Perron, P. (2003). Computation and analysis of multiple structural change models. *Journal of Applied Econometrics*, 18(1), 1-22.

Balcilar, M., Bouri, E., Gupta, R. & Roubaud, D. (2017). Can volume predict Bitcoin returns and volatility? A quantiles-based approach. *Economic Modelling*, 64, 74-81.

Bariviera, A. F., Basgall, M. J., Hasperué, W. & Naiouf, M. (2017). Some stylized facts of the Bitcoin market. *Physica A*: *Statistical Mechanics and Its Applications*, 484, 82-90.

Bauwens, L., Preminger, A. & Rombouts, J. V. (2010). Theory and inference for a Markov switching GARCH model. *Econometrics Journal*, 13(2), 218–244.

Bauwens, L., Dufays, A. & Rombouts, J. V. K. (2014a). Marginal likelihood for Markov-switching and change points GARCH models. *Journal of Econometrics*, 178(3), 508-522.

Bauwens, L., Backer, B. D. & Dufays, A. (2014b). A Bayesian method of change-point estimation with recurrent regimes: Application to GARCH models. *Journal of Empirical Finance*, 29, 207-229.

Bazzi, M., Blasques, F., Koopman, S. J. & Lucas, A. (2017). Time-varying transition probabilities for Markov regime-switching models. *Journal of Time Series Analysis*, 38(3), 458-478.

Bollerslev, T. (1986). Generalized autoregressive conditional heteroscedasticity. *Journal of Econometrics*, 31(3), 307-327.

Bouoiyour, J. & Selmi, R. (2015). What does Bitcoin look like? *Annals of Economics and Finance*, 16(2), 449-492.

Bouoiyour, J. & Selmi, R. (2016). Bitcoin: A beginning of a new phase? *Economics Bulletin*, 36(3), 1430-1440.

Bouri, E., Azzi, G. & Dyhrberg, A. H. (2017). On the return-volatility relationship in the Bitcoin market around the price crash of 2013. *Economics*, 11(2), 1-16.

Bouri, E., Gil-Alana, L. A., Gupta, R. & Roubaud, D. (2019a). Modelling long memory volatility in the Bitcoin market: Evidence of persistence and structural breaks. *International Journal of Finance and Economics*, 24(1), 412-426.

Bouri, E., Lau, C. K. M., Lucey, B. & Roubaud, D. (2019b). Trading volume and the predictability of return and volatility in the cryptocurrency market. *Finance Research Letters*, 29, 340-346.

Brière, M., Oosterlinck, K. & Szafarz, A. (2015). Virtual currency, tangible return: Portfolio diversification with Bitcoin. *Journal of Asset Management*, 16(6), 365-373.

Cai, J. (1994). A Markov model of switching-regime ARCH. *Journal of Business & Economic Statistics*, 12(3), 309-316.

Caporale, G. M., Pittis, N. & Spagnolo, N. (2003). IGARCH models and structural breaks. *Applied Economics Letters*, 10(12), 765-768.

Caporale, G. M. & Zekokh, T. (2019). Modelling volatility of cryptocurrencies using Markov-switching GARCH models. *Research in International Business and Finance*, 48, 143-155.

Chaim, P. & Laurini, M. P. (2018). Volatility and return jumps in Bitcoin. *Economics Letters*, 173, 158-163.

Cheah, E. T. & Fry, J. (2015). Speculative bubbles in Bitcoin markets? An empirical investigation into the fundamental value of Bitcoin. *Economics Letters*, 130, 32-36.

Christoffersen, P. F. (1998). Evaluating interval forecasts. *International Economic Review*, 39(4), 841-862.

Chu, J., Chan, S., Nadarajah, S. & Osterrieder, J. (2017). GARCH modelling of cryptocurrencies. *Journal of Risk and Financial Management*, 10(4), Article#17.

Ciaian, P., Rajcaniova, M. & Kancs, D. (2016). The economics of Bitcoin price formation. *Applied Economics*, 48(19), 1799-1815.

Corbet, S., Lucey, B., Urquhart, A. & Yarovaya, L. (2019). Cryptocurrencies as a financial asset: A systematic analysis. *International Review of Financial Analysis*, 62, 182-199.

Corbet, S., Larkin, C., Lucey, B. M., Meegan, A. & Yarovaya, L. (2020). The impact of macroeconomic news on Bitcoin returns. *European Journal of Finance*, 26(14), 1396-1416.

Da, Z., Engelberg, J. & Gao, P. (2011). In search of attention. *Journal of Finance*, 66(5), 1461-1499.

Diebold, F. X., Lee, J. H. & Weinbach, G. C. (1994). Regime switching with time-varying transition probabilities. *Business Cycles: Durations, Dynamics and Forecasting*, 1, 144-165.

Diebold, F. X. & Mariano, R. S. (1995). Comparing predictive accuracy. *Journal of Business & Economic Statistics*, 13(3), 253-263.

Dueker, M. J. (1997). Markov switching in GARCH processes and mean-reverting stock-market volatility. *Journal of Business & Economic Statistics,* 15(1), 26-34.

Dwyer, G. P. (2015). The economics of Bitcoin and similar private digital currencies. *Journal of Financial Stability*, 17, 81-91.

Dyhrberg, A. H. (2016). Hedging capabilities of Bitcoin. Is it the virtual gold? *Finance Research Letters*, 16, 139-144.

ElBahrawy, A., Alessandretti, L., Kandler, A., Pastor-Satorras, R. & Baronchelli, A. (2017). Evolutionary dynamics of the cryptocurrency market. *Royal Society Open Science*, 4(11), Article#170623.

Elliot, R. J., Lau, J. W., Miao, H. & Siu, T. K. (2012). Viterbi-based estimation for Markov switching GARCH model. *Applied Mathematical Finance*, 19(3), 219-231.

Engle, R. F. (1982). Autoregressive conditional heteroscedasticity with estimates of the variance of United Kingdom inflation. *Econometrica*, 50(4), 987-1008.

Engle, R. F. & Manganelli, S. (2004). CAViaR: Conditional autoregressive value at risk by regression quantiles. *Journal of Business & Economic Statistics*, 22(4), 367-381.

Filardo, A. J. (1994). Business-cycle phases and their transitional dynamics. *Journal of Business & Economic Statistics*, 12(3), 299-308.

Francq, C. & Zakoian, J. M. (2019). *GARCH models: Structure, statistical inference and financial applications* (2nd ed.). John Wiley & Sons.

Garcia, D., Tessone, C. J., Mavrodiev, P. & Perony, N. (2014). The digital traces of bubbles: Feedback cycles between socio-economic signals in the Bitcoin economy. *Journal of the Royal Society Interface*, 11(99), Article#20140623.

Glosten, L. R., Jagannathan, R. & Runkle, D. E. (1993). On the relation between the expected value and the volatility of the nominal excess return on stocks. *Journal of Finance*, 48(5), 1779-1801.

Gosset, W. S. (1908). The probable error of a mean. *Biometrika*, 6(1), 1-25.

Gray, S. F. (1996). Modeling the conditional distribution of interest rates as a regime-switching process. *Journal of Financial Economics*, 42(1), 27-62.

Haas, M., Mittnik, S. & Paolella, M. S. (2004). A new approach to Markov-switching GARCH models. *Journal of Financial Econometrics*, 2(4), 493-530.

Hamilton, J. D. (1989). A new approach to the economic analysis of nonstationary time series and the business cycle. *Econometrica*, 57(2), 357-384.

Hamilton, J. D. & Susmel, R. (1994). Autoregressive conditional heteroscedasticity and changes in regime. *Journal of Econometrics*, 64(1-2), 307-333.

Hansen, P. R. (2005). A test for superior predictive ability. *Journal of Business & Economic Statistics*, 23(4), 365-380.

Hansen, P. R., Lunde, A. & Nason, J. M. (2011). The model confidence set. *Econometrica*, 79(2), 453-497.

Katsiampa, P. (2017). Volatility estimation for Bitcoin: A comparison of GARCH models. *Economics Letters,* 158, 3-6.

Katsiampa, P. (2019). An empirical investigation of volatility dynamics in the cryptocurrency market. *Research in International Business and Finance*, 50, 322-335.

Klaassen, F. (2002). Improving GARCH volatility forecasts with regime-switching GARCH. *Empirical Economics*, 27(2), 363-394.

Kristoufek, L. (2015). What are the main drivers of the Bitcoin price? Evidence from wavelet coherence analysis. *PloS One*, 10(4), Article#e0123923.

Kupiec, P. H. (1995). Techniques for verifying the accuracy of risk measurement models. *Journal of Derivatives*, 3(2), 73-84.

Lahmiri, S., Bekiros, S. & Salvi, A. (2018). Long-range memory, distributional variation and randomness of Bitcoin volatility. *Chaos*, *Solitons & Fractals*, 107, 43-48.

Liu, J., Wu, S. & Zidek, J. V. (1997). On segmented multivariate regression. *Statistica Sinica*, 7(2), 497-525.

Mensi, W., Al-Yahyaee, K. H. & Kang, S. H. (2019). Structural breaks and double long memory of cryptocurrency prices: A comparative analysis from Bitcoin and Ethereum. *Finance Research Letters*, 29, 222-230.

Mikosch, T. & Stărică, C. (2004). Nonstationarities in financial time series, the long-range dependence, and the IGARCH effects. *Review of Economics and Statistics*, 86(1), 378-390.

Nakamoto, S. (2008). Bitcoin: A peer-to-peer electronic cash system, https://bitcoin.org/bitcoin.pdf.

Nelson, D. B. (1991). Conditional heteroskedasticity in asset returns: A new approach. *Econometrica*, 59, 347-370.

Panagiotidis, T., Stengos, T. & Vravasinos, O. (2019). The effects of markets, uncertainty and search intensity on Bitcoin returns. *International Review of Financial Analysis*, 63, 220-242.

Parino, F., Beiró, M. G. & Gauvin, L. (2018). Analysis of the Bitcoin blockchain: Socio-economic factors behind the adoption. *EPJ Data Science*, 7(1), Article#38.

Patton, A. J. (2011). Volatility forecast comparison using imperfect volatility proxies. *Journal of Econometrics*, 160(1), 246-256.

Philip, A., Chan, J. S. K. & Peiris, S. (2018). A new look at cryptocurrencies. *Economics Letters,* 163, 6-9.

Risteski, D. & Davcev, D. (2014). Can we use daily internet search query data to improve predicting power of EGARCH models for financial time series volatility? *In Proceedings of the International Conference on Computer Science and Information System* (*ICSIS'2014*), *October 17-18*, *2014*, *Dubai* (*United Arab Emirates*).

Rivin, I. & Scevola, C. (2018). The CCI30 Index. arXiv: 1804.06711.

Thies, S. & Mólnar, P. (2018). Bayesian change point in analysis of Bitcoin returns. *Finance Research Letters*, 27, 223-227.

Trimborn, S. & Härdle, W. K. (2016). CRIX an index for blockchain based currencies. SFB 649 Discussion Paper 2016-021, Economic Risk, Berlin.

Urquhart, A. (2018). What causes the attention of Bitcoin? *Economics Letters*, 166, 40-44.

Williams, M. T. (2014) Virtual currencies-Bitcoin risk. In *World Bank Conference*, *October 21*, *2014*, *Washington*, *D.C*.

Zakoian, J. M. (1994). Threshold heteroscedasticity models. *Journal of Economic Dynamics and Control*, 18(5), 931-955.

LIST OF PUBLICATIONS AND PAPERS PRESENTED

List of publications

1. **Tan, C. Y.**, Koh, Y. B., Ng, K. H. & Ng, K. H. (2021). Dynamic volatility modelling of Bitcoin using time-varying transition probability Markov-switching GARCH model. *North American Journal of Economics and Finance*, 56, Article#101377.